



Head and otolith morphology of the genera *Hymenocephalus*, *Hymenogadus* and *Spicomacrurus* (Macrouridae), with the description of three new species

Schwarzahns, Werner

DOI:

[10.11646/zootaxa.3888.1.1](https://doi.org/10.11646/zootaxa.3888.1.1)

Publication date:

2014

Document version

Publisher's PDF, also known as Version of record

Document license:

[CC BY](https://creativecommons.org/licenses/by/4.0/)

Citation for published version (APA):

Schwarzahns, W. (2014). *Head and otolith morphology of the genera Hymenocephalus, Hymenogadus and Spicomacrurus (Macrouridae), with the description of three new species*. Magnolia Press. Zootaxa, Vol.. 3888 <https://doi.org/10.11646/zootaxa.3888.1.1>



Zootaxa 3888 (1): 001–073
www.mapress.com/zootaxa/

Copyright © 2014 Magnolia Press

Monograph

ISSN 1175-5326 (print edition)

ZOOTAXA

ISSN 1175-5334 (online edition)

<http://dx.doi.org/10.11646/zootaxa.3888.1.1>

<http://zoobank.org/urn:lsid:zoobank.org:pub:1B437AE1-CF28-4C1B-95B6-C31A295905A0>

ZOOTAXA

3888

Head and otolith morphology of the genera *Hymenocephalus*, *Hymenogadus* and *Spicomacrurus* (Macrouridae), with the description of three new species

WERNER SCHWARZHANS

Ahrensburger Weg 103, D-22359 Hamburg, and Natural History Museum of Denmark, Copenhagen

E-mail: wwschwarz@aol.com



Magnolia Press
Auckland, New Zealand

Accepted by W. Holleman: 7 Aug. 2014; published: 28 Nov. 2014

Licensed under a Creative Commons Attribution License <http://creativecommons.org/licenses/by/3.0>

WERNER SCHWARZHANS

Head and otolith morphology of the genera *Hymenocephalus*, *Hymenogadus* and *Spicomacrurus* (Macrouridae), with the description of three new species

(*Zootaxa* 3888)

73 pp.; 30 cm.

28 Nov. 2014

ISBN 978-1-77557-583-2 (paperback)

ISBN 978-1-77557-584-9 (Online edition)

FIRST PUBLISHED IN 2014 BY

Magnolia Press

P.O. Box 41-383

Auckland 1346

New Zealand

e-mail: zootaxa@mapress.com

<http://www.mapress.com/zootaxa/>

© 2014 Magnolia Press

All rights reserved.

No part of this publication may be reproduced, stored, transmitted or disseminated, in any form, or by any means, without prior written permission from the publisher, to whom all requests to reproduce copyright material should be directed in writing.

This authorization does not extend to any other kind of copying, by any means, in any form, and for any purpose other than private research use.

ISSN 1175-5326 (Print edition)

ISSN 1175-5334 (Online edition)

Table of contents

Abstract	4
Introduction	4
Materials and methods	5
Head morphology (Figs. 1 A–F, Tables 2, 3)	6
Otolith morphology (Fig. 2 A–C, Tab. 4)	9
Character analysis (Tables 1–4)	10
Taxonomy	16
Species Descriptions	18
Key to the species of <i>Hymenocephalus</i> , <i>Hymenogadus</i> and <i>Spicomacrus</i>	18
Species Descriptions	19
<i>Spicomacrus</i> Okamura, 1970	19
<i>Spicomacrus adelscottii</i> (Iwamoto & Merrett, 1997)	20
<i>Spicomacrus dictyogadus</i> Iwamoto, Shao & Ho, 2011	20
<i>Spicomacrus kuronumai</i> (Kamohara, 1938)	21
<i>Spicomacrus mcoskeri</i> Iwamoto, Shao & Ho, 2011	22
<i>Hymenogadus</i> Gilbert & Hubbs, 1920	23
<i>Hymenogadus gracilis</i> (Gilbert & Hubbs, 1920)	25
<i>Hymenogadus tenuis</i> (Gilbert & Hubbs, 1917)	26
<i>Hymenocephalus</i> Giglioli, 1884	26
<i>Hymenocephalus longibarbis</i> Group	27
<i>Hymenocephalus longibarbis</i> (Günther, 1887)	27
<i>Hymenocephalus longipes</i> Smith & Radcliffe, 1912	29
<i>Hymenocephalus iwamotoi</i> Group	30
<i>Hymenocephalus iwamotoi</i> n.sp.	30
<i>Hymenocephalus aterrimus</i> Group	33
<i>Hymenocephalus aterrimus</i> Gilbert, 1905	33
<i>Hymenocephalus barbatulus</i> Gilbert & Hubbs, 1920	35
<i>Hymenocephalus nesaeae</i> Merrett & Iwamoto, 2000	36
<i>Hymenocephalus papyraceus</i> Jordan & Gilbert, 1904	37
<i>Hymenocephalus sazoonovi</i> n.sp.	38
<i>Hymenocephalus striatulus</i> Group	41
<i>Hymenocephalus billsam</i> Marshall & Iwamoto, 1973	41
<i>Hymenocephalus lethonemus</i> Jordan & Gilbert, 1904	42
<i>Hymenocephalus nascens</i> Jordan & Hubbs, 1920	43
<i>Hymenocephalus striatulus</i> Gilbert, 1905	45
<i>Hymenocephalus antraeus</i> Group	47
<i>Hymenocephalus antraeus</i> Gilbert & Cramer, 1897	47
<i>Hymenocephalus hachijoensis</i> Okamura, 1970	49
<i>Hymenocephalus heterolepis</i> (Alcock, 1889)	50
<i>Hymenocephalus punt</i> n.sp.	52
<i>Hymenocephalus italicus</i> Group	55
<i>Hymenocephalus italicus</i> Giglioli, 1884	55
<i>Hymenocephalus striatissimus</i> Group	58
<i>Hymenocephalus aeger</i> Gilbert & Hubbs, 1920	58
<i>Hymenocephalus megalops</i> Iwamoto & Merrett, 1997	59
<i>Hymenocephalus striatissimus</i> Jordan & Gilbert, 1904	60
<i>Hymenocephalus torvus</i> Smith & Radcliffe, 1912	61
<i>Hymenocephalus grimaldii</i> Group	63
<i>Hymenocephalus grimaldii</i> Weber, 1913	63
<i>Hymenocephalus neglectissimus</i> Sazonov & Iwamoto, 1992	64
<i>Hymenocephalus semipellucidus</i> Sazonov & Iwamoto, 1992	65
Unidentifiable species	65
<i>Hymenocephalus</i> sp. 1	66
<i>Hymenocephalus</i> sp. 2	66
Fossil record	67
Phylogenetic interpretation	68
Geographical distribution and speciation (Figs. 5, 7, 12, 16, 21, 27, 29, 37)	68
Phylogenetic trends and polarities of characters (Fig. 39)	69

Conclusions	71
Acknowledgements	71
References	71

Abstract

The fishes of the genus *Hymenocephalus* live over continental slope terrain, chiefly between 300 and 1000 m water depths, in all tropical oceans, except the eastern Pacific. They are characterized by an elongated light organ with two lenses, striations on jugular and thorax, and by an extraordinary development of sensory reception organs: strongly enlarged eyes, exceptionally large and specialized sagittal otoliths and extremely wide and deep head canals resembling caverns and housing the cephalic sensory organ for motion reception (lateral line system).

The purpose of this study is to evaluate the potential that a detailed analysis of the head and otolith morphology can offer for distinguishing the various species and assessment of their interrelationships. About 500 specimens were investigated, representing all 22 nominal species of the genus *Hymenocephalus*, except for *H. barbatulus* (specimens of which could not be located), the two species of the related genus *Hymenogadus* and three of the four species of *Spicomacrurus*. Because of the delicate and thin nature of the head bones and head skin typical for the fishes of the genus *Hymenocephalus* and the deteriorating effects of formalin to the aragonitic otoliths, only a fraction of the studied specimens actually contributed useful data, although that fraction represented all species studied.

Otoliths in particular and aspects of the cephalic canal system were found to contribute additional characters that help to verify the status of certain controversial species such as *H. heterolepis*, *H. nascens* and species within the *H. striatissimus* and *H. grimaldii* Groups. *Hymenocephalus longiceps* is revised to represent a junior synonym of *H. longibarbis*. Eight species groups are defined within the genus *Hymenocephalus*. Three new species are being described in the course of this review: *H. iwamotoi* from off northwestern Australia, *H. sazonovi* from the Sala y Gomez and Nazca Ridges, and *H. punt* from northern Somalia and the Gulf of Aden, now raising the count of valid species in the genus to a total of 24.

The specializations of the sensory reception organs show a variety of developments with well-expressed phylogenetic polarities that are discussed in the context of their evolution and interrelationships. A well-documented case of polarity reversal of certain characters in the *H. aterrimus* Group is interpreted as a functional adaptation to migration of these fishes into a deeper water environment that favors different specializations of the sensory reception

Key words: Head morphology, otoliths, new species, *Hymenocephalus*, *Hymenogadus*, *Spicomacrurus*

Introduction

The fishes of the macrourid genus *Hymenocephalus* Giglioli, 1884 are found along the continental slopes of the tropical and subtropical seas of the world except for the Pacific coast of South America (but for a single specimen caught off Peru, USNM 149049). They occur predominantly at depths between 300 and 600 m where they feed mostly on planktonic euphasids and copepods (Okamura, 1970) and often seem to socialize in schools. At this water depth there is still some dim, high-frequency light and it is also within or close to the zone with highly effective long-distance sound transmission. It may have to do with their specific environment in life that evolution has favored the development of extraordinary sensory reception organs in the fishes of the genus *Hymenocephalus*. They show strongly enlarged eyes positioned in orbits resembling parabolic mirrors and oriented perpendicular to the fish axis. The sagittal otolith ('otolith' in the following), which is part of the sound-receiving sensory organ in fishes, is amongst the largest found in teleosts relative to the size of the brain capsule, and it shows some very distinct specialized features. It is so big and the head bones are so translucent that very often it can be seen shining through the head from above. The orbit sizes reach up to 50% of the head length in certain species and the sagittal otolith can attain a size of about 20% of the head length. The head bones are thin and large parts of the head over the occiput, around the eyes, along the rim of the preopercle and the mandible are occupied by an extremely wide and deep cavern or canal system housing the cephalic sensory organ for motion reception (lateral-line system) with large sensory papillae or neuromasts of one mm in diameter or more. The canals are covered by a very thin integument ('hymen'), which is almost never found fully intact on fishes brought to surface. The integument is stretched over the cephalic canals ('caverns') with the support of a number of bony projections from the skull ('supporters'), not unlike the canvas of a tent stretched over its poles. As far as can be reconstructed, the canal systems do not seem to be segmented, but, where reasonably preserved, the integument does show regular linear

bracing elements, and sometimes the floor of the canals show similar features too. The cephalic canals appear to be a generally closed systems without pores or with only few and small pores in the hymen, unlike the development of a similar expansive canal system observed in the ophidiid genus *Porogadus* Goode & Bean, 1885, which shows numerous very large pores. In essence one must assume that the fishes of the genus *Hymenocephalus* have developed superb visual, auditory and motion reception senses, which probably are related to their way of living (see above).

The purpose of this study is to evaluate whether a detailed analysis of the head and the otolith morphology can contribute to a better distinction of the species contained in the genus, which so far have mainly been recognized by the combination of pectoral and pelvic fin counts, gill raker counts, head profile, eye size, barbel presence and length, luminous organ details and, occasionally, coloration patterns. Of the 28 nominally valid species and subspecies currently recognized within the three genera reviewed, a number of species present taxonomic challenges for distinction or have been the subject of divergent views as to their validity. Specimens, including several types, of all these species were examined, and the related genera *Spicomacrurus* and *Hymenogadus*, except for *H. barbatulus* Gilbert & Hubbs, 1920, of which the two unique syntypes could not be located at USNM. Otoliths were extracted representing all other species except for the unique holotypes of *Hymenogadus tenuis* and *Spicomacrurus dictyogadus*. However, an x-ray showed that the otoliths of *H. tenuis* are very similar in outline to the ones of its closest relative, *H. gracilis*, and those of *S. dictyogadus* appear to be similar to those of the other species of the genus.

The otolith morphology was found to be particularly useful as an additional character of diagnostic value, while the head morphology added only few previously unused characters. The main taxonomic findings are:

Hymenocephalus italicus and *H. heterolepis* can be clearly distinguished by the combination of eye size and otolith morphology.

Hymenocephalus longibarbis and *H. longiceps* cannot be distinguished by any morphological means and are therefore considered synonyms.

Several subspecies of *H. striatissimus* in the western Pacific have been recognized, based on the observations by Gilbert & Hubbs (1920) of a large number of specimens. These are *H. striatissimus aeger*, *H. striatissimus torvus* and *H. striatissimus striatissimus*. They are here considered valid at species rank following the use of additional characters from head and otolith morphology, but their distinction remains based on relatively few and subtle differences, which suggest a close interrelationship and a relatively recent speciation. A subsequently described subspecies, *Hymenocephalus striatissimus hachijoensis* Okamura, 1970, is also listed at species rank, supported by additional distinctive characters of its otolith morphology, and is in fact not considered to be closely related to the other taxa.

Hymenocephalus lethonemus and *H. nascens* differ in very subtle characters, which also exhibit some degree of overlap. Nevertheless, the subtle differences appear to be statistically meaningful and hence both nominal species are provisionally kept as valid.

Population variations were studied for the geographically widespread species *H. italicus*, *H. longibarbis* and *H. aterrimus*. No consistent differences were identified between the various populations, but the few specimens recorded as *H. aff. aterrimus* by Sazonov & Iwamoto, 1992 from the Sala y Gomez and Nazca ridges were found distinct from *H. aterrimus* based on additional characters from otolith morphology, and are here described as *H. sazonovi* n.sp.

In addition to the above, two new species are recognized in the material studied, and are herein described: *H. iwamotoi* n.sp. from off northwestern Australia and *H. punt* n.sp. from off Somalia and Yemen. With these, the genera *Hymenocephalus*, *Hymenogadus* and *Spicomacrurus* now contain 30 species, of which 24 species are in the genus *Hymenocephalus*. There is evidence for two more unnamed species from isolated specimens or otoliths, which are not identifiable because of inadequate material available, but highlight the potential for further species to be recognized. Descriptions are given for these otoliths.

Materials and methods

A total of about 500 specimens of the genera *Hymenocephalus*, *Hymenogadus* and *Spicomacrurus* were studied for this review. The distribution maps were created using Microsoft Encarta 2001 digital world atlas. They are based

on a combination of published data, which are referenced, and specimens investigated, the latter being marked specifically.

Institutional abbreviations follow Fricke & Eschmeyer (2011).

Full descriptions are only given for new species and are based on their holotypes. The descriptions of other species focus on detailed head and otolith morphology, which have not been part of previous species descriptions and which add new information.

Meristic counts are given for pelvic and pectoral fins and gill rakers on the inner face of the 1st gill arch and the outer face of the 2nd gill arch of all specimens where possible, and are summarized on Table 1. Pelvic fin rays were counted for both left and right fins, gill rakers from the right side and pectoral fin rays from the better preserved fin of the individual specimens, sometimes from both sides. Fin rays are often fragile and fins are often poorly preserved or incomplete. The first ray of both pelvic and pectoral fins is usually much longer than the subsequent ones, often by a factor of two, but since they are so rarely intact or since their preservation status is difficult to judge, no specific measurements were taken to make use of such characters. Some uncertainty in pectoral fin ray counts may result from the poor preservation of one to three very short rays in the lower part of the pectoral fins. The first dorsal-fin rays have been counted in a representative number; fin rays of the second dorsal and anal fins have not been counted because of the uncertainty of the completeness of the tail. Counts are compared with published data and the range is adjusted accordingly when needed and referenced accordingly. In the case of gill raker counts only those from the outer face of the 2nd gill arch are referred in text and tables since no major variation was observed to the counts on the inner face of the 1st gill arch. Meristic values are given for the holotype first followed by paratype values in parentheses.

Morphometric characters are given as percentage of total length (TL) and head length (HL), in the case of interorbital width in percentage of head width (HW) and in the case of infraorbital supporter length in percentage of orbit diameter (OD). The head width is measured across the head just behind the position of the postorbital canal, in front of the opercle, and because of the flexibility of this area could result in distortions. The size of the orbit is measured as the horizontal diameter of its edges; this can result in slightly lower values than the greatest diameter, which is also used in publications. In some species orbits are oval with the greatest diameter oblique to the axis of the fish. The horizontal diameter is preferred here, because it appears to be less affected by head distortion resulting from preservation. Barbel lengths are measured from tip to base. Barbels are difficult to spread from the head for lateral figures and therefore have been projected from ventral views. Since many of the morphometric measurements of the head depend on good preservation of the fragile head bones, as already stated, only few selected specimens have been used and measurements were done with the aid of a camera lucida; 'n' is the number of specimens measured. A minimum range of 5% was assumed for any morphometric measurement in the absence of actual measured ranges, with the value placed at the center of the range or inside regular 5% increments, whichever more plausible. The prime morphometric measurements used are summarized in Table 2.

Number of precaudal vertebrae was counted from radiographs for holotype and selected paratype specimens only.

The number of otoliths investigated per species varied greatly depending on preservation due to exposure to formalin and otherwise was kept to a maximum of 10 specimens, except in a few instances where certain interspecific variations were investigated. Following abbreviations are used in the otolith descriptions: OL = otolith length; OH = otolith height; OT = otolith thickness; OCL = ostial colliculum length; CCL = caudal colliculum length; TCL = total colliculum length, including cases of non-separated / fused colliculi; PCL = pseudocolliculum length. Morphometric otolith characters are given as ratios: OL:OH, OL:OT, CCL:OCL, TCL:PCL.

The information given under 'Distribution' and shown on the geographic distribution maps is based on studied specimens and information from literature and collection files as far as was accessible for this study. Locations with specimens examined for this study are marked.

Head morphology (Figs. 1 A–F, Tables 2, 3)

The cavernous nature of the head with its thin skin cover (integument), as well as the thin and fragile skull bones lead to many collected specimens being rather poorly preserved with the integument rarely preserved to any larger extent and the skull being deformed or squashed or otherwise affected. Consequently, only few specimens of most

species were found to be preserved well enough to warrant in-depth morphological analysis. This fact also prohibited any statistically meaningful degree of observation of the variability of the head morphology. The following morphological terms are used for the description of the heads of *Hymenocephalus* species:

Eye / orbit. The eyes are positioned in orbits resembling parabolic mirrors and are very large, ranging between 25 and 50% of the head length (HL). They are oriented laterally with only slight inclination dorsally or, in the most advanced species, almost entirely vertically. A ridge-like thin bone-structure marks the orbit. The largest orbit diameter is usually slightly inclined towards the fish axis. Although the eye-size is not the only aspect of importance for the visual capacity in fishes (see Marshall, 1979), the extremely large eye found in some of the species and the ‘parabolic’ appearance of the orbit suggest enhanced sight efficiency.

Barbel. The barbel is inserted at the chin when present. It is composed of firm tissue and is usually well preserved even in otherwise poorly preserved fishes. The length of the barbel, which is often diagnostic, is described in relation to the orbit, i.e. minute (not reaching a vertical line through the anterior rim of the orbit), reaching a vertical line through the anterior rim of the orbit, reaching a vertical line through the middle of the eye or reaching a vertical line through the rear margin of the orbit, or is given as percentage of HL.

Snout. The snout projects further than the upper jaw to various extents and can be pointed, blunt or rounded. Although often poorly preserved at the tip, its profile and relative length given in percentage of HL is still of diagnostic value in certain cases.

Canals and supporters. (Figs. 1 A–C) Eight different paired canal systems extend over the head. A system of broad cephalic canals (‘caverns’) is seen above the snout on the frontal. It is separated towards the middle by a high, thin median nasal ridge. Its integument is segmented into three segments, which however are rarely recognizable. The first two segments are paired on either side of the frontal ridge, the third is very wide, across the entire width of the cavern and located behind the abruptly terminated frontal ridge. A large, round nasal cavern is located in front of the eye and contains the olfactory organ, which is of moderate size (Marshall, 1979) and contains 4 to 7 paired olfactory lamellae. A thin, half-moon-shaped bony ridge separates the nasal cavern anteriorly from the frontal canals, whereas posteriorly it is bound by the orbit. The supraorbital canal connects anteriorly to the third, central and unpaired segment of the frontal canal and extends from midway above the eye backwards to a position above the rear part of the opercle over the temporal bones (‘temporal canal’ in Garman, 1899, and Marshall, 1979). The supraorbital width of the canal system is measured at its widest point. The integument spanning the supraorbital canal is divided into 4 to 6 segments, which are usually recognizable even when damaged, by evidence of similar segmentation of tissue lining the floor of the canal and the presence of small spinous supporters along its dorsal margin. A skin flap is often seen above the 3rd or 4th segment of the supraorbital canal housing a narrow, un-segmented supratemporal canal. This feature, however, is very easily damaged or otherwise is poorly identifiable or not observable. The infraorbital canal extends from below the tip of the snout to a position behind the eye, where it curves upwards. The infraorbital width is measured at the shortest vertical distance from the lower rim of the orbit to the mouth cleft. The infraorbital canal is divided into 5 or 6 segments recognized in the integument as well as by tissue linings on the floor of the canal. The first segment is the longest and its middle section it is partly covered by a fragile, often flexible lateral nasal bone, the ‘infranasal supporter’, which is dorsally connected to the skull below the nasal ridge. The following three to four segments are supported by a thin bony ridge extending below the eye. This longitudinal ridge, the ‘infraorbital supporter’, ranges in development from broad along its entire stretch to thin anteriorly and expanded into a broad supporter only above the 4th and / or 5th segment. The last segment (the 5th or 6th, respectively) is curved upwards behind the infraorbital supporter. The integument of the infraorbital canal is the only one in which one to four small pores have been observed on segments 1 to 3 and 5. An un-segmented postorbital canal behind the eye connects the infraorbital canal with the supraorbital canal, separated on each end by a narrowing joint with a bony ridge at the floor of the canal. An un-segmented preopercular canal runs along the distal margin of the preoperculum and ventrally turns around a broad, angular ‘preopercular supporter’. The width of the preopercular canal system is measured at its widest point. The length of the preopercular supporter is measured from its distal tip to the anterior concavity where it begins. The un-segmented mandibular canal runs inside of the mandible from near the tip of the lower jaw to the ‘mandibular hook’ and connects upwards to the preopercular canal. The mandibular hook is a small, sharp, curved spine at the posterior termination of the mandible in most of the species.

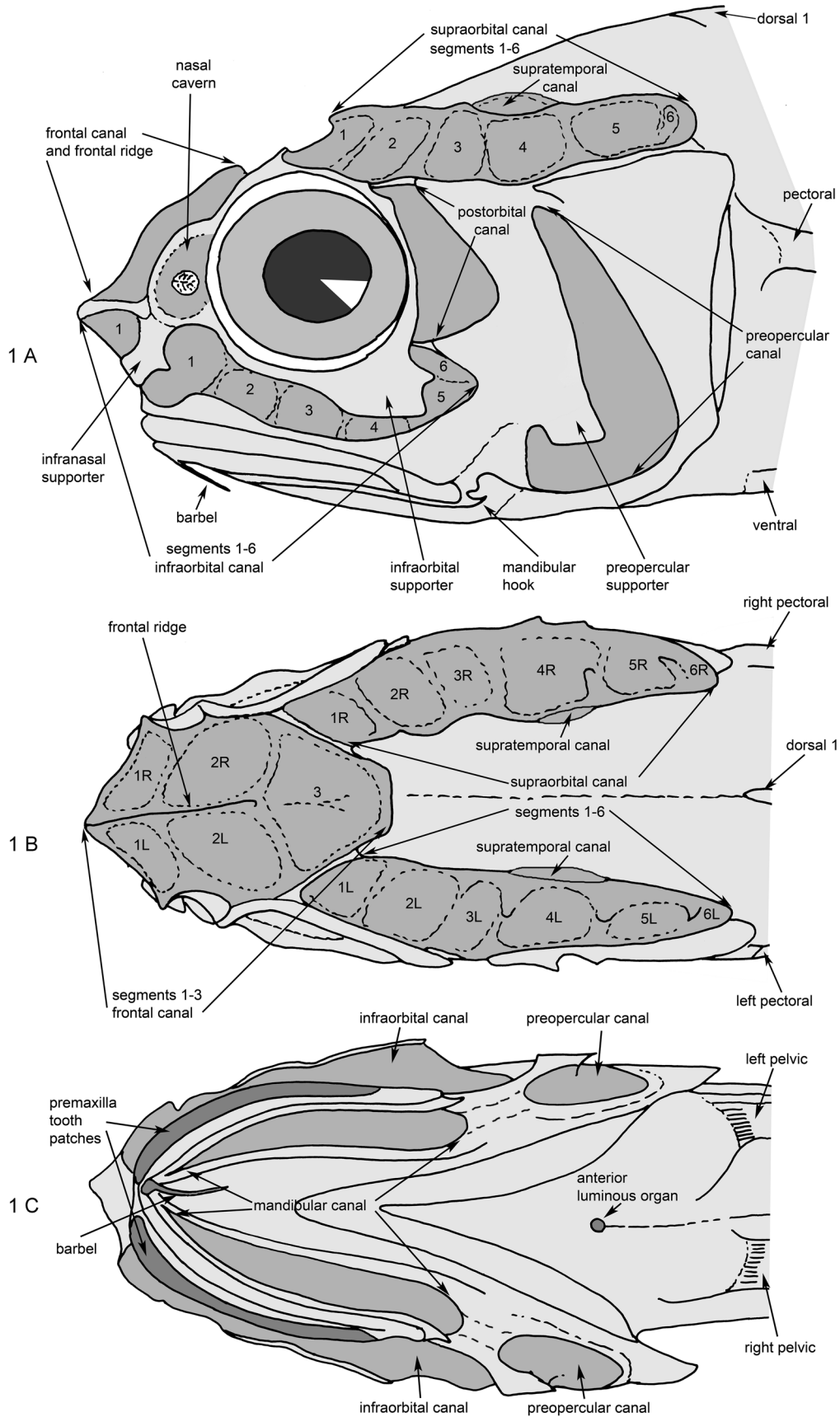


FIGURE 1. Head morphology and sensory system of *Hymenocephalus*: A—Head morphology in lateral view. B—Head morphology in dorsal view. C—Head morphology in ventral view.

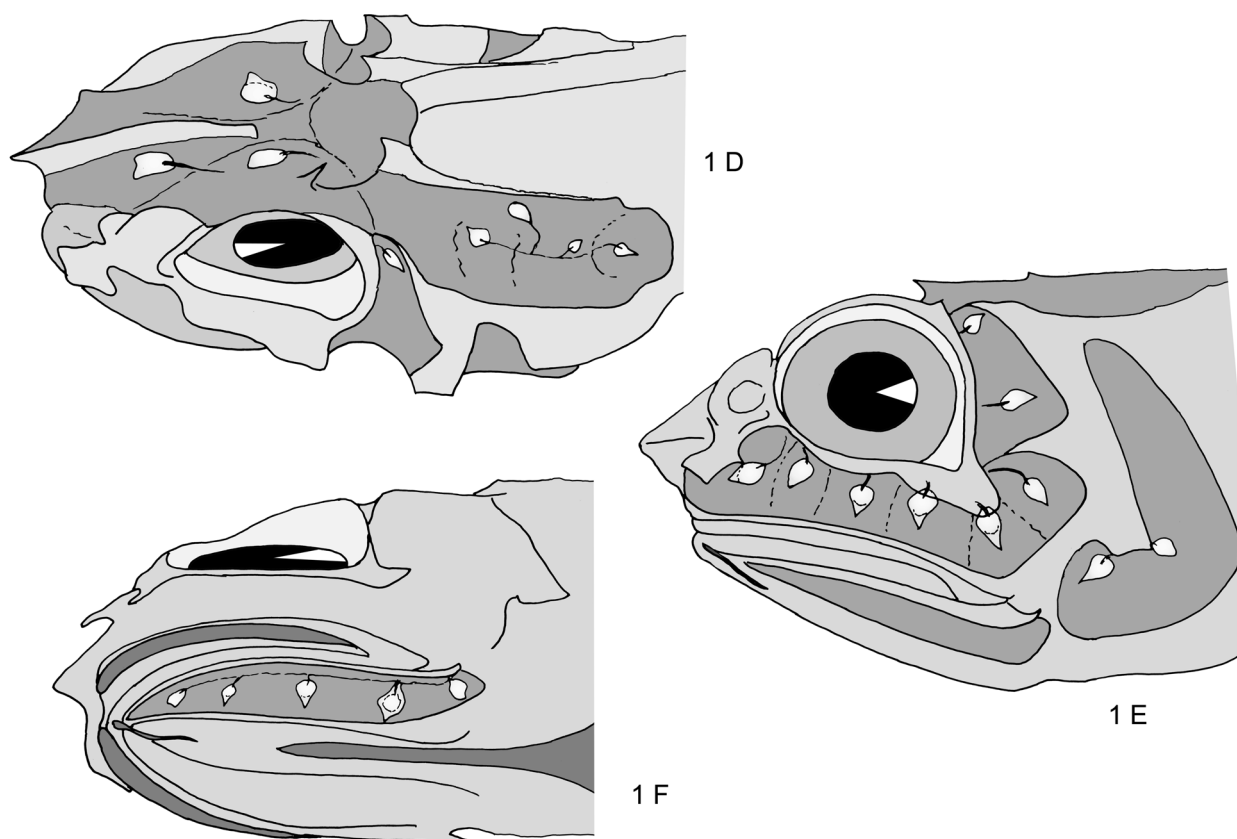


FIGURE 1. D—Neuromasts in head canals in oblique dorso-lateral view. E—Neuromasts in head canals in oblique lateral view. F—Neuromasts in head canals in oblique ventro-lateral view.

Neuromasts. (Figs. 1 D–F) The floor of the canals carries large, leaf-shaped sensory papillae or neuromasts (see Marshall, 1979), which can reach a length of 1 mm or more, but are only rarely well preserved. Some specimens of *Hymenocephalus punt* n.sp. are well preserved, and as a result of the dusty dark coloration of the head and the lighter color of the sensory papillae, the neuromasts stand out exceptionally well. They are best seen on the floor of the infraorbital canal, where there are 5 or 6 large neuromasts, one per segment. The floor of the unsegmented postorbital canal has 2 or 3 neuromasts, and the floor of the unsegmented mandibular canal 4 or 5 neuromasts. The frontal canal has at least 2 neuromasts, one pair of neuromasts attached towards the rear of the frontal ridge, the second pair above the eye. The floor of the supraorbital canal seems to carry smaller neuromasts, which are more difficult to assess and may amount to 4 or more. The neuromasts in the supraorbital canal are not positioned along a continuous sequence; one neuromast is located higher than the rest. The neuromasts on the floor of the preopercular canal are also difficult to assess and seem to consist of only 2 patches at the lower part next to the preopercular supporter.

Otolith morphology (Fig. 2 A–C, Tab. 4)

The otolith terminology follows Koken (1884) and Weiler (1942) with amendments by Schwarzhans (1978) and is shown in Fig. 2. A feature typical, but not unique for otoliths of many gadiforms, is the ridge-like pseudocolliculum located ventral to the collum between the ostial and the caudal colliculi, and in *Hymenocephalus* often extending for a significant stretch below these two colliculi.

The otoliths of *Hymenocephalus* are characterized by their massive, compressed appearance and the presence of a broad and mostly well-developed predorsal lobe. They are mostly higher than long, while those of the related genera *Hymenogadus* and *Spicomacrurus* are more elongate with an expanded posterior tip. The sulcus is a horizontal groove on the inner face of the otolith with the anterior part being the ostium and the posterior part the cauda, and it is typically homosulcoid with ostium and cauda being equally wide and terminating close to the otolith rims anteriorly and posteriorly. The colliculi are well marked and usually farther from the anterior and

posterior otolith rims than the sulcus. In *Hymenocephalus* the ostial and caudal colliculi are about equal in length, while in *Hymenogadus* the caudal colliculum is about twice as long as the ostial colliculum.

Hymenocephalus contains species with both colliculi fused into a single large colliculum (Fig. 2 B), a character development commonly observed in benthic and benthopelagic fishes (Schwarzahns, 2010). The collum carries a distinct ventral pseudocolliculum in all species of *Hymenocephalus*, but not or indistinctly so in *Hymenogadus* and *Spicomacrurus*. As a result, the ventral margin of the sulcus is convex in otoliths of *Hymenocephalus*, at least for its central part, while it is indented at the collum in the other two genera. The pseudocolliculum extends considerably in several species of *Hymenocephalus* and in some reaches the largest relative size known of any teleost otolith. Otoliths of *Spicomacrurus* resemble those of *Hymenogadus* in most aspects including the more elongate shape and lack of an extended pseudocolliculum, but with a much less developed predorsal lobe.

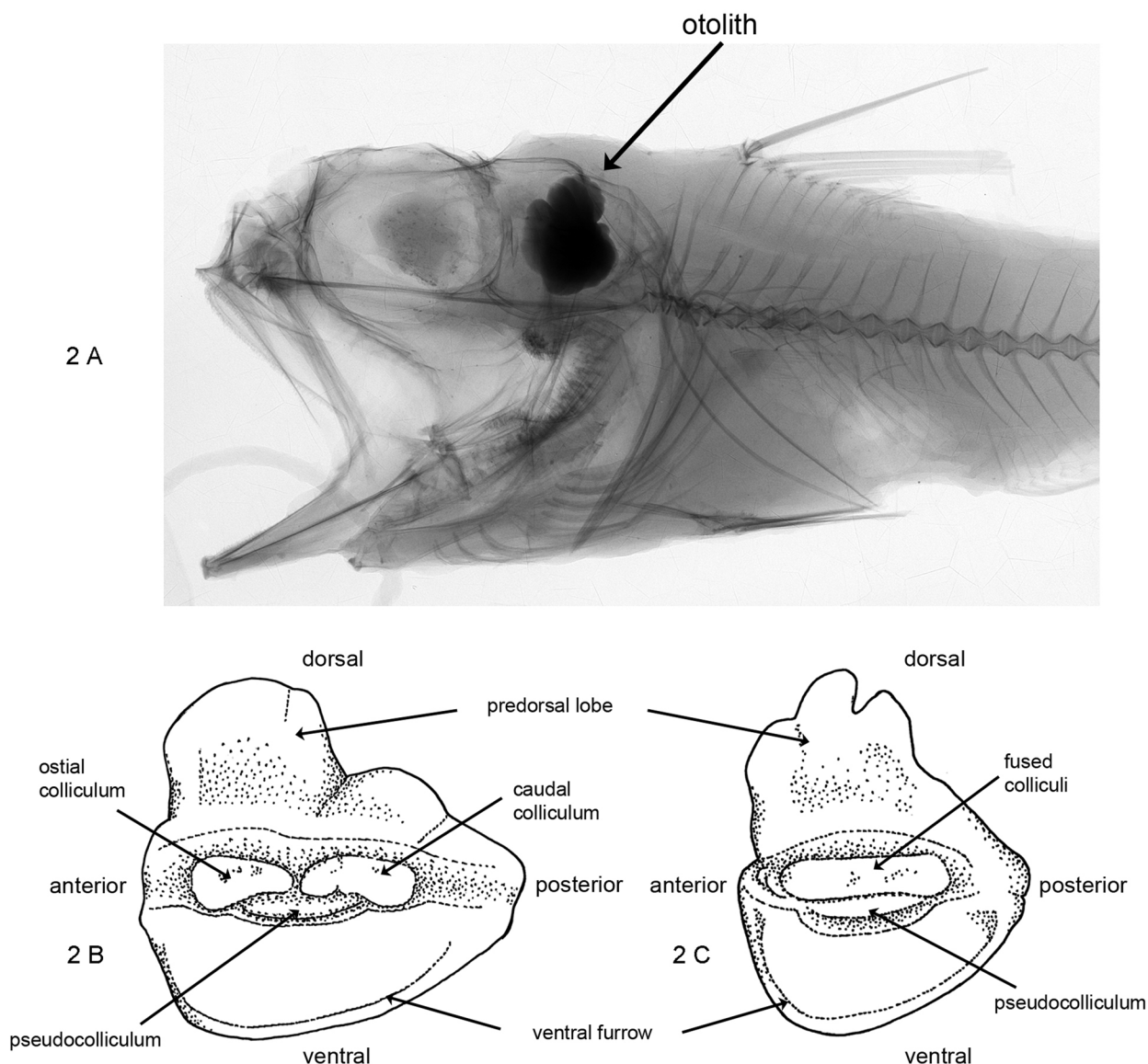


FIGURE 2. Otolith location and morphology of *Hymenocephalus*: A—Radiograph of the head of *Hymenocephalus striatissimus*, USNM 50934, depicting position of otolith inside brain capsule. B—Otolith morphology of inner face of right otolith of *Hymenocephalus nascens*, WAM P.32344-001. C—Otolith morphology of inner face of right otolith of *Hymenocephalus torvus*, MNHN 2005-0928.

Character analysis (Tables 1–4)

The fishes of the genus *Hymenocephalus* exhibit a set of specializations expressed in head and otolith morphology as well as pelvic fin ray counts. These characters seem to have developed in parallel to a large extent, while the

development of a barbel and its length has not. The main characters used for evaluation of evolutionary trends are the following.

1. Number of pelvic fin rays. There are three different clusters observed in *Hymenocephalus*, 13–15 pelvic fin rays, 10–12 pelvic fin rays and 7–9 pelvic fin rays. Species of *Hymenogadus* and *Spicomacrurus* have 8–10 pelvic fin rays, indicating that the derived character state might be a higher number of fin rays.

2. Head size. Head lengths (HL) are in the range of 12–25% of the total length (TL) with the majority of the values between 15 and 19%. *Hymenogadus* species have a smaller head of only 12–16% TL. *Hymenocephalus aterrimus* and related species have larger heads, 20–25% TL.

3. Snout length and profile. *Hymenocephalus* species show a tendency towards reduced snout length, which in the most advanced forms results in a blunt tip. It is difficult to cluster the ranges observed because the tip of the snout is well preserved only in a minority of the specimens examined, but there is a well-preserved specimen available of each species that allowed recognition of two clusters, one a long-snouted cluster with snout lengths of 20–26% HL, and a short-snouted, more advanced cluster with snout lengths of 10–20% HL.

4. Nasal bones. In most species of *Hymenocephalus*, the tip of the snout is formed by a thin, weak, laterally flattened mesial extension of the nasal bones. Species with long snouts contain forms with pointed tips (most strongly developed in *H. papyraceus*) or depressed snout tips (*H. longibarbis* and *H. longipes*), while species with short snouts, which is considered a derived character state, show a blunt or rounded snout profile. The genus *Spicomacrurus* is remarkable for a spectacular specialization of the nasal bones characterized by stout, large, median and lateral nasal processes forming three broad spatulate and inferior projections (Iwamoto *et al.*, 2011).

5. Orbit diameter. The most reliable measure related to eye size is the horizontal orbit diameter, measured between the sharp bony edges of the orbit. Orbit diameters show four different range clusters of which the one around 30% HL (28–33%) is regarded as the most plesiomorphic. From this stage relative orbit diameter increases in two clusters to 34–40% HL and finally 40–50% HL (*H. megalops*, *H. neglectissimus* and *H. semipellucidus*). There is also one distinct trend to reduction of eye and orbit diameters to ranges of 20–27% HL found in *H. aterrimus* and related species.

6. Eye orientation. In *Spicomacrurus* as well as *Hymenogadus* and some species of *Hymenocephalus* (*H. longibarbis* and *H. longipes*), the axis of the eye orientation has a slight v-shaped inclination towards the dorsal, which is best depicted in dorsal views. This inclination results in a narrow interorbital space that becomes gradually larger in species of the genus *Hymenocephalus*. In the most advanced forms the eyes are completely lateralized at 90° to the axis of the head. The different clusters are best characterized by relating interorbital width to head width (HW) resulting in the following clusters: 35–50% HW (including all *Spicomacrurus* and *Hymenogadus*, with *S. mccoskeri* representing a group of its own at 25% HW), 50–60% HW and 60–80% HW.

7. Head canal sizes and integument cover. The extensive head canal systems described above are observed in all specimens of the genus *Hymenocephalus* while they are mostly obscure due to more rigid skull bones and skin cover in the genus *Spicomacrurus*. The infraorbital width ranges from 5–25% HL. Three clusters are observed in this category: <10% HL (in *Spicomacrurus* and few *Hymenocephalus* species, namely *H. antraeus*, *H. neglectissimus* and *H. semipellucidus*), 10–20% HL in the majority of species and >20% HL in *H. aterrimus* and *H. sazovovi* n.sp.. The width of the supraorbital canal system ranges from 4–20% HL and shows no obvious clustering except for the very narrow widths of less than 5% HL found only in *Spicomacrurus*. The width of the preopercular canals system ranges from 5–20% HL. Three clusters can be defined, however, with somewhat fluent limits: <10% HL (in *Spicomacrurus*, *Hymenogadus* and few *Hymenocephalus* species, i.e. *H. hachijoensis* and *H. neglectissimus*), 10–16% HL in the majority of species and higher values to 20% HL only reached in *H. aterrimus* and *H. grimaldii*. A final value of some use is the interspace between the postorbital and preopercular canal systems reaching 3–14% HL. Low values <7% HL are found in the majority of *Hymenocephalus* species and intermediate values from 6–10% HL in a second large cluster of *Hymenocephalus* species mainly of the *striatulus* and *antraeus* groups (see below). Values above 10% HL are found in *Hymenogadus* and only few *Hymenocephalus* species, such as *H. longibarbis*, *H. longipes*, *H. aterrimus*, *H. billsam* and *H. sazovovi* n.sp.

8. Integument supporters. Of the three prominent supporters associated with the canal systems, the infraorbital and the preopercular supporters show the highest degree of variance, particularly in *Hymenocephalus*. The infraorbital supporter is broad throughout its length (50–100% of OD) in *H. striatissimus* and *H. longibarbis* and related species of the two, while it is anteriorly narrowed and only posteriorly expanded (25–50% OD) or developed into an elongate narrow posterior strip in the remainder of the *Hymenocephalus* and *Hymenogadus* species. The length of the preopercular supporter ranges from barely expanded (<5% HL) in *Hymenogadus* and

TABLE 4. Key otolith morphometrics and characters of the genera *Hymenocephalus*, *Hymenogadus* and *Spicomacrus*: colliculi and collum status, OL:OH, CCL:OCL, TCL:PCL.

	colliculi status		collum status		otolith length : otolith height (OL:OH)											caudal : ostial colliculum (CCL:OCL)					total colliculi length : pseudocolliculum length (TCL:PCL)								
	separate	fused	indented	convex	0.7	0.8	0.9	1.0	1.1	1.2	1.3	1.4	1.5	1.6	1.7	1.8	1.9	1.0	1.2	1.4	1.6	1.8	2.0	2.2	2.4	2.6	2.8	7.0-12.0	
Spicomacrus																													
<i>adelscottii</i>																													
<i>dictyogadus</i>																													
<i>kuronumai</i>																													
<i>mccoskeri</i>																													
Hymenogadus																													
<i>gracilis</i>																													
<i>tenuis</i>																													
Hymenocephalus																													
<i>longibarbis</i> group																													
<i>longibarbis</i>																													
<i>longipes</i>																													
iwamotoi group																													
<i>iwamotoi</i>																													
aterrimus group																													
<i>aterrimus</i>																													
<i>barbatulus</i>																													
<i>nesaeae</i>																													
<i>papyraceus</i>																													
<i>sazonovi</i>																													
striatulus group																													
<i>billsam</i>																													
<i>lethonemus</i>																													
<i>nascens</i>																													
<i>striatulus</i>																													
antraeus group																													
<i>antraeus</i>																													
<i>hachijoensis</i>																													
<i>heterolepis</i>																													
<i>punt</i>																													
italicus group																													
<i>italicus</i>																													
striatissimus group																													
<i>aeger</i>																													
<i>megalops</i>																													
<i>striatissimus</i>																													
<i>torvus</i>																													
grimaldi group																													
<i>grimaldi</i>																													
<i>neglectissimus</i>																													
<i>semipellucidus</i>																													

many *Hymenocephalus* species related to *H. longibarbis*, *H. aterrimus*, *H. striatulus* and *H. neglectissimus* to 9–13% HL in just a few species, namely *H. iwamotoi* n.sp., *H. papyraceus* and *H. grimaldii*. The outline of the preopercular supporter shows five main shapes: 1) rounded angles rather than projecting supporters in *Spicomacrus* and *Hymenogadus gracilis*; 2) a projecting supporter with a sharp tip and a mostly well recognizable obtuse angle on the posterior margin of the supporter (*H. billsam* and related species); 3) a very short, forked supporter usually with three individual short peaks in *H. aterrimus* and *H. sazónovi* n.sp.; 4) a projecting supporter with a cut termination and a straight back margin in the majority of *Hymenocephalus* species, and 5) a thin and long supporter in *H. papyraceus* and *H. grimaldii*.

9. Otolith proportions. (otolith length to height = OL:OH) Five clusters can be observed, whereby the ones with the highest OL:OH ratio (the most high-bodied otoliths) are considered to be the most advanced. The otoliths of *Spicomacrus* are the most slender (and thin) with an OL:OH ratio of 1.5–1.9. In *Hymenogadus* the OL:OH ratio ranges from 1.35–1.65. Otoliths of the genus *Hymenocephalus* are compact, robust and high bodied. Three clusters of OL:OH ratios are observed within *Hymenocephalus*: 1.0–1.2, 0.85–1.0 and 0.7–0.85, the last cluster found in *H. grimaldii*, *H. megalops*, *H. neglectissimus* and *H. semipellucidus*.

10. Predorsal lobe of otolith. A distinct predorsal lobe is another typical character of the genera *Hymenogadus* and *Hymenocephalus*, except for *H. aterrimus* where it is low or completely reduced with the dorsal rim being evenly curved. The predorsal lobe can be broad and massive or narrow and protruding; it can be oriented straight upwards or slightly inclined anteriorly. In very compressed otoliths (*H. grimaldii*, *H. semipellucidus*) the predorsal lobe can become so massive as to almost entirely occupy the dorsal rim. In *Spicomacrus* the predorsal lobe is generally rather low and much less spectacular than in *Hymenogadus* or *Hymenocephalus*.

11. Sulcus proportions. (caudal colliculum length to ostial colliculum length = CCL:OCL) In all species of the genus *Hymenocephalus* the ostial and caudal colliculi are of about equal length (the ratio mostly varying between 0.7 and 1.2), and usually terminate at some distance from the anterior and posterior rims of the otolith. However, the ostial and caudal colliculi are fused ('not separated') in a number of species, such as *H. striatissimus* and several related species, and *H. italicus*, which prohibits calculation of the CCL:OCL ratio. In line with common observations elsewhere (Schwarzahns, 2010) the fusion of the colliculi is considered derived. In otoliths of *Hymenogadus* and *Spicomacrus* the caudal colliculum is longer than the ostial colliculum, the CCL:OCL ratio being 1.6–2.1 in *Hymenogadus* and 1.1–1.5 in *Spicomacrus*.

12. Expression of pseudocolliculum. In *Spicomacrus* and *Hymenogadus* the collum is about as wide as the height of each of the colliculi and shows a rather indistinct and short ventral pseudocolliculum. The ventral sulcus margin at the collum is indented. In *Hymenocephalus* the collum becomes gradually narrower with the approach of the colliculi until it is fused in certain species and the collum completely disappears. The pseudocolliculum is 'oversized' in all *Hymenocephalus* species extending below a good portion of the neighboring colliculi, and the ventral margin of the collum is convex. The pseudocolliculum extends in some species of *Hymenocephalus* to almost entirely underlie the colliculi, particularly in those species with fused colliculi. These represent the longest pseudocolliculum observed in any teleost otolith.

Taxonomy

Species Groups

The genus *Hymenogadus* was originally established as subgenus of *Hymenocephalus* by Gilbert & Hubbs (1920) and elevated to generic ranking by Okamura (1970), who also established *Spicomacrus* as a subgenus of *Hymenogadus*. Okamura stated that his *Hymenogadus* and *Hymenocephalus*, which he considered closely related, are "the most distinct of any in the subfamily Macrourinae, as already pointed out by Gilbert & Hubbs (1916)". Amongst the characters distinguishing these genera from the others he mentioned "the presence of peculiar ventral striae consisting of black and silvery lines alternating with each other, the elongation of the luminous organ provided with external lenses at both ends". I consider all three closely related genera valid as characterized below. With the characters defined and described above the genus *Hymenocephalus* can be conveniently subdivided into eight species groups (see also for comparison the character matrix, Table 1), which includes further characters such as barbel, gill raker counts and pectoral fin rays.

The genus *Spicomacrus* Okamura, 1970 contains four rare species in the western Pacific: *S. adelscottii* (Iwamoto & Merrett, 1997), *S. dictyogadus* Iwamoto, Shao & Ho, 2011, *S. kuronumai* (Kamohara, 1938) and *S. mccoskeri* Iwamoto, Shao & Ho, 2011. The genus is remarkable for a spectacular specialization of the nasal bones characterized by stout, large, median and lateral nasal processes forming three broad spatulate and inferior projections. It is further defined by the following combination of characters: 8–10 pelvic fin rays; orbit diameter 28–33% HL; orientation of eye axis v-shaped resulting in an interorbital width of 25–40% HW; no integument supporters developed except for a broad, rounded preopercular edge; canals covered by thick skin, not enlarged as evidenced by infraorbital, supraorbital and preopercular canal width all less than 10% HL; index OL:OH = 1.5–1.9; index CCL:OCL = 1.3–1.6; pseudocolliculum short and indistinct, ventral margin of collum indented; predorsal lobe poorly developed.

The genus *Hymenogadus* Gilbert & Hubbs, 1920 contains only two species, the cosmopolitan *H. gracilis* Gilbert & Hubbs, 1920 and *H. tenuis* (Gilbert & Hubbs, 1917) known from the unique holotype collected off Hawaii. The genus is defined by the following combination of characters: serrated first dorsal spine; 8 pelvic fin rays; head size 12–16% HL; pointed snout at 15–20% HL; orbit diameter 35–40% HL; orientation of eye axis slightly v-shaped upwards resulting in an interorbital width of 35–40% HW; preopercular integument supporter broad and short; infraorbital and preopercular canal widths less than 10% HL; index OL:OH = 1.65–1.35; index CCL:OCL = 1.8–2.5; pseudocolliculum short and indistinct, ventral margin of collum indented.

The *Hymenocephalus longibarbis* Group comprises the species *H. longibarbis* (Günther, 1887) and *H. longipes* Smith & Radcliffe, 1912. It represents the most primitive species group of the subgenus *Hymenocephalus* and is defined by the combination of the following characters: 8 pelvic fin rays; snout depressed, not significantly projecting; orbit diameter 28–33% HL; orientation of eye axis slightly v-shaped upwards resulting in an interorbital width of 40–50% HW; postorbital-preopercular interspace more than 10% HL; infraorbital supporter extending below entire orbit (>80% OD); index OL:OH = 1.0–1.2; colliculi separated; TCL:PCL = 1.8–2.2. These are all considered plesiomorphic characters within the genus, but apomorphic in respect to the out-group (*Hymenogadus*) except for the orbit diameter, the long infraorbital supporter, the index OL:OH and the expression of the pseudocolliculum. Günther (1887) established the subgenus *Mystaconurus* as a subgenus of *Macrurus* for *Macrurus (Mystaconurus) longibarbis* Günther, 1887.

The *Hymenocephalus iwamotoi* Group contains only the new species *H. iwamotoi* n.sp. from off NW Australia. It differs from the *H. longibarbis* Group in the short, blunt, not depressed snout, the larger orbit diameter (35–40% HL), the interorbital width (60–65% HW), the long preopercular supporter (7–12% HL) and the more compressed otolith (OL:OH = 1.0–0.8).

The *Hymenocephalus aterrimus* Group comprises the species *H. aterrimus* Gilbert, 1905, *H. barbatulus* Gilbert & Hubbs, 1920, *H. nesaeae* Merrett & Iwamoto, 2000, *H. papyraceus* Jordan & Gilbert, 1904 and *H. sazonomi* n.sp. Gilbert & Hubbs (1920) established the subgenus *Papyrocephalus* for the then known species of the group, with *H. aterrimus* as the type species. This species group is defined by the following combination of characters: number of pelvic fin rays 12–14, except 10–11 in *H. papyraceus* and 7 in *H. barbatulus*; head size 21–25% TL; nasal bones very weak and snout short, except pointed and projecting in *H. papyraceus*; orbit diameter 20–27% HL; infraorbital canal widened (15–25% HL); preopercular supporter short and forked in *H. aterrimus* and *H. sazonomi* n.sp.; otolith size reduced, predorsal lobe reduced in *H. aterrimus*; index OL:OH = 0.8–1.0; colliculi separated; TCL:PCL = 1.8–2.8. The species of this group occur generally deeper than those of the other species groups at depth down to 1000 m (vs predominantly between 300 and 600 m). It is assumed that the deeper habitat has triggered certain functional morphological adaptations such as the further thinning and weakening of the skull bones, the reduction of the eye size, the reduction of the otolith size (see also Wilson, 1985) and the size increase of the head canal system. In all these aspects *H. aterrimus* shows the most advanced morphology.

The *Hymenocephalus striatulus* Group contains the species *H. billsam* Marshall & Iwamoto, 1973, *H. lethonemus* Jordan & Gilbert, 1904, *H. nascens* Gilbert & Hubbs, 1920 and *H. striatulus* Gilbert, 1905. This species group is defined by the following combination of characters: 11–15 pelvic fin rays; snout pointed, projecting, 20–26% HL; orbit diameter 28–33% HL; eye advanced lateralized resulting in an interorbital width of 50–57% HW; infraorbital supporter extended only below rear part of orbit (25–50% OD); preopercular supporter with pointed tip and obtuse angle on rear margin; index OL:OH = 1.0–1.2; colliculi separated, usually rounded towards collum; TCL:PCL = 2.0–2.5; predorsal lobe narrow, across anterior half of dorsal rim only.

The *Hymenocephalus antraeus* Group comprises the species *H. antraeus* Gilbert & Cramer, 1897, *H. hachijoensis* Okamura, 1970, *H. heterolepis* (Alcock, 1889) and *H. punt* n.sp. This species group is defined by the following combination of characters: 10–12 pelvic fin rays (8 in *H. hachijoensis*); snout blunt or rounded, 15–20% HL; orbit diameter 30–40% HL; eye advanced lateralized resulting in an interorbital width of 50–65% HW; infraorbital supporter extends only below rear part of orbit (20–50% OD, up to 70% OD in *H. lethonemus*); preopercular supporter with blunt tip and straight rear margin (except with obtuse angle in *H. antraeus*); index OL:OH = 0.9–1.1; colliculi separated, usually closely placed at collum; TCL:PCL = 1.5–1.7 (1.9–2.2 in *H. punt* n.sp.); predorsal lobe broad, massive, usually extending across middle of dorsal rim. This species group is closely related to the *H. striatulus* group differing mainly in the shorter, blunter snout and in the otoliths with the more massive predorsal lobe and the longer pseudocolliculum expressed in the smaller index TCL:PCL (except *H. punt* n.sp.).

The *Hymenocephalus italicus* Group contains only the species *H. italicus* Giglioli, 1884 known from both sides of the Atlantic and the western Indian Ocean. It is considered derived from the *H. antraeus* Group differing mainly in the fused colliculi and additionally in the larger orbit diameter from *H. heterolepis* (about 35% HL vs about 30% HL), a species with which it has commonly been synonymized.

The *Hymenocephalus striatissimus* Group contains the species *H. aeger* Gilbert & Hubbs, 1920, *H. megalops* Iwamoto & Merrett, 1997, *H. striatissimus* Jordan & Gilbert, 1904 and *H. torvus* Smith & Radcliffe, 1912. This species group is defined by the following combination of characters: 7–8 pelvic fin rays; snout blunt, 10–18% HL; orbit diameter mostly 34–42% HL, 40–45 (48)% HL in *H. megalops*; postorbital-preopercular interspace narrow, <7% HL; infraorbital supporter extended below larger part to entire length of orbit (60–90% OD); preopercular supporter with blunt tip and straight rear margin index; OL:OH = 0.8–1.0; colliculi fused; TCL:PCL = 1.3–1.4; predorsal lobe very broad and large.

The *Hymenocephalus grimaldii* Group comprises the species *H. grimaldii* Weber, 1913, *H. neglectissimus* Sazonov & Iwamoto, 1992 and *H. semipellucidus* Sazonov & Iwamoto, 1992. This species group is defined by the following combination of characters: 8 pelvic fin rays; snout blunt, 10–22% HL; orbit diameter 37–50 (55)% HL; infraorbital width very narrow in *H. neglectissimus* and *H. semipellucidus* (<10% HL); preopercular supporter very elongate and narrow in *H. grimaldii* (8–13% HL); index OL:OH = 0.65–0.85; colliculi fused; TCL:PCL = 1.2–1.3; predorsal lobe broad, occupying nearly the entire dorsal rim, sometimes reduced in height.

Key to the species of *Hymenocephalus*, *Hymenogadus* and *Spicomacrurus*

The following key considers mainly characters shown in Tables 1–3, plus a number of more descriptive features. Additional characters have been used in other published keys, for instance in Cohen *et al.* (1990) or Iwamoto *et al.* (2011), which are not incorporated in this key and might be considered as complementary.

1a	Head with large nasal bones with stout, median, lateral, often spatulate processes; cephalic canals under thick skin (<i>Spicomacrurus</i>)	2
1b	Head with soft, non-spatulate nose flaps; extensive cephalic canal system with thin integument cover	5
2a	Lateral nasal processes short, not spatulate; snout <20% HL	<i>Spicomacrurus dictyogadus</i>
2b	Lateral nasal processes extensive, spatulate; snout 20–30% HL	3
3a	Interorbital width 25% HW; nasal bones broadly separated by rostral cartilage	<i>Spicomacrurus mccoskeri</i>
3b	Interorbital width 35–40% HW; nasal bones closely adjoining along mesial edge	4
4a	Snout 20% HL; OL:OH = 1.4–1.6	<i>Spicomacrurus kuronumai</i>
4b	Snout 26% HL; OL:OH = 1.8	<i>Spicomacrurus adelscottii</i>
5a	Pelvic fin rays 7–9	6
5b	Pelvic fin rays 10–15	19
6a	Denticles present on first dorsal spine; ventral striae not joined mesially behind pelvic fins; precaudal vertebrae 11–12; otolith with indented collum and very short pseudocolliculum (TCL:PCL >7), CCL:OCL = 1.6–2.0 (otolith of <i>Hymenogadus tenuis</i> not studied) (<i>Hymenogadus</i>)	7
6b	No denticles on first dorsal spine; ventral striae joined mesial behind pelvic fins; precaudal vertebrae 10; otolith with convex collum, TCL:PCL <3, CCL:OCL = 0.7–1.3 (otolith of <i>Hymenocephalus barbatulus</i> not studied)	8
7a	Pectoral fin rays 14–17; gill rakers on inner face of 2 nd arch 13–19; barbel 27–33% HL	<i>Hymenogadus gracilis</i>
7b	Pectoral fin rays 12; gill rakers on inner face of 2 nd arch 10; barbel 12% HL	<i>Hymenogadus tenuis</i>
8a	Barbel long, reaching to rear end of vertical through orbit, 40–60% HL	9
8b	Barbel reaching maximally to vertical through center of orbit, <35% HL, or absent	10

9a	Orbit diameter 30–33% HL; interorbital width 45–48% HW; OL:OH = 1.1–1.3	<i>Hymenocephalus longibarbis</i>
9b	Orbit diameter 35–38% HL; interorbital width 65% HW; OL:OH <1.0	<i>Hymenocephalus iwamotoi</i>
10a	Orbit diameter <23% HL; snout length >20% HL	<i>Hymenocephalus barbatus</i>
10b	Orbit diameter >28% HL; snout length <20% HL (up to 22% HL in <i>H. grimaldii</i>)	11
11a	Barbel absent	12
11b	Barbel present, at least 10% HL	13
12a	Pectoral fin rays 9–12; pelvic fin not colored; orbit diameter 34–38% HL; interorbital width 70–80% HW; preopercular supporter long, narrow; OL:OH = 0.75–0.8, colliculi fused, TCL:PCL = 1.15–1.25	<i>Hymenocephalus grimaldii</i>
12b	Pectoral fin rays 13–15; pelvic fin black tipped; orbit diameter 28–33% HL; interorbital width 40–50% HW; preopercular supporter broad, short; OL:OH = 1.1–1.25, colliculi separate, TCL:PCL = 1.7–2.1	<i>Hymenocephalus longipes</i>
13a	Barbel reaching to vertical through center of orbit, 30–35% HL; colliculi separate	<i>Hymenocephalus hachijoensis</i>
13b	Barbel reaching vertical through anterior rim of orbit, 10–25% HL; colliculi fused	14
14a	Orbit diameter 40–50% HL; interorbital width 40–55% HW	15
14b	Orbit diameter 33–42% HL; interorbital width 60–70% HW	17
15a	Dark colored blotch on nape extending backwards beyond pectoral fin tips, with fading contours; ventral striae reaching to about ½ of distance from pelvic bases to periproct; pectoral fin rays 15–19	<i>Hymenocephalus semipellucidus</i>
15b	Dark colored blotch on nape not extending beyond pectoral fin tips, with sharp contours; ventral striae reaching to about ⅔ to full distance from pelvic bases to periproct; pectoral fin rays 13–15	16
16a	Snout 10–15% HL; infraorbital width 5–8% HL; otolith with narrow, pointed predorsal lobe	<i>Hymenocephalus neglectissimus</i>
16b	Snout 14–18% HL; infraorbital width 10–12% HL; otolith with broad predorsal lobe	<i>Hymenocephalus megalops</i>
17a	Barbel 20–25% HL; OL:OH = 0.9–1.0	<i>Hymenocephalus aeger</i>
17b	Barbel 10–20% HL; OL:OH = 0.8–0.9	18
18a	Pelvic fin rays 7, rarely 8; pectoral fin rays 12–14; snout 15–20% HL	<i>Hymenocephalus torvus</i>
18b	Pelvic fin rays 8; pectoral fin rays 14–17; snout 10–14% HL	<i>Hymenocephalus striatissimus</i>
19a	Orbit diameter 20–27% HL; head size 21–25% TL; infraorbital width 16–25% HL	20
19b	Orbit diameter 28–40% HL; head size 15–20% TL; infraorbital width 5–17% HL	23
20a	Pelvic fin rays 10–11; pectoral fin rays 16–18; minute barbel present	<i>Hymenocephalus papyraceus</i>
20b	Pelvic fin rays 12–14; pectoral fin rays 13–16; barbel absent	21
21a	Snout 25–30% HL; infraorbital width 16–17% HL	<i>Hymenocephalus nesaeae</i>
21b	Snout 20–24% HL; infraorbital width 20–25% HL	22
22a	Gill rakers inner side 2 nd arch 21–25; OL:OH = 1.0–1.2, TCL:PCL = 2.2–2.8	<i>Hymenocephalus aterrimus</i>
22b	Gill rakers inner side 2 nd arch 18–20; OL:OH = 0.8, TCL:PCL = 1.8	<i>Hymenocephalus sazónovi</i>
23a	Orbit diameter 28–33% HL	24
23b	Orbit diameter 35–40% HL	30
24a	Barbel absent or rudimentary (<5% HL); snout 20–26% HL	25
24b	Barbel present (3–15% HL); snout 17–20% HL	28
25a	Pelvic fin rays 14–15; OL:OH = 0.9–1.0	<i>Hymenocephalus striatulus</i>
25b	Pelvic fin rays 11–13 (except 13–14 in <i>H. billsam</i>); OL:OH = 1.05–1.2	26
26a	Barbel rudimentary (3–5% HL); otolith TCL:PCL = 2.6–2.8	<i>Hymenocephalus billsam</i>
26b	Barbel absent (rarely base visible); otolith TCL:PCL = 1.8–2.6	27
27a	Pelvic fin rays usually 11, rarely 12; OL:OH = 1.05–1.1	<i>Hymenocephalus lethonemus</i>
27b	Pelvic fin rays 12–13, rarely 11; OL:OH = 1.1–1.2	<i>Hymenocephalus nascens</i>
28a	Pelvic fin rays 13–14, rarely 12	<i>Hymenocephalus billsam</i>
28b	Pelvic fin rays 10–12	29
29a	Barbel reaching vertical through anterior rim of orbit (11–15% HL); pectoral fin rays 14–15, rarely 13; ventral striae reaching to about ⅓ to ½ of distance from pelvic bases to periproct; OL:OH = 1.0–1.05, TCL = PCL = 1.9–2.2	<i>Hymenocephalus punt</i>
29b	Barbel not reaching vertical through anterior rim of orbit (5–10% HL); pectoral fin rays 11–13; ventral striae reaching to about ⅔ of distance from pelvic bases to periproct; OL:OH = 0.9–0.95, TCL = PCL = 1.5–1.7	<i>Hymenocephalus heterolepis</i>
30a	Barbel minute (<5% HL); otolith with separate colliculi	<i>Hymenocephalus antraeus</i>
30b	Barbel short (7–12% HL); otolith with fused colliculi	<i>Hymenocephalus italicus</i>

Species Descriptions

Spicomacrus Okamura, 1970

Spicomacrus Okamura 1970: 63, as subgenus of *Hymenogadus* Gilbert & Hubbs, 1920, type species by original designation

Hymenocephalus kuronumai Kamohara, 1938.

Hymenocephalus (*Spicomacrus*): Iwamoto & Merrett 1997: 514.

Spicomacrus: Iwamoto, Shao & Ho, 2011: 514.

Diagnosis. Modified from Iwamoto *et al.* (2011) Leading spine of dorsal fin smooth. Ventral striae consisting of fine parallel lines of dark, alternating with silvery pigment associated with light-producing function on abdominal wall, parts of chest, and shoulder girdle, not joint at median line behind pelvic fin bases. Head not cavernous. Nasal bones forming broad, horizontal, lateral, and medial plate-like processes; nasal bones of both sides in broad contact (two species), or widely separated by rostral cartilage (two species). Gill rakers 9–15. Additional diagnostic features from otolith morphology are: Elongate shape of otoliths (OL:OH = 1.45–1.95); otoliths thin due to slightly concave outer face; relatively low and short predorsal lobe; ventral sulcus margin at collum indented; pseudocolliculum indistinct, short.

Comparison. *Spicomacrurus* is remarkable for the spectacular specialization of its broad spatulate nasal bones (see above). It further differs from the related genera *Hymenogadus* and *Hymenocephalus* by the lack of the cavernous cephalic canal system covered by thin skin (integument). It shares with *Hymenogadus* the short ventral striae, which are not joined along the mesial line behind the pelvic fin bases, and the rather slender otoliths with the narrow, ventrally indented collum and the short pseudocolliculum.

Species. Four species, all from the western Pacific, *S. adelscottii*, *S. dyctiogadus*, *S. kuronumai* and *S. mccoskeri*.

***Spicomacrurus adelscottii* (Iwamoto & Merrett, 1997)**

Figs. 3C–D, 4A–B, 5

Hymenocephalus (Spicomacrurus) adelscottii Iwamoto & Merrett, 1997: 514 (type locality: 11°54'S, 179°31'W); Iwamoto & Williams, 1999: 176.

Material examined. 1 specimen WAM P.28073-004, 154+ mm TL, 17°45'S, 118°32'E, 600–690 m.

Diagnosis. Pelvic fin rays 9; nasal bones closely adjoining along mesial edges, forming three horizontal plate-like processes; OL:OH = 1.75.

Comparison. *Spicomacrurus adelscottii* most closely resembles *S. kuronumai*, differing in the number of pelvic fin rays (9 vs 8), the more elongate head shape (head length : height = 2.1 vs 1.7) and the more elongate otolith (OL:OH = 1.75 vs 1.45–1.6). The occiput does not show any relict of scales or scale pockets as do the studied specimens of *S. kuronumai*.

Description. Head morphology (Figs. 3C–D): Head length to height about 2.1 with relatively firm head bones and platy spatulate nasal bones closely adjoining along mesial edges. No indication of scales on head. Snout length 26% HL, orbit diameter 29% HL, interorbital width 40% HW. Barbel 18% HL, reaching vertical through center of orbit. Infraorbital, supraorbital and preopercular canal systems narrow with widths <8% HL, covered by rather thick, firm skin. One small pore visible in anterior section of infraorbital skin. Preopercular angle broad, not projecting.

Otolith morphology (Fig. 4A–B): Thin, elongate otoliths with slightly convex inner and slightly concave outer face. OL:OH = 1.75; OH:OT = 4. Predorsal lobe moderately developed, narrow; ventral rim shallow; anterior tip blunt, posterior tip moderately pointed. Sulcus slightly suprmedian with narrow, ventrally-indented collum. Colliculi large, reaching close to anterior and posterior rims of otolith, caudal colliculum about 1½ times the length of ostial colliculum; pseudocolliculum indistinct, short; TCL:PCL = 9. Dorsal depression large; ventral furrow distinct, turning upwards and away from ventral rim posteriorly.

Distribution. (Fig. 5) Known from only two specimens, the holotype off northern Fiji, and the examined specimen from off Western Australia.

***Spicomacrurus dictyogadus* Iwamoto, Shao & Ho, 2011**

Figs. 3A–B, 5

Spicomacrurus dictyogadus Iwamoto, Shao & Ho, 2011: 518 (type locality: 16°18'S, 167°46'E).

Discussion. The unique holotype of *S. dictyogadus* (MNHN 2009-1455) was visually inspected, but no otolith was extracted and no additional observations were made to the description of Iwamoto *et al.* (2011), and the figure

included is based on their detailed photographs. The species is remarkable for its blunter head profile with barely protruding, short and not spatulate nasal bones, characters which are considered plesiomorphic in respect to the other members of the genus.

***Spicomacrus kuronumai* (Kamohara, 1938)**

Figs. 3E–F, 4E–G, 5

Hymenocephalus kuronumai Kamohara, 1938: 70 (type locality: Tosa Bay).

Hymenogadus (Spicomacrus) kuronumai: Okamura, 1970: 64.

Spicomacrus kuronumai: Iwamoto, Shao & Ho, 2011: 515.

Material examined. 2 specimens; 1 specimen NSMT 46796, 164 mm TL, 34°57'N, 138°43'E, 315–500m; 1 specimen NSMT 103488, 157 mm TL, 31°29–32'N, 128°30–31'E, 550–596 m.

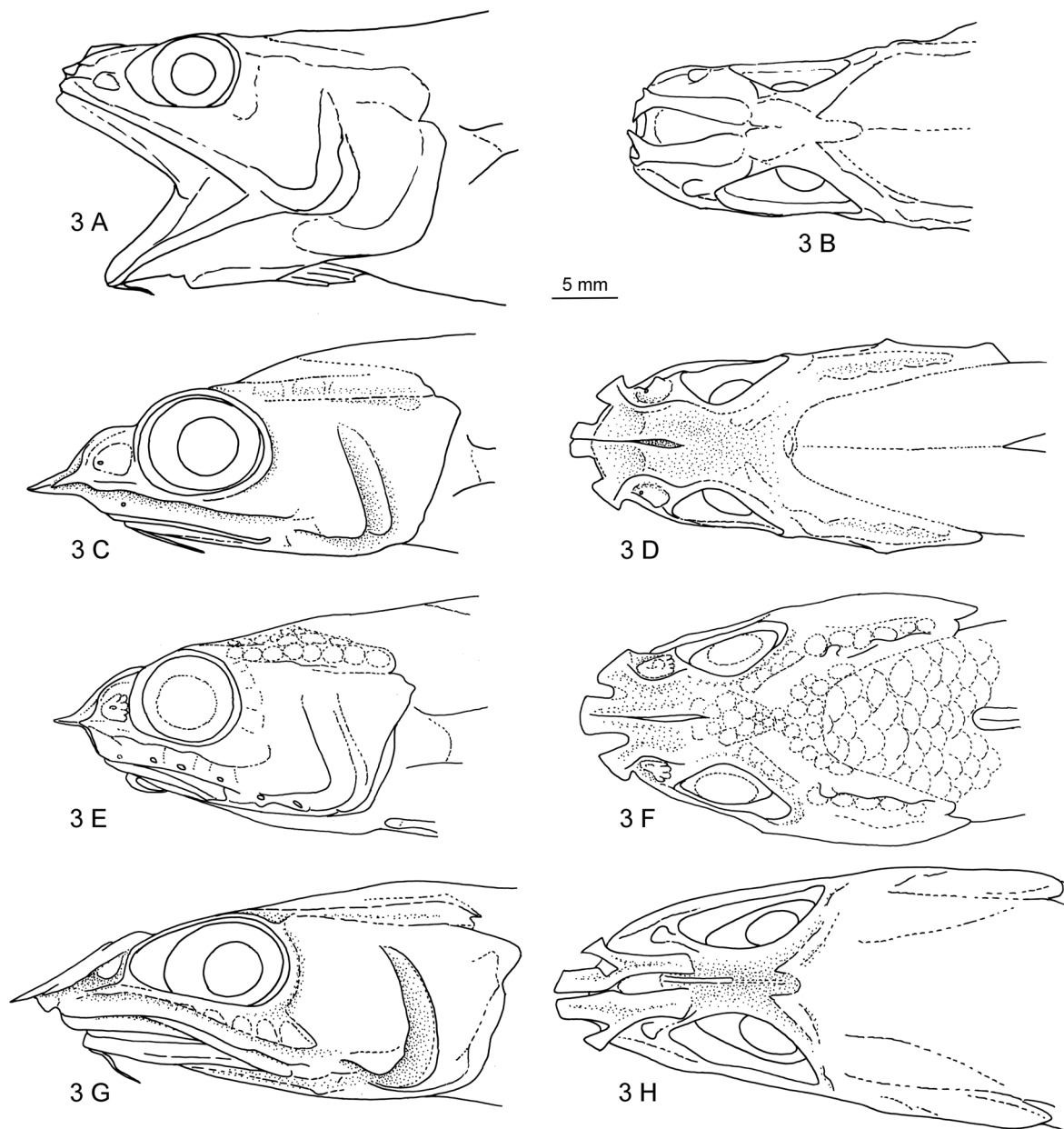


FIGURE 3. Heads of the species of *Spicomacrus*: A–B—*Spicomacrus dictyogadus*, holotype, MNHN 2009-1455, redrawn from Iwamoto, Shao & Ho (2011), A—Lateral view, B—Dorsal view. C–D—*Spicomacrus adelscottii*, WAM P.28073-004, C—Lateral view, D—Dorsal view. E–F—*Spicomacrus kuronumai*, E—Lateral view, NSMT P46796, F—Dorsal view, NSMT P103488. G–H—*Spicomacrus mccoskeri*, MNHN 1994-0881, G—Lateral view, H—Dorsal view.

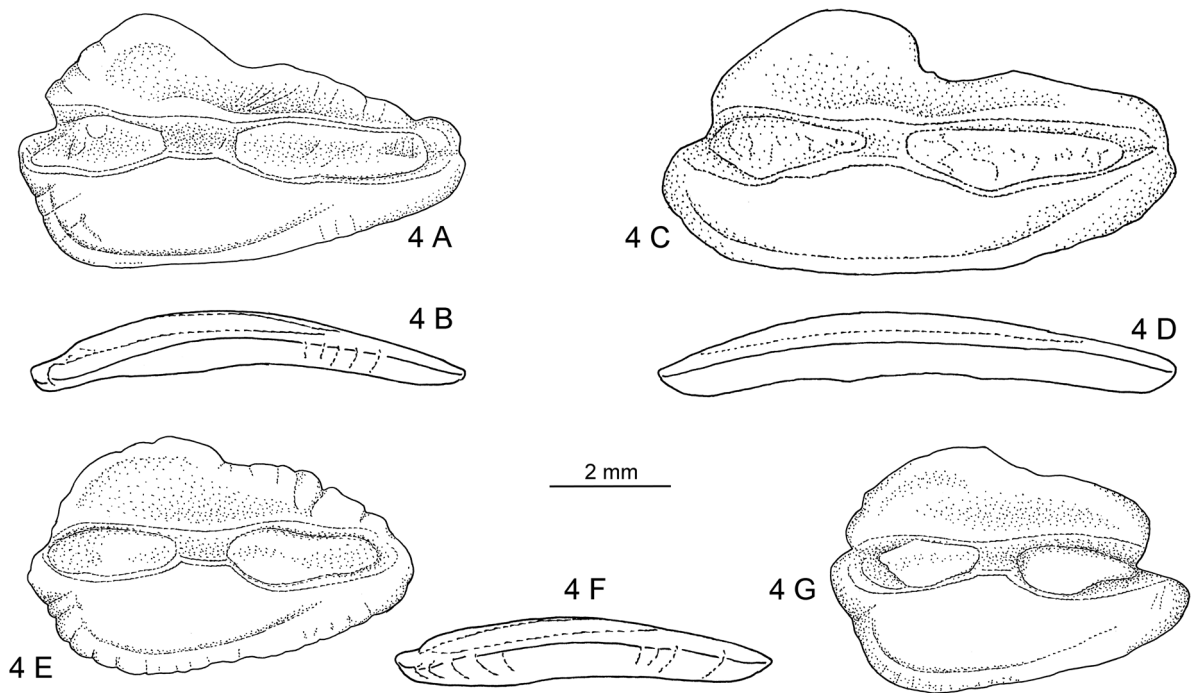


FIGURE 4. Otoliths of the species of *Spicomacrurus*: A–B—*Spicomacrurus adelscottii*, WAM P.28073-004, A—Inner face, B—Ventral view. C–D—*Spicomacrurus mccoskeri*, MNHN 1994-0881, C—Inner face, D—Ventral view. E–G—*Spicomacrurus kuronumai*, E–F—NSMT P46796, E—Inner face, F—Ventral view, G—NSMT P103488, inner face.

Diagnosis. Pelvic fin rays 8; nasal bones closely adjoining along mesial edges, forming three horizontal plate like processes; OL:OH = 1.45–1.6.

Comparison. For distinction from *S. adelscottii* see above. *Spicomacrurus kuronumai* also resembles *S. mccoskeri*, from which it differs in the number of pelvic fin rays (8 vs 9), the robust head shape (head length : height = 1.7 vs 2.3) and the more compressed otolith (OL:OH = 1.45–1.6 vs 1.95). *Spicomacrurus kuronumai* shows scale pockets on the occiput, a character otherwise only shared with *S. dictyogadus*.

Description. Head morphology (Figs. 3E–F): Head length to height about 1.7 with relatively firm head bones and platy spatulate nasal bones closely adjoining along mesial edges. Scales or scale pockets present on occiput in small patches behind nasal bones and in front of nape and in a row covering the skin over the supraorbital canal. Snout length 20% HL, orbit diameter 30–33% HL, interorbital width 35% HW. Barbel 15% HL, reaching vertical through center of orbit. Infraorbital, supraorbital and preopercular canal systems narrow with widths <10% HL, covered by rather thick, firm skin. Few small pores visible in skin of infraorbital and in posterior mandibular positions. Preopercular angle broad, not projecting.

Otolith morphology (Figs. 4E–G): Thin and moderately elongate otoliths with slightly convex inner and flat outer face. OL:OH = 1.45–1.6; OH:OT = 6. Predorsal lobe low, rather indistinct; ventral rim similarly deep; anterior tip blunt, posterior tip rounded. Rims often somewhat ornamented; postdorsal section deeply indented in one specimen (Fig. 4G). Sulcus slightly suprmedian with narrow, ventrally indented collum. Colliculi large, reaching close to anterior and posterior rims of otolith, caudal colliculum only slightly longer than ostial colliculum (CCL:OCL = 1.0–1.2); pseudocolliculum indistinct, short; TCL:PCL = 7–8. Dorsal depression large; ventral furrow distinct, turning upwards and away from ventral rim posteriorly.

Distribution. (Fig. 5) Off southeastern Japan (Okamura, 1970) to northern Taiwan (Iwamoto *et al.*, 2011).

Spicomacrurus mccoskeri Iwamoto, Shao & Ho, 2011

Figs. 3G–H, 4C–D, 5

Spicomacrurus mccoskeri Iwamoto, Shao & Ho, 2011: 523 (type locality: 19°45'S, 158°45'E).

Material examined. 1 specimen MNHN 1994-0881 (paratype), 173+ mm TL, 19°43'S, 158°48'E, 710 m.

Diagnosis. Pelvic fin rays 9; nasal bones broadly separated by rostral cartilage, forming three horizontal plate like processes; barbel short, 12% HL, reaching only to vertical through anterior part of orbit; interorbital width narrow, 25% HW; OL:OH = 1.95.

Comparison. *Spicomacrurus mccoskeri* is readily recognized by the slender head (head length : height = 2.3), the narrow interorbital width (25% HW), the broad rostral cartilage, which it shares with *S. dictyogadus* and the elongate otolith (OL:OH = 1.95).

Description. Head morphology (Fig. 3G–H): Head length to height about 2.3 with relatively firm head bones and platy spatulate nasal bones mesial separated by rostral cartilage. No scale pockets visible on head. Snout length 25% HL, orbit diameter 30% HL, interorbital width 25% HW. Barbel 12% HL, reaching vertical through anterior part of orbit. Infraorbital, supraorbital and preopercular canal systems narrow with widths <10% HL, covered by rather thick, firm skin. Infraorbital supporter visible through skin cover. No pores visible. Preopercular angle broad, slightly expanded.

Otolith morphology (Fig. 4C–D): Thin and very elongate otoliths with slightly convex inner and slightly concave outer face. OL:OH = 1.95; OH:OT = 4. Predorsal lobe moderately developed, narrow; ventral rim shallow; anterior tip blunt, posterior tip moderately pointed. Sulcus slightly suprmedian with narrow, ventrally indented collum. Colliculi large, reaching close to anterior and posterior rims of otolith, caudal colliculum slightly longer than ostial colliculum (CCL:OCL = 1.3); pseudocolliculum indistinct, short; TCL:PCL = 12. Dorsal depression large; ventral furrow distinct, posteriorly reaching towards tip of caudal colliculum.

Distribution. (Fig. 5) Known only from off the Chesterfield Plateau, Coral Sea.

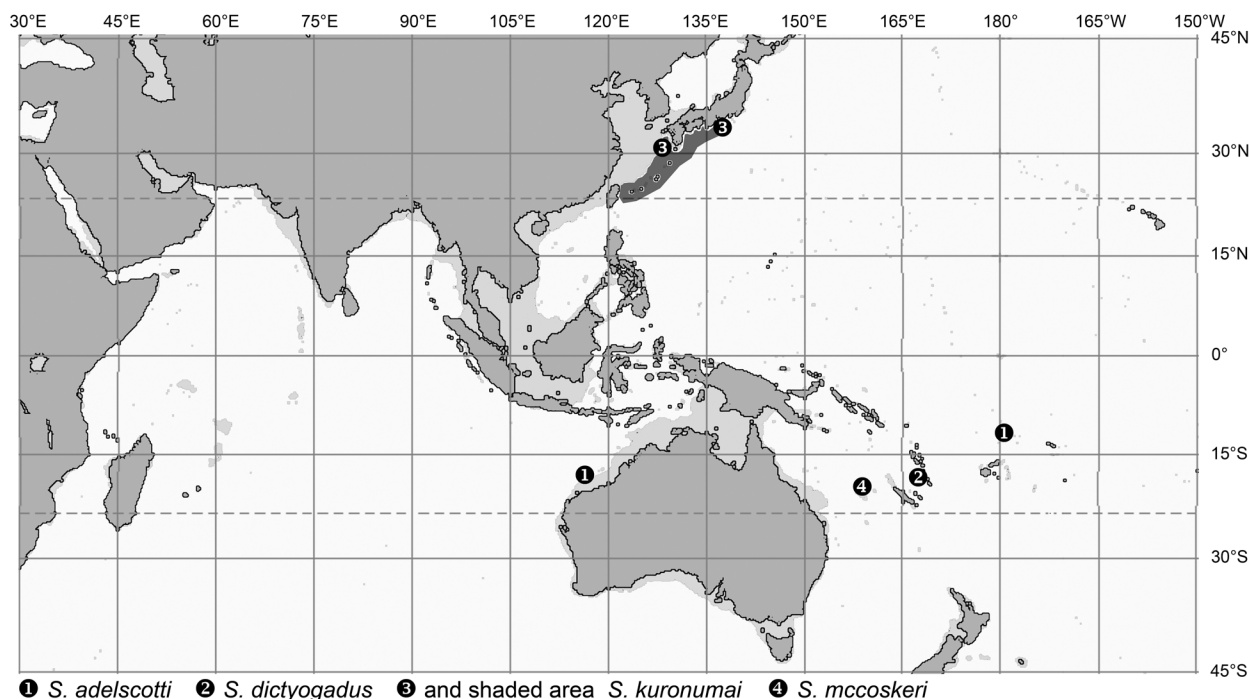


FIGURE 5. Geographical distribution of the species of *Spicomacrurus*.

Hymenogadus Gilbert & Hubbs, 1920

Hymenogadus Gilbert & Hubbs, 1920: 521, as subgenus of *Hymenocephalus* Giglioli, 1884, type species by original designation *Hymenocephalus gracilis* Gilbert & Hubbs, 1920.

Hymenogadus: Okamura, 1970: 58.

Hymenocephalus: Marshall & Iwamoto, 1973: 602; Sazonov & Iwamoto, 1992: 55; Iwamoto & Merrett, 1997: 518.

Diagnosis. Modified from Okamura (1970). First spine of dorsal fin serrated. Ventral striae consisting of fine parallel lines of dark, alternating with silvery pigment associated with a light-producing function on abdominal

wall, parts of chest, and shoulder girdle, not joint at median line behind pelvic fin bases. Head cavernous, with moderately thin skin cover. Median and lateral processes of snout sharply pointed, not plate-like. Gill rakers 10–19. Additional diagnostic features from axial skeleton and head morphology are: 11–12 precaudal vertebrae (based on radiographs). Widening of sensory canal systems on head; development of incipient infranasal, infraorbital and preopercular supporters; *Hymenocephalus*-like snout with broad, blunt, soft tip. Additional diagnostic features from otolith morphology are: Moderately elongate shape of otoliths (OL:OH = 1.25–1.55); elevated, but short predorsal lobe; ventral sulcus margin at collum indented; pseudocolliculum indistinct, short.

Comparison. *Hymenogadus* resembles *Spicomacrus* in a number of aspects, such as body shape, extent of ventral striae not joined behind the pelvic fin bases, otolith with an indented ventral sulcus margin at the collum, and short, indistinct pseudocolliculum. Certain other characters remind of the status seen in *Hymenocephalus*, such as the widening of the sensory canal system on the head, albeit covered by a thicker more robust skin than in *Hymenocephalus*, the lack of the spatulate nasal bones, the incipient developments of infranasal, infraorbital and preopercular supporters and the expanded, though short predorsal lobe in the otoliths.

Species. Two species, one nearly cosmopolitan (*H. gracilis*), except for Hawaii, where it is replaced by the second, probably endemic species (*H. tenuis*).

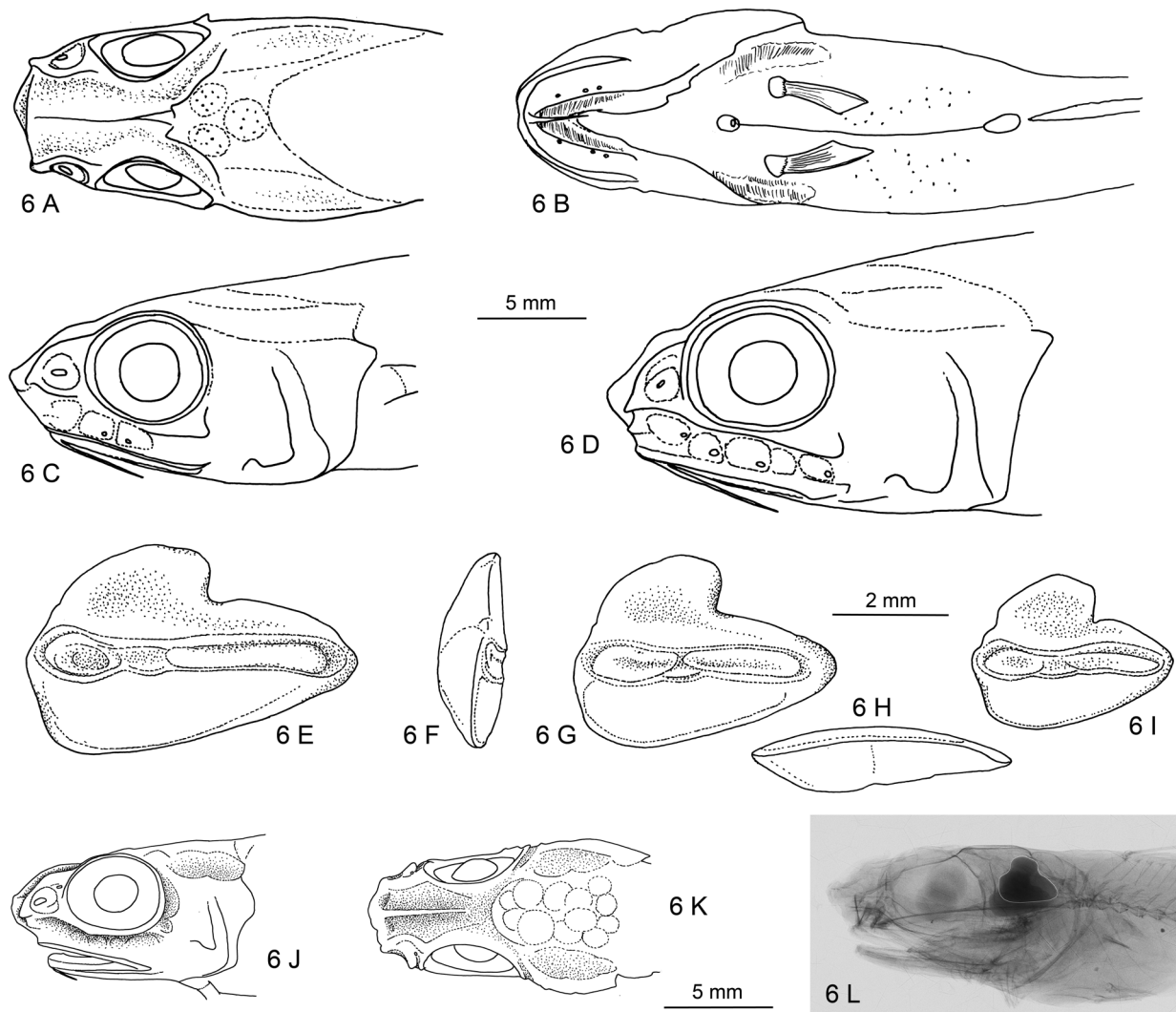


FIGURE 6. Heads and otoliths of the species of *Hymenogadus*: A–I—*Hymenogadus gracilis*, A–D—ZMH 11113, A—Dorsal view of head, B—Ventral view of head and trunk, C–D—Lateral views of head, E—Inner face of otolith, coll. Schwarzhans (leg. IRSNB), F–H—USNM 131873, F—Anterior view of otolith, G—Inner face of otolith, H—Ventral view of otolith, I—ZMH 107658, inner face of otolith. J–L—*Hymenogadus tenuis*, holotype, J—Lateral view of head, K—Dorsal view of head, L—Radiograph of head depicting otolith.

***Hymenogadus gracilis* (Gilbert & Hubbs, 1920)**

Figs. 6A–I, 7

Hymenocephalus (Hymenogadus) gracilis Gilbert & Hubbs, 1920: 522 (type locality: Philippines, off southern Luzon).

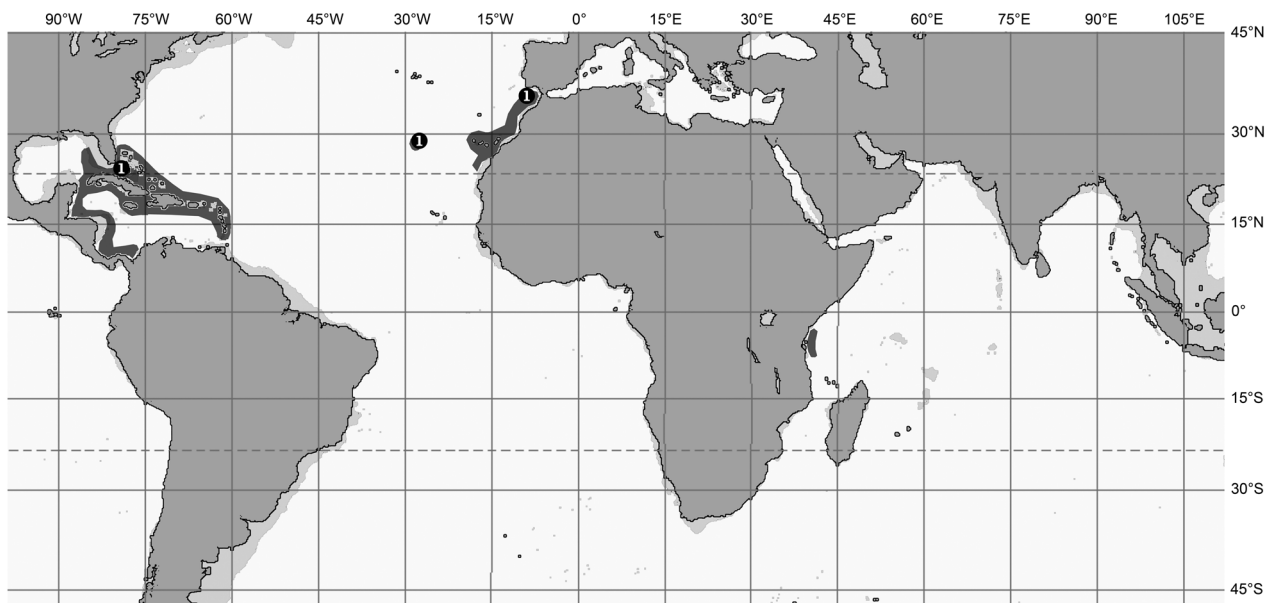
Hymenogadus gracilis: Okamura, 1970: 61.

Hymenocephalus (Hymenogadus) gracilis: Marshall & Iwamoto, 1973: 602; Sazonov & Iwamoto, 1992: 55; Iwamoto & Merrett, 1997: 518.

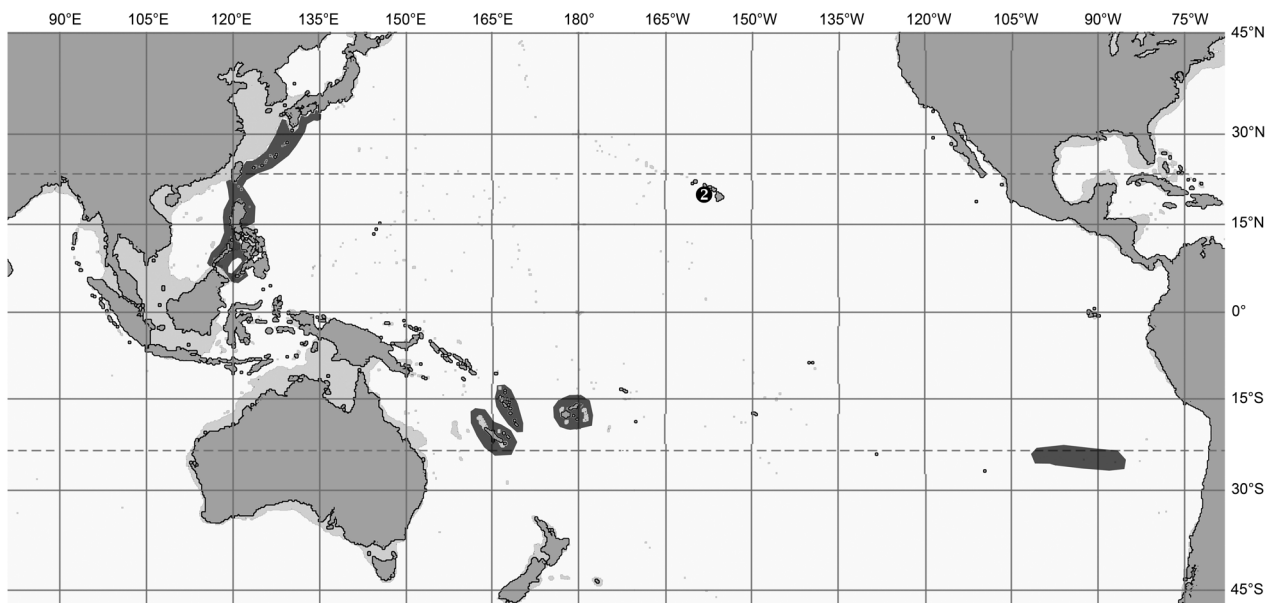
Material examined. 12 specimens; 2 specimens ZMH 107658, 53 and 65 mm TL, Great Meteor Bank, 30°00'N, 28°30'W, 300 m; 8 specimens ZMH 111113, 34°N, 07°W; 1 specimen USNM 131873, 27°22'N, 78°07'W, 0–618 m; 1 specimen (otolith only), off Morocco, coll. IRSNB (courtesy D. Nolf).

Diagnosis. Pelvic fin rays 8; pectoral fin rays 14–17; barbel long, 27–33% HL, reaching vertical through center of orbit; gill rakers 13–19; OL:OH = 1.25–1.55, increasing with size.

Comparison. *Hymenogadus gracilis* is very similar to *H. tenuis*, differing in the longer barbel (27–33% vs 12% HL), the higher number of pectoral fin rays (14–17 vs 12) and the higher number of gill rakers (13–19 vs 10).



1 and shaded area *H. gracilis*



1 and shaded area *H. gracilis* 2 *H. tenuis*

FIGURE 7. Geographical distribution of the species of *Hymenogadus*.

Description. Head morphology (n = 2) (Fig. 6A–D): Head slender with projecting, broad, soft-tipped snout. No scale pockets visible on head, but present on nape. Snout length 17–20% HL, orbit diameter 35–38% HL, interorbital width 35–40% HW. Barbel 27–33% HL, reaching vertical through center of orbit or slightly further, but not to rear margin of orbit. Frontal, infraorbital, supraorbital and postorbital canals widened (infraorbital, supraorbital and postorbital widths 7–12% HL), covered by thin, but often well-preserved skin; preopercular and supratemporal canals fully skin covered and indistinct. Infranasal supporter small; infraorbital supporter narrow, extended and slightly expanded below and behind rear part of orbit, 30–50% OD; preopercular supporter broad, short (<3% HL). Few small pores visible in infraorbital skin.

Otolith morphology (n = 4) (Figs. 6E–I): Moderately thick, elongate otoliths with slightly convex inner and outer faces, the latter thickest opposite to ostium on inner face. OL:OH = 1.25–1.55, increasing with size; OH:OT = 3. Predorsal lobe expanded, somewhat posteriorly inclined, reaching to about mid-point of dorsal rim and there terminating in a sharp notch; ventral rim shallow; anterior tip rounded, posterior tip pointed. Sulcus median with narrow sulcus and narrow, ventrally indented collum. Colliculi large, reaching close to anterior and posterior rims of otolith, caudal colliculum longer than ostial colliculum (CCL:OCL = 1.6–2.1); pseudocolliculum indistinct, short; TCL:PCL = 7–10. Dorsal depression small, indistinct; ventral furrow thin, running very close to ventral rim of otolith.

Distribution. (Fig. 7) *Hymenogadus gracilis* is a notably widespread species in the North Atlantic and the Indo West-Pacific from off East Africa to Japan and the Sala-y-Gomez Ridge in the southeastern Pacific at 300–450 m water depth according to Iwamoto & Merrett (1997), but excluding the Hawaiian Islands.

***Hymenogadus tenuis* (Gilbert & Hubbs, 1917)**

Figs. 6J–L, 7

Hymenocephalus tenuis Gilbert & Hubbs, 1917: 173 (type locality: Hawaii, off southern Oahu).

Material examined. The unique holotype: USNM 78177, 75 mm TL, south coast of Oahu, Hawaii, 485–512 m, Albatross, 5 June 1902.

Diagnosis. Pelvic fin rays 8; pectoral fin rays 12; barbel short, 12% HL, reaching vertical through anterior edge of orbit; gill rakers 10; OL:OH = 1.3, from x-ray.

Comparison. See *H. gracilis*.

Description. Head morphology (Fig. 6J–K): Head slender with projecting, broad, soft-tipped snout. No scale pockets visible on head, but present on nape. Snout length 20% HL, orbit diameter 38% HL, interorbital width 40% HW. Barbel 12% HL, reaching vertical through anterior edge of orbit. Frontal, infraorbital, supraorbital and postorbital canals widened (infraorbital, supraorbital and postorbital widths 5–12% HL), covered by thin, but mostly preserved skin; preopercular and supratemporal canals fully skin covered and indistinct. Infranasal supporter small; infraorbital supporter narrow, not expanded below rear part of orbit; preopercular supporter narrow, pointed, short, 4% HL. No pores visible.

Otolith morphology (Fig. 6L): No otolith was extracted from the unique holotype, but a high quality x-ray shows an otolith with a very similar outline and similar proportions (OL:OH = 1.3) to those of *H. gracilis*, but seemingly with a more symmetrical and not-inclined predorsal lobe.

Distribution (Fig. 7). Apparently endemic to Hawaii.

***Hymenocephalus* Giglioli, 1884**

Hymenocephalus Giglioli, 1884: 228, type species by original designation *Hymenocephalus italicus* Giglioli, 1884.

Mystacourus Günther, 1887: 124, as a subgenus of *Macrurus* (correct *Macrourus*) Bloch, 1786, type species by original designation *Macrurus (Mystacourus) longibarbis* Günther, 1887.

Papyrocephalus Gilbert & Hubbs, 1920: 539, as a subgenus of *Hymenocephalus* Giglioli, 1884, type species by original designation *Hymenocephalus aterrimus* Gilbert, 1905.

Diagnosis. Modified from Cohen *et al.* (1990): Leading spine of dorsal fin not serrated. Ventral striae consisting of fine parallel lines of dark, alternating with silvery pigment associated with a light-producing function on abdominal wall, parts of chest, and shoulder girdle, and joining at median line behind pelvic fin bases. Head cavernous with

thin, membranous skin cover. Median and lateral processes of snout variably pointed or blunt, weak, often flexible. Gill rakers 15–29. Additional diagnostic features from axial skeleton and head morphology are: 10 precaudal vertebrae (based on radiographs); well-developed infranasal, infraorbital and preopercular supporters; snout broad, usually projecting, with soft tip. Additional diagnostic features from otolith morphology are: large, high-bodied, compressed otoliths (OL:OH=0.75–1.3); large to very large, massive predorsal lobe; ventral sulcus margin at collum convex; pseudocolliculum distinct, long to very long, extending forward and backward below colliculi.

Comparison. *Hymenocephalus* resembles *Hymenogadus* in many aspects, and it appears as if several of its morphological features have been taken to the extremes, particularly when concerning head and otolith morphology. Differences are (*Hymenocephalus* first) wide head canal system with thin integument cover which is rarely preserved (vs head canal system less widened and covered by thin, but usually sufficiently robust skin to be preserved), well-developed infranasal, infraorbital and preopercular supporters (vs incipient development), ventral striae joined behind the pelvic fin bases (vs not joined), otoliths compressed (OL:OH = 0.75–1.3 vs 1.25–1.55), with convex ventral sulcus margin at collum (vs indented) and long to very long pseudocolliculum (TCL:PCL = 1.15–2.8 vs 7.0–10.0). I consider *Hymenocephalus* as derived from near *Hymenogadus* with the latter representing a plesiomorphic sister group to *Hymenocephalus*, while *Spicomacrurus* in this concept would represent a different lineage of specialization distinct from the other two genera.

Species. Including the three new species described in the following, the synonymization of *H. longiceps* with *H. longibarbis* and the upgrading of former subspecies of *H. striatissimus* to species rank as proposed here, the genus now contains 24 species considered valid. There are, however, indications of at least two further undescribed species to be expected in the genus subject to more material becoming available and also subject to statistical reviews or application of other methods such as DNA-analyses. The species considered valid herein are, in alphabetical order: *H. aeger*, *H. antraeus*, *H. aterrimus*, *H. barbatulus*, *H. billsam*, *H. grimaldii*, *H. hachijoensis*, *H. heterolepis*, *H. italicus*, *H. iwamotoi* n.sp., *H. lethonemus*, *H. longibarbis*, *H. longipes*, *H. megalops*, *H. nascens*, *H. neglectissimus*, *H. nesaeae*, *H. papyraceus*, *H. punt* n.sp., *H. sazonomi* n.sp., *H. semipellucidus*, *H. striatissimus*, *H. striatulus* and *H. torvus*.

See ‘Species Groups’ above for distinction and definition of the various species groups, in which the species of *Hymenocephalus* have been provisionally placed.

***Hymenocephalus longibarbis* Group**

***Hymenocephalus longibarbis* (Günther, 1887)**

Figs. 8A–L, 12

Macrurus longibarbis Günther 1887: 139 (type locality: Fiji, 19°09’S, 179°41’E).

Hymenocephalus longibarbis: Iwamoto & Merrett, 1997: 520; Iwamoto & Williams, 1999: 177; Merrett & Iwamoto 2000: 757.

Hymenocephalus longiceps Smith & Radcliffe, 1912: 111 (type locality: Philippines, off Luzon, 13°10’N, 123°59’E).

Hymenocephalus longiceps: Gilbert & Hubbs, 1916: 145; Gilbert & Hubbs, 1920: 520; Okamura, 1970: 45.

Hymenocephalus striatissimus: Weber, 1913: 168.

Material examined. 27 specimens; 1 specimen BMNH 1887.12.7.94 (holotype), 140 mm TL, 19°09’S, 179°41’E, 576 m, Challenger; 1 specimen AMS I.23423-018, 160 mm TL, 18°01’S, 118°23’E; 1 specimen AMS I.32433-008, 255 mm TL, 10°29’S, 144°01’E; 3 specimens AMS I.40292-002, 166, 180, 216+ mm TL, 36°29’S, 150°21’E; 1 specimen (otolith only) BSKU 106798, 210 mm TL, Kagoshima, off Kyushu Island; 1 specimen (otolith only) BSKU 106800, 193 mm TL, Kagoshima, off Kyushu Island; 1 specimen BSKU 110100, 173 mm TL, Suruga Bay; 1 specimen BSKU 110104, 98 mm TL, Suruga Bay; 1 specimen LACM 42620-1, 144+ mm TL, E of Sydney; 3 specimens (2 otoliths only) MNHN 2006-0020, 176 mm TL, 08°16’S, 160°04’E, 464–523 m; 1 specimen MNHN 2006-0159, 182+ mm TL, 07°44’S, 156°29’E, 518–527 m; 1 specimen (otolith only) MNHN 2008-2433, 15°07’S, 167°03’E, 420–670 m; NSMT P.94559, 185 mm TL, KH-02-4 station S1-C; 1 specimen (otolith only) USNM 149296, 16°38’N, 119°57’E; 1 specimen USNM 149298, 125+ mm TL, 05°52’N, 120°31’E; 1 specimen USNM 149299, 188 mm TL, 00°15’N, 127°24’E; 2 specimens WAM P.28058-014, 200 and 211 mm TL, 18°05’S, 118°10’E; 1 specimen WAM P.28071-020, 159 mm TL, 18°08’S, 118°31’E; 4 specimens ZMUC reg. 1.2.1928, 95, 99, 125 and 127 mm TL, off Jolo, Philippines.

Diagnosis. Pelvic fin rays 8; pectoral fin rays 13–17; snout barely projecting; head bones rather firm; barbel very long, 50–60% HL, reaching vertical through posterior edge of orbit; orbit diameter 30–33% HL; interorbital width 45–48% HW; gill rakers 16–20; ventral striae reaching close to periproct; OL:OH = 1.1–1.3; TCL:PCL = 1.8–2.1.

Comparison. *Hymenocephalus longibarbis* resembles *H. longipes*, differing primarily in the very long barbel (vs no barbel) and the absence of black pigmentation on the pelvic fin (vs black tip).

Description. Head morphology (n = 3) (Fig. 8A–C): Head with rounded, soft-tipped snout, barely projecting. Snout length 15–20% HL, orbit diameter 30–33% HL, interorbital width 45–50% HW. Barbel 50–60% HL,

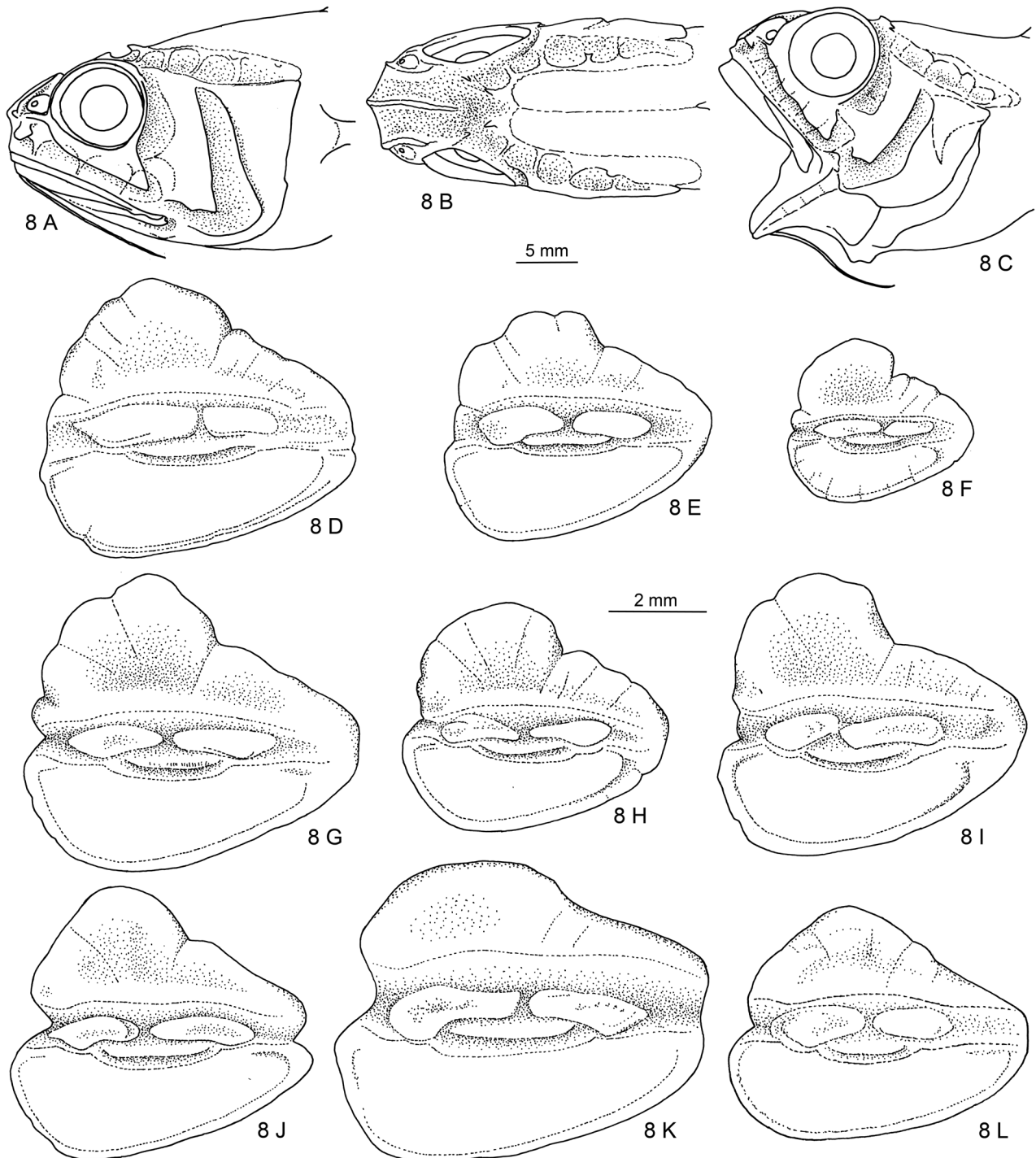


FIGURE 8. *Hymenocephalus longibarbis*: A–B—USNM 149298, A—Lateral view of head, B—Dorsal view of head. C—Holotype, BMNH 1887.12.7.94, lateral view of head. D–L—Otoliths, inner faces, D—BSKU 106798, E—BSKU 110100, F—BSKU 110104, G—USNM 149296, H—LACM 42620-1, I—MNHN 2006-0159, J,L—WAM P.28058-014, K—AMS I.32433-008.

reaching vertical through posterior edge of orbit. Head canals well developed, infraorbital width 12–15% HL, supraorbital canal with 6 segments, width 7–10% HL, supratemporal canal narrow, above segment 4 of supraorbital canal (information provided by N. Nakayama, BSKU), preopercular canal width 10–15% HL, postorbital-preopercular interspace 9–11% HL. Infranasal supporter small; infraorbital supporter moderately widened throughout length below orbit, expanded beyond rear of orbit, 90–110% OD; preopercular supporter broad, with straight rear margin, short (3–5% HL).

Otolith morphology (n = 20) (Fig. 8D–L): Otolith moderately high bodied; OL:OH = 1.1–1.3; OL:OT about 3. Predorsal lobe large, mostly triangular in shape, often crenulated marginally, gently inclining towards rear part of otolith. Anterior rim irregular, broadly rounded; posterior tip moderately pointed, sometimes with incision at cauda. Ventral rim deep, smooth and regularly curved, deepest anterior of middle. Inner face slightly convex along horizontal axis, with slightly supramedian sulcus. Ostial and caudal colliculi moderately large, closely separated at collum, terminating at some distance from anterior and posterior tips of otolith; pseudocolliculum moderately enlarged. CCL:OCL = 0.7–1.3; TCL:PCL = 1.8–2.1. Dorsal depression moderately wide; ventral furrow thin, close to ventral rim.

Discussion. When Smith and Radcliffe (1912) described *H. longiceps*, they stated that “the species resembles *H. longibarbis* Günther, and may prove to be identical with it”. Okamura (1970) noted that the two species could be differentiated by *H. longiceps* having more pectoral fin rays and a shorter barbel. Iwamoto & Merrett (1997) discussed the relationship of the two nominal species and concluded that the difference of pectoral fin rays given as 11 for the holotype of *H. longibarbis* (vs 14–17 for *H. longiceps*) is based on an erroneous measure by Günther and that differences in barbel lengths are not verified. Both observations are clearly supported by my review of the holotype of *H. longibarbis* as well as the many other specimens of both nominal species reviewed from a large variety of locations. Iwamoto & Merrett nevertheless retained both species based on differences in snout length (apparently measured slightly differently from my method, which arrives at slightly lower values) and small differences in interorbital and suborbital width. I failed to verify these differences, and consider *H. longiceps* as a junior synonym of *H. longibarbis*.

Notwithstanding the above, one can observe certain statistical variations in the otolith shapes which appear to relate to geographical differences. Otoliths of specimens from Japan (Fig. 6D–F) exhibit a more intense marginal crenulation and a more regular triangular shape of the dorsal rim than the ones from the Philippines to NE Australia (Fig. 6G–J). Some specimens from off Australia, particularly off Western Australia (Fig. 6K–L), show a relatively low predorsal lobe. However, I was unable to relate these subtle differences in otolith morphology to any other morphological differences of the fishes and therefore regard them as representing intraspecific variations.

Distribution (Fig. 12). Following the synonymization of *H. longiceps*, *H. longibarbis* now maintains a rather wide geographical distribution in the West Pacific from southern Japan in the north to the Philippines and Indonesia and further south to New Caledonia and northern Australia from Queensland to Western Australia.

***Hymenocephalus longipes* Smith & Radcliffe, 1912**

Figs. 9A–G, 12

Hymenocephalus longipes Smith & Radcliffe, 1912: 109 (type locality: 09°38'N, 121°11'E).

Hymenocephalus longipes: Gilbert & Hubbs, 1920: 527.

Material examined. 6 specimens; 1 specimen MNHN 2011–0226, 146 mm TL, 11°57'N, 121°28'E, 388–404 m; 2 specimens (otoliths only) USNM 99474, 11°10'N, 121°28'E; 1 specimen USNM 150156, 137 mm TL, 10°08'N, 123°52'E; 1 specimen (otolith only) USNM 150157, 10°10'N, 123°53'E; 1 specimen USNM 150158, 155 mm TL, 08°48'N, 123°35'E; 1 specimen (otolith only) USNM 150160, 12°52'N, 123°23'E.

Diagnosis. Pelvic fin rays 8; pectoral fin rays 13–15; pelvic fins with black-colored tips; snout barely projecting; head bones rather firm; barbel absent; orbit diameter 28–33% HL; interorbital width 40–50% HW; gill rakers 19–21; ventral striae reaching close to periproct; OL:OH = 1.1–1.25; TCL:PCL = 1.7–2.1.

Comparison. See *H. longibarbis*.

Description. Head morphology (n = 3) (Fig. 9A–C): Head with rounded, soft-tipped snout, not projecting. Snout length 15% HL, orbit diameter 28–33% HL, interorbital width 40–50% HW. Barbel absent. Head canals well developed, infraorbital width 10–12% HL, supraorbital canal with 6 segments, width 5–10% HL, supratemporal

canal indistinct, preopercular canal width 7–12% HL, postorbital-preopercular interspace 11–13% HL. Infranasal supporter small; infraorbital supporter moderately widened throughout length below orbit, expanding beyond rear part of orbit, 80–100% OD; preopercular supporter broad, blunt, with straight rear margin short (3–5% HL).

Otolith morphology ($n = 7$) (Fig. 9D–G): Otolith moderately high bodied; OL:OH = 1.1–1.25; OL:OT about 4. Predorsal lobe large, with pointed tip, triangular in shape, rather gently inclining towards rear part of otolith with some undulation. Anterior rim irregular, broadly rounded to blunt; posterior tip moderately pointed. Ventral rim deep, smooth and regularly curved, deepest anterior of middle. Inner face very slightly convex along horizontal axis, with median sulcus. Ostial and caudal colliculi moderately large, narrowly placed at collum, terminating at considerable distance from anterior and posterior tips of otolith; pseudocolliculum moderately enlarged. CCL:OCL = 0.9–1.0; TCL:PCL = 1.7–2.1. Dorsal depression wide; ventral furrow thin, close to ventral rim.

Distribution (Fig. 12). Known from a relatively small area within the Sulu Sea and southern Luzon to northern Mindanao.

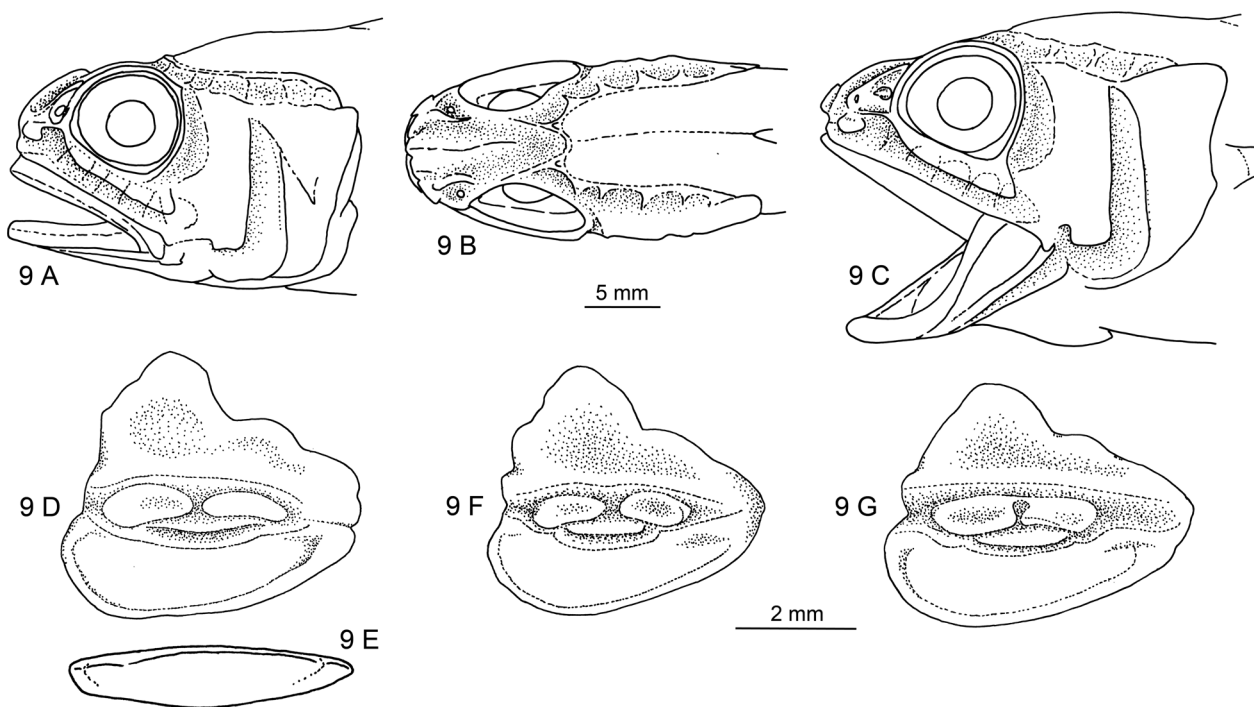


FIGURE 9. *Hymenocephalus longipes*: A–B—USNM 150156, A—Lateral view of head, B—Dorsal view of head. C—MNHN 2011-0226, lateral view of head. D–G—Otoliths, D—MNHN 2011-0226, inner face, E—MNHN 2011-0226, ventral view, F–G—USNM 150160.

Hymenocephalus iwamotoi Group

Hymenocephalus iwamotoi n.sp.

Figs. 10A–B, 11A–I, 12

Material examined (30 specimens, (58+) 74–103 mm TL). Holotype WAM P.25401-003, 86+ mm TL, off northwestern Australia, vicinity of Browse Island, 13°47'S, 123°18'E, 242 m, 23 December 1969, identified as *Hymenocephalus* sp. by Iwamoto, 2003; Paratypes: WAM P.25401-020, 29 specimens, (58+) 74–103 mm, same data as holotype. 69 further specimens from the same location not investigated in detail and not characterized as type-specimens, WAM P.25401-021.

Diagnosis. A small species, not exceeding 105 mm TL. Pelvic fin rays 8 (7–9); pectoral 12–13; first dorsal II + 6–7; gill rakers 17–20. Barbel long 40–46% HL, reaching vertical through rear end of orbit. Orbit 35–38% HL. Snout rounded, barely protruding, short 15–19% HL. Posterior luminescent lens round; ventral striae extending to near periproct. Otolith compressed (OL:OH = 0.95); colliculi separated, small; pseudocolliculum small (TCL:PCL = 1.8–2.0).

Comparison. *Hymenocephalus iwamotoi* is readily recognized by the combination of the characters given in the diagnosis, which represent a mixture of assumed plesiomorphic characters, such as the otolith with the separated colliculi and the short pseudocolliculum, the low number of gill rakers, and the long infraorbital supporter, and perceived apomorphic characters such as the blunt head profile, the large orbit and the low number of fin rays in the first dorsal. It shows the longest barbel of any *Hymenocephalus* species together with *H. longibarbis*. Because of its unique combination of characters, I propose a species group of its own for *H. iwamotoi*.

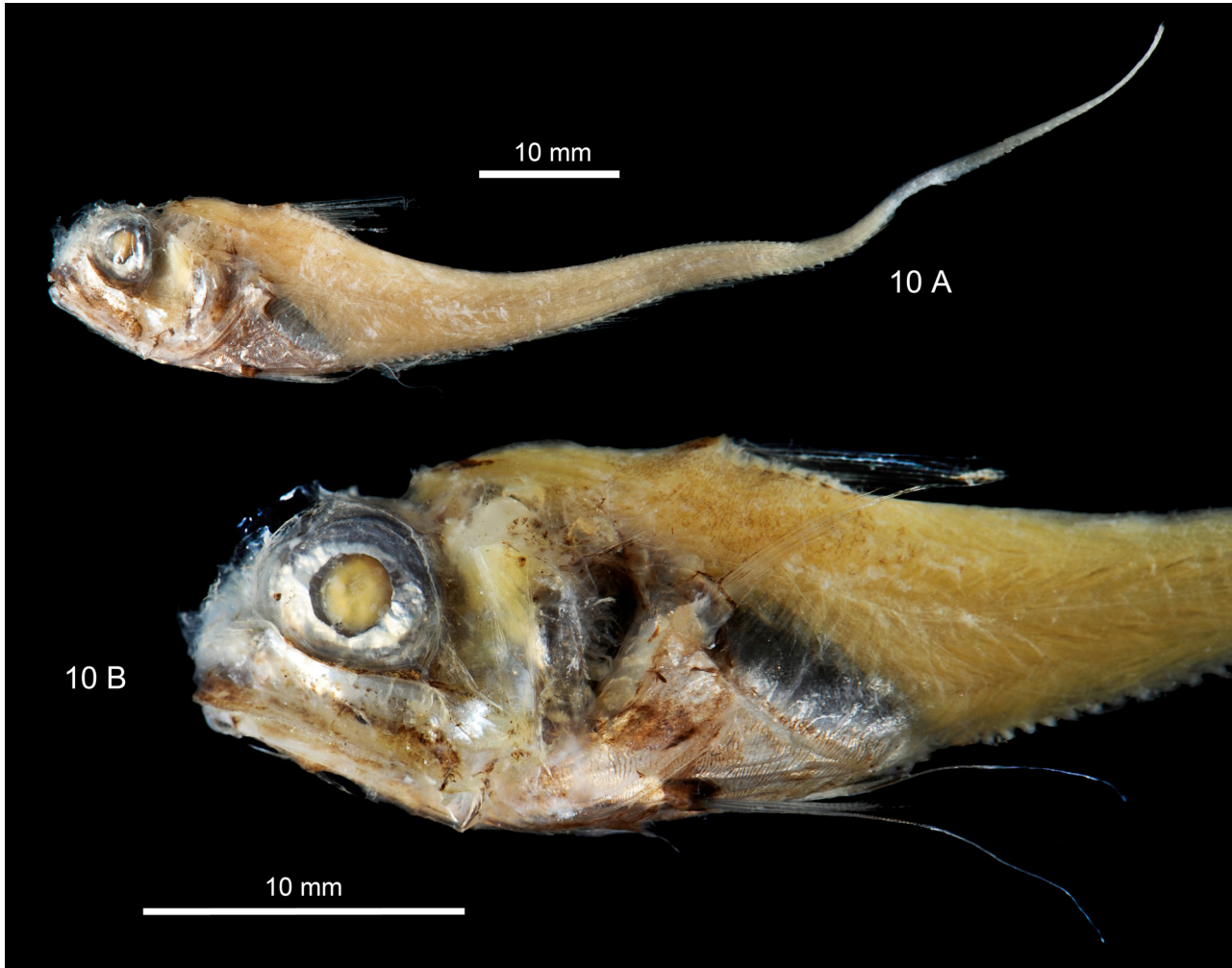


FIGURE 10. *Hymenocephalus iwamotoi*: A—Holotype, WAM P.25401-003, TL 86+ mm (photo M. Krag). B—Paratype, WAM 25401-020, TL 90+ mm, head close-up (photo M. Krag).

Description. Counts (from 31 specimens): 1D. II,7 (II,6–7); P. 12 (12–13, one specimen 14); V. 8 (7–9, predominantly 8); gill rakers on first arch, inner side 18 (17–20); gill rakers second arch, outer side 18 (18–20).

Measurements (from holotype and two best-preserved paratypes): head length 13.7–15.0 mm, about 18–20% TL; head height 78–82% HL; head width 55% HL (holotype only); barbel 40–46% HL; snout 15–19% HL; orbit 35–38% HL; postorbital 43–49%HL; interorbital 35% HL / 63% HW (holotype only); upper jaw length 56–59% HL; pre-anal about 150% HL; pre-dorsal to 1D about 100% HL; pre-dorsal to 2D about 230% HL; distance base 1D to 2D about 130% HL; 1st dorsal fin length 70–80% HL; pectoral fin length 70% HL; ventral fin length, 1st ray 110% HL, 2nd ray 50% HL; supraorbital canal width 12.0–14.5% HL; infraorbital width 14.5–17% HL; minimal infraorbital canal width 7.0–7.5% HL.

The following description is based on the holotype (Fig. 10A). Body slender, highest and widest at rear part of head just behind orbit, tapering rather regularly behind first dorsal into the usual whip-like tail. Origin of first dorsal, pectoral and ventral fins about on same vertical. First ray of ventral more than twice the length of subsequent rays. Second dorsal rudimentary; anal well developed.

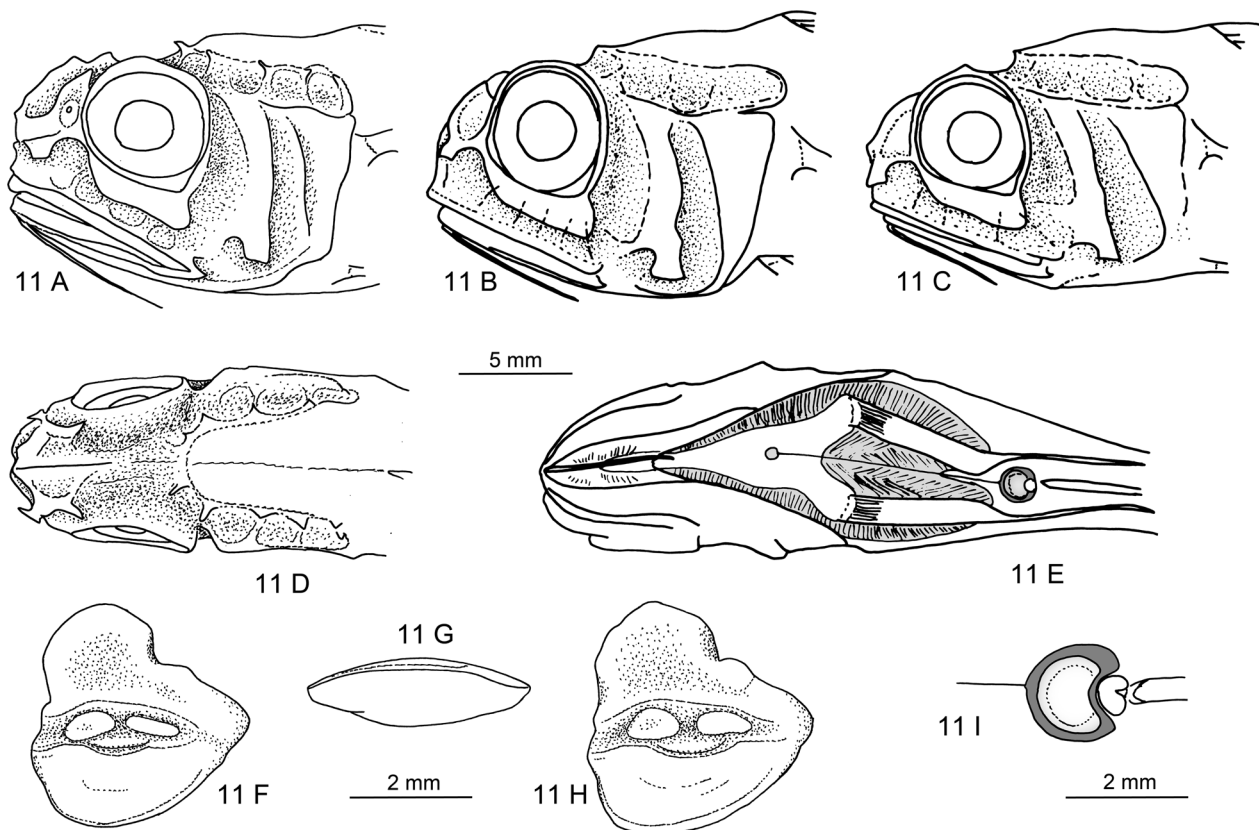


FIGURE 11. *Hymenocephalus iwamotoi*: A—Holotype, WAM P.25401-003, TL 86+ mm, lateral view of head. B—Paratype, WAM P.25401-020, TL 90+ mm, lateral view of head. C—Paratype, WAM P.25401-020, TL 58+ mm, lateral view of head. D—Holotype, dorsal view of head. E—Holotype, ventral view of head and trunk. F—H—Non-types, WAM P.25401-020, F, H—inner faces, G—ventral view. I—Holotype, detail view of posterior lens of ventral luminescent organ.

Teeth all small, on narrow bands of both jaws.

Luminescent striae (Fig. 11E) silvery, extending as a narrow band along both sides of isthmus below gill covers, reaching up to bases of pectoral fins and behind ventral fin bases, where they join along medial line, and expanding almost to periproct region. Some dark striae on gular region. Anterior lens of ventral luminescent organ small, pale; posterior lens (Fig. 11I) before periproct about three times as large, round, surrounded by thin dark tissue.

Axial skeleton (based on radiographs). Number of precaudal vertebrae 10; vertebrae 1 to 3 much shorter than subsequent vertebrae. Neural spines of vertebrae 1 and 2 nearly twice as long as vertebra 3; neural spines 3 to 9 depressed and with blunt tips; neural spines 3 to 7 short and of equal length, spines 8 to 9 increasing in length. Bases of neural spines 4 to 8 enlarged. Parapophyses on vertebrae 7 to 10. Pleural ribs on vertebrae 5 to 8. First fin ray of 1D supported by two pterygiophores both inserted behind neural spine 2. Last pterygiophore of 1D inserted behind neural spine 7 or 8. First pterygiophore of 2D above vertebra 18 to 20. First pterygiophore of anal fin slightly prolonged, inserted in front of first haemal spine on first caudal vertebrae (11).

Head morphology (Figs. 10B, 11A–D): Head stout, with rounded anterior profile, snout barely protruding beyond mouth and nasal flap. Bones thin and fragile; eyes large; barbel long, reaching vertical through rear end of orbit. Head canals well developed, covered with very thin, mostly fragmented integument. Infraorbital, supraorbital and preopercular canal widths 10–17% HL, supraorbital canal with 4 segments, supratemporal canal not identified, postorbital-preopercular interspace 7–10% HL. Infranasal supporter small; infraorbital supporter broad, constantly widened below entire stretch of orbit, 70–90% OD; preopercular supporter narrow, with straight rear margin, long (7–11% HL); mandibular hook small.

Otolith morphology (Fig. 11F–H): Otolith high bodied; OL:OH = 0.95; OL:OT about 3. Predorsal lobe massive, slightly anteriorly inclined, terminating posteriorly in a marked incision above middle of otolith. Anterior rim irregular, nearly vertical; posterior tip moderately pointed at or slightly above level of sulcus. Ventral rim deep,

smooth and regularly curved, deepest anterior of middle. Inner face slightly convex along horizontal axis, with narrow, median sulcus. Ostial and caudal colliculi small, the latter often distinctly narrower than the ostial colliculum; pseudocolliculum moderately enlarged. CCL:OCL = 1.1–1.2; TCL:PCL = 1.8–2.0. Dorsal depression wide; ventral furrow distinct, close to ventral rim.

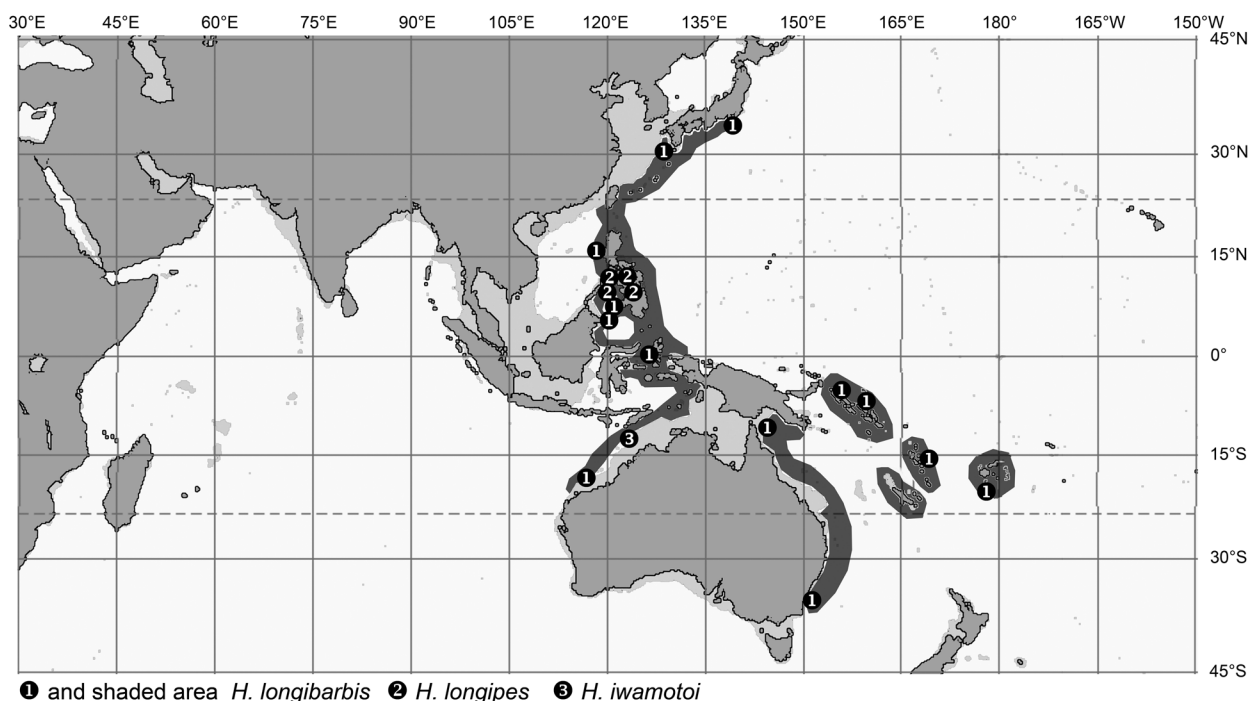


FIGURE 12. Geographical distribution of *Hymenocephalus longibarbis*, *H. longipes* and *H. iwamotoi*.

Coloration (in alcohol): Very light, yellowish on tail and dorsum; silvery and light yellow colors on head; area of ventral striae silvery, very little dark pigments; some small, indistinct darker pigments on tail below bases of fin rays of 2nd dorsal.

Distribution. Known only from the type location off Browse Island, probably endemic to the northwest Australian shelf edge.

Etymology. The new species is named in honor of Tomio Iwamoto (San Francisco, U.S.A.) in recognition of his outstanding contribution to the knowledge of the family Macrouridae. He was also the first ichthyologist to see the specimens, then identified as *Hymenocephalus* sp.

Hymenocephalus aterrimus Group

Hymenocephalus aterrimus Gilbert, 1905

Figs. 13A–L, 16

Hymenocephalus aterrimus Gilbert 1905: 666 (type locality: off Kauai, Hawaii).

Hymenocephalus aterrimus: Marshall & Iwamoto, 1973: 607; Iwamoto & Merrett, 1997: 516; Merrett & Iwamoto 2000: 757.

Hymenocephalus (Papyrocephalus) aterrimus Gilbert & Hubbs, 1920: 539.

Material examined. 33 specimens; 3 specimens AMS I.29753-001, 105–125 mm TL, 31°53'S, 153°16'E, 878–933 m; 1 specimen AMS I.30304-006, 105+ mm TL, 32°13'S, 153°06'E, 820–857 m; 1 specimen BSKU 111021, 148+ mm TL, 28°23'S, 113°01'E, 855 m; 2 specimens LACM 57120-1, 96+ and 110+ mm TL, north off Maui, TC-61-65; 5 specimens MCZ 51405, 119–135 mm TL, off Havana, 860 m; 2 specimens MNHN 1994-0872, 122 and 129+ mm TL, 23°07'S, 166°51'E, 850 m; 4 specimens MNHN 1994-0876, 74+–118 mm TL, 12°31'S, 174°22'W, 715–730 m; 2 specimens MNHN 1997-0670, 85+ and 110 mm SL, 21°10'S, 165°53'E, 786–800 m; 1 specimen MNHN 2000-1067, 08°57'S, 140°15'W, 708–738 m; 3 specimens USNM 216161, 195–205 mm TL,

24°40'N, 80°00'W, 732–860 m; 4 specimens USNM 405734, 122–130+ mm TL, 16°58'N, 87°53'W; 3 specimens USNM 405736, 80+–154 mm TL, 16°58'N, 80°07'W, 732 m; 2 specimens USNM 51677, 117+–140+ mm TL, off southern Oahu, Hawaii, 386 m.

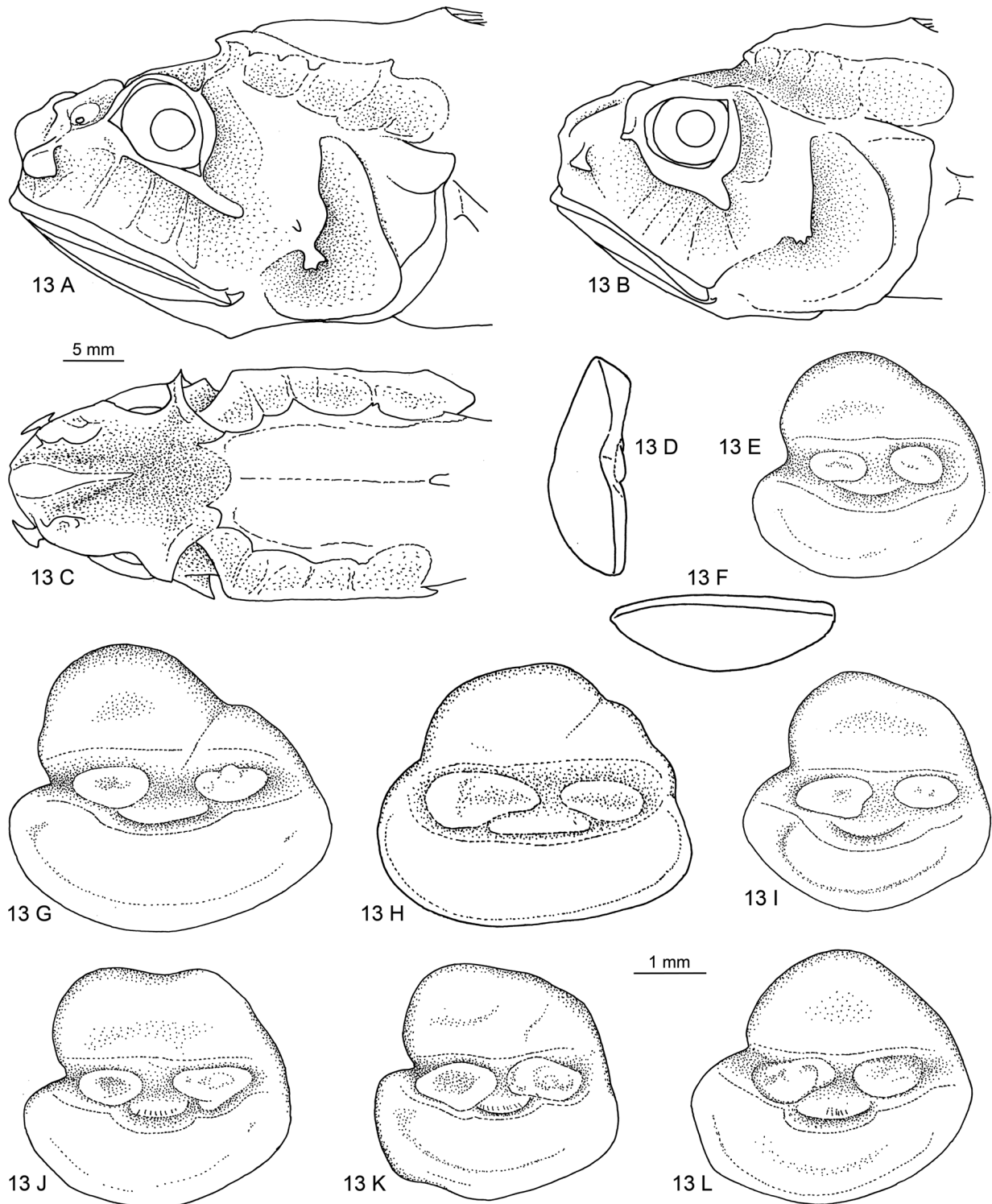


FIGURE 13. *Hymenocephalus aterrimus*: A—USNM 216161, lateral view of head. B—USNM 51677, cotype, lateral view of head. C—USNM 216161, dorsal view of head. D–L—Otoliths, E, G–L—Inner faces, D—Anterior view, F—Ventral view, D–F—MNHN 1997-0670, G—USNM 405736, H—BSKU-ED915, I—MNHN 1994-0876/2, J—MCZ 51405/1, K—AMS I.30384-006, L—MNHN 1994-0872.

Diagnosis. Black-colored large-headed fish (head size 21–25% TL); pelvic fin rays 13–14; pectoral fin rays 13–16; snout projecting, 20–24% HL; head bones papery thin, often distorted; barbel absent; orbit diameter small,

20–24% HL; interorbital width 60–70% HW; infraorbital width 20–25% HL; postorbital-preopercular interspace 10–14% HL; preopercular supporter very small, forked; gill rakers 21–25; ventral striae reaching to about $\frac{1}{3}$ from pelvic fin bases to periproct; otolith small with rounded outline, no predorsal lobe developed; colliculi separated; OL:OH = 1.0–1.2; TCL:PCL = 2.2–2.8.

Comparison. *Hymenocephalus aterrimus* is readily recognized by the large head, black color, small eyes, wide infraorbital space, small preopercular supporter, relatively small otolith without predorsal lobe, and clearly separated colliculi. It closely resembles *H. barbatulus*, from which it differs primarily in the larger number of pelvic fin rays (13–14 vs 7) and pectoral fin rays (13–16 vs 10), and *H. sazónovi* n.sp., from which it differs in the head and otolith shape and the larger number of gill rakers (21–25 vs 19–20).

Description. Head morphology (n = 3) (Fig. 13A–C): Head large, with very soft bones, snout bluntly rounded, long, (snout length 20–24% HL), orbit diameter 20–24% HL, interorbital width 60–70% HW. Barbel absent. Head canals well developed, large, infraorbital width 20–25% HL, supraorbital canal with 4 to 5 segments, width 13–17% HL, supratemporal canal not identified, preopercular canal width 19–23% HL, postorbital-preopercular interspace 10–14% HL. Infranasal supporter small; infraorbital supporter short, expanding only beyond rear part of orbit, 30–60% OD; preopercular supporter short, forked (3–4% HL).

Otolith morphology (n = 24) (Fig. 13D–L): Otolith smaller than usually in the genus, with regularly curved outline and with low or indistinct predorsal lobe; OL:OH = 1.0–1.2; OL:OT about 3. All rims smooth and regularly curved; dorsal rim somewhat reduced, ventral rim broad, shallow. Inner face almost flat, with median sulcus. Ostial and caudal colliculi small, terminating at moderate distance from anterior and posterior tips of otolith; pseudocolliculum short. CCL:OCL = 0.8–1.2; TCL:PCL = 2.2–2.8. Dorsal depression indistinct; ventral furrow thin, moderately close to ventral rim.

Discussion. *Hymenocephalus aterrimus* seems to reside in deeper water than most other species of the genus with most of the catches from 700 to nearly 1000 m water depth. As already mentioned, this deeper habitat may have resulted in certain functional adaptations such as the reduction of eye and otolith size, the enlargement of the head canal system and the development of very thin, papery head bones. As a result of the fragile head bones, very few specimens have been found in collections that were adequate for a detailed study of the head morphology. *Hymenocephalus aterrimus* is also an unusually widely distributed species in the genus (see below), and because of this, I investigated specimens from different locations to find out whether regional differences could be seen. However, as a result of the generally poor preservation of the specimens my studies were primarily focused on meristic values and otoliths. Meristic values of pectoral fin rays and gill rakers show a rather wide variability, but no pattern of regional differentiation. Otoliths do not exhibit any valuable regional variation. It was therefore concluded that *H. aterrimus* represents a single, well-defined species with a very wide geographical distribution range, except for specimens on the Nazca and Sala y Gomez ridges in the SE Pacific, which represent a related, but separate species—*H. sazónovi* n.sp. (see below).

Distribution (Fig. 16). The geographical distribution pattern of *H. aterrimus*, although wide, is somewhat patchy and discontinuous. In the Atlantic it is known from the Caribbean and the continental slope of northern South America. It has not been recorded from the eastern Atlantic or the Indian Ocean. In the Pacific it has been caught off subtropical western and eastern Australia, off several islands in the southern Pacific (New Caledonia, Vanuatu, Wallis & Futuna, Marquesas Islands), and off Hawaii in the central northern Pacific.

***Hymenocephalus barbatulus* Gilbert & Hubbs, 1920**

Figs. 14A–B, 16

Hymenocephalus (Papyrocephalus) barbatulus Gilbert & Hubbs, 1920: 539 (type locality: 07°35'S, 126°38'E).

Discussion. *Hymenocephalus barbatulus* was described based on the holotype and one paratype from the same location off eastern Mindanao, Philippines, from 695 m. It differs from the other species in the *aterrimus* Group in the low pelvic and pectoral fin ray counts (7 and 10). Neither holotype nor paratype was located in the collection of USNM. According to information provided by S. Raredon (USNM) they were last checked in 1980. The figures shown are copies of the original drawing by Gilbert & Hubbs (1920: fig. 34) (Fig. 14A) and a secondary drawing in Cohen et al. (1990: fig. 511) (Fig. 14B); both depict an overall head morphology similar to that of *H. aterrimus*.

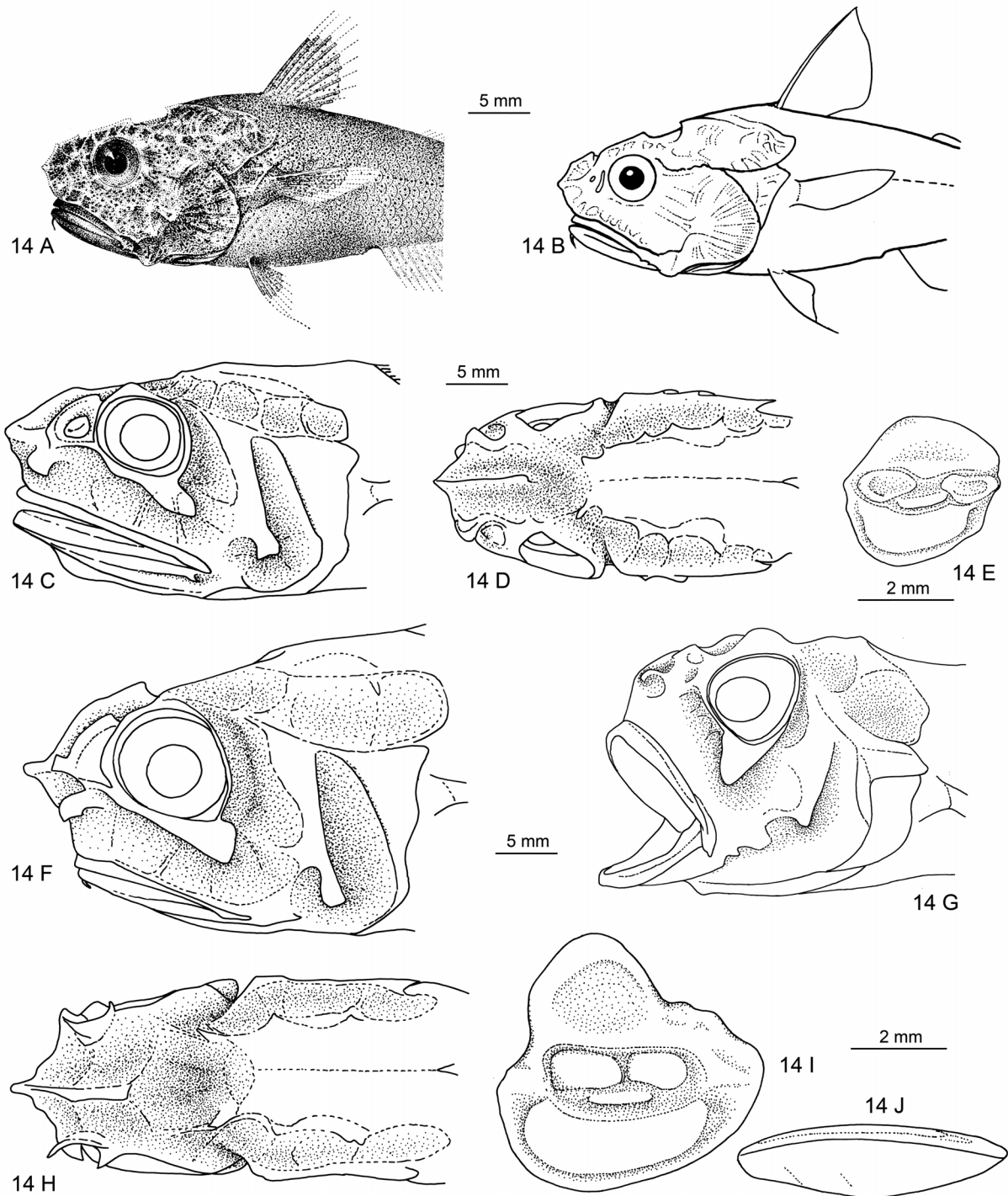


FIGURE 14. A–B: *Hymenocephalus barbatulus*: A—Figure from Gilbert & Hubbs (1920). B—Figure from Cohen et al. (1990). C–E: *Hymenocephalus nesaeae*: Holotype, MNHN 1995-0869, C—Lateral view of head, D—Dorsal view of head, E—inner face of otolith. F–J: *Hymenocephalus papyraceus*: F—BSKU 099483, lateral view of head, G—Holotype, USNM 50935, lateral view of head, H—BSKU 099483, dorsal view of head, I—BSKU 44761, inner face of otolith, J—BSKU 44761, ventral view of otolith.

***Hymenocephalus nesaeae* Merrett & Iwamoto, 2000**

Figs. 14C–E, 16

Hymenocephalus nesaeae Merrett & Iwamoto, 2000: 759 (type locality: 18°53'S, 169°52'E).

Material examined. 2 specimens; 1 specimen MNHN 1995-0869 (holotype), 143+ mm TL, 18°53'S, 169°52'E, 919–1000 m; 1 specimen MNHN 1995-0999 (paratype), 130 mm TL, 18°51'S, 168°50'E, 980–990 m.

Diagnosis. Pelvic fin rays 13–14; pectoral fin rays 13–15; snout projecting, 25–30% HL; barbel absent; orbit diameter small, 25% HL; interorbital width 55% HW; infraorbital width 16–17% HL; preopercular supporter moderately long, straight, 6% HL; gill rakers 25–26; ventral striae reaching to about $\frac{1}{3}$ from pelvic fin bases to periproct; otolith small with rounded outline, no predorsal lobe developed, colliculi separated, reaching close to anterior and posterior rims of otolith; OL:OH = 1.05; TCL:PCL = 2.8.

Comparison. *Hymenocephalus nesaeae* resembles *H. aterrimus* in the large head, the small eyes and the pelvic and pectoral fin ray counts, but differs in the narrower sensory canal systems on the head: infraorbital width 16–17% HL (vs 20–25% HL), supraorbital canal width 10% HL (vs 13–17% HL), preopercular canal width 12% HL (vs 19–23% HL). The preopercular supporter is larger and not forked as in *H. aterrimus* (infraorbital supporter length 6% HL vs 3–4% HL). The relatively small otolith is characteristic with its rounded outline and the colliculi reaching close to the anterior and posterior rims of the otolith, which resemble otoliths of the genus *Coryphaenoides* more than they do those of *Hymenocephalus*. Another similar species is *H. papyraceus*, from which *H. nesaeae* differs in pelvic and pectoral fin rays counts (13–14 vs 10–11 and 13–15 vs 16–18 respectively), number of gill rakers (24–26 vs 18–22), narrower supraorbital and preopercular canal widths (10% vs 17–20% HL and 12% vs 14–17% HL respectively), longer preopercular supporter (11 vs 6% HL), and the different otolith shape. *Hymenocephalus nesaeae* represents the most plesiomorphic morphology in the *aterrimus* group.

Description. Head morphology (n = 1) (Fig. 14C–D): Head large, snout projecting, long, (snout length 26% HL), orbit diameter 25% HL, interorbital width 55% HW. Barbel absent. Head canals well developed, large, infraorbital width 16% HL, supraorbital canal with 5 segments, width 10% HL, supratemporal canal narrow, above segments 3 to 4 of supraorbital canal, preopercular canal width 12% HL, postorbital-preopercular interspace 6% HL. Infranasal supporter small; infraorbital supporter short, expanding only beyond rear part of orbit, 60% OD; preopercular supporter moderately long, straight (6% HL).

Otolith morphology (n = 1) (Fig. 14E): Otolith smaller than usual for the genus, with round outline and without distinct predorsal lobe; OL:OH = 1.05. All rims smooth and rather regularly curved. Inner face almost flat, with median sulcus. Ostial and caudal colliculi small, terminating very close to anterior and posterior tips of otolith; pseudocolliculum short. CCL:OCL = 0.95; TCL:PCL = 2.8. Dorsal depression indistinct; ventral furrow distinct, moderately close to ventral rim.

Distribution (Fig. 16). So far only known from off Vanuatu.

Hymenocephalus papyraceus Jordan & Gilbert, 1904

Figs. 14F–J, 16

Hymenocephalus papyraceus Jordan & Gilbert, 1904: 614 (type locality: Sagami Bay, Japan).

Hymenocephalus papyraceus: Okamura, 1970: 56.

Material examined. 12 specimens; 6 specimens BSKU 44292-44297, 120+ –132+ mm TL, central Tosa Bay off Kochi, 600 m; 1 specimen BSKU 44761, 170 mm TL, central Tosa Bay off Kochi, 600 m; 1 specimen BSKU 99483, 171 mm TL, off southern Japan (no further data); 1 specimen BSKU 101959, R/V Hakuro-maru (KH 73-2, St. 4); BSKU NMIC-ZF-03092, 147 mm TL, off southern Japan (no further data); 1 specimen USNM 50935 (holotype), 112 mm TL, Sagami Bay, 220–485 m; 1 specimen ZMMGU P-18258, 30°30'N, 129°19'E.

Diagnosis. Pelvic fin rays 10–11; pectoral fin rays 16–18; snout projecting, with thin, pointed tip, 20–25% HL; barbel short, 4–5% HL, not reaching vertical through anterior margin of orbit; orbit diameter moderate, 25–30% HL; interorbital width 70–80% HW; infraorbital width 16–20% HL; preopercular supporter very long, straight, 10–11% HL; gill rakers 18–22; ventral striae reaching to about $\frac{1}{3}$ distance from pelvic fin bases to periproct; otolith with moderately high predorsal lobe, colliculi separated, closely placed across narrow collum, terminating far from anterior and posterior rims of otolith; OL:OH = 1.05; TCL:PCL = 2.1.

Comparison. *Hymenocephalus papyraceus* resembles *H. aterrimus* and *H. nesaeae*. From *H. aterrimus* it differs in the number of pelvic and pectoral fin rays (10–11 vs 13–14 and 16–18 vs 13–16, respectively), the smaller preopercular canal width (14–17 vs 19–23% HL), the smaller postorbital-preopercular interspace (4–6 vs

10–14% HL), the long and slender preopercular supporter (11 vs 3–4% HL) and the otolith with a distinct predorsal lobe. For difference with *H. nesaeae* see above.

Description. Head morphology (n = 3) (Fig. 14F–H): Head large, snout projecting, long, with thin pointed tip, which is easily damaged, snout length 20–25% HL, orbit diameter 25–30% HL, interorbital width 70–80% HW. Barbel short, 4–5% HL, not reaching vertical through anterior margin of orbit. Head canals well developed, large, infraorbital width 16–20% HL, supraorbital canal with 4 segments, width 17–20% HL, supratemporal canal rather distinct and wide, above segment 3 of supraorbital canal, preopercular canal width 14–17% HL, postorbital-preopercular interspace 4–6% HL. Infranasal supporter small; infraorbital supporter short, expanding only beyond rear part of orbit, 40–60% OD; preopercular supporter very long, thin and straight (11% HL).

Otolith morphology (n = 1) (Fig. 14I–J): Otolith moderate in size, ventrally well rounded, dorsally with a distinct predorsal lobe, postdorsally somewhat undulating and regularly inclined towards rounded posterior tip; OL:OH = 1.05; OH:OT = 3.5. Inner face slightly convex, with median sulcus. Ostial and caudal colliculi small, narrowly placed across collum, terminating at considerable distance from anterior and posterior tips of otolith; pseudocolliculum moderately short. CCL:OCL = 0.85; TCL:PCL = 2.1. Dorsal depression small; ventral furrow distinct, moderately close to ventral rim, anteriorly and posteriorly turning away and upwards.

Distribution (Fig. 16). *Hymenocephalus papyraceus* is only known off the southeastern coast of Japan, chiefly the Sagami and Tosa Bays and off Kagoshima.

***Hymenocephalus sazonomi* n.sp.**

Figs. 15A–F, 16

Hymenocephalus sp. cf. *aterrimus*: Sazonov & Iwamoto, 1992: 54.

Material examined (3 specimens, 84+ –131+ mm TL). Holotype ZMMGU P-18128, 84+ mm TL, Nazca Ridge, 340–780 m, *Prof. Mesiatzev* cruise 13; Paratypes: ZMMGU P-17729, 121–131+ mm TL, Sala y Gomez Ridge, 1070–1100 m, *Prof. Mesiatzev* cruise 13, trawl 10.

Diagnosis. A stout species, much less slender than typical for the genus, with very thin head bones. Pelvic fin rays 12–13; pectoral 15–16; gill rakers 18–20. Barbel absent. Orbit 21% HL. Snout blunt, with high frontal ridge, barely protruding, short, 23% HL. Ventral striae extending about $\frac{2}{3}$ distance from pelvic fin bases to periproct region. Infraorbital canal wider than other canal systems; preopercular supporter very small. Otolith compressed (OL:OH = 0.8); colliculi separated, small; pseudocolliculum small (TCL:PCL = 1.8).

Comparison. *Hymenocephalus sazonomi* no doubt is closely related to the widespread *H. aterrimus* Gilbert, 1905, with which it was tentatively associated when first described by Sazonov & Iwamoto (1992). It differs from *H. aterrimus* in the deeper head and the high frontal ridge, as already noted by Sazonov & Iwamoto, and the lower number of gill rakers on the inner side of the first gill arch and the outer side of the second gill arch, respectively (18–20 vs 21–27) and the high-bodied otolith with a strongly developed predorsal lobe, which is strongly reduced and rounded in *H. aterrimus*. This additional otolith character particularly supports the recognition of a separate species.

Description. Counts (from 2 specimens): 1D. II,9 (II,9–10); P. 16 (15–16); V. 13 (12–13); first gill raker inner side 20 (18–20); second gill raker outer side 20 (19–20).

Measurements (from holotype, supplemented in part from one paratype and from Sazonov & Iwamoto, 1992): head length 26.5–35.0 mm, about 25–30% TL; head height 85% HL; head width 50% HL; snout 23% HL; orbit 21% HL; postorbital 56% HL; interorbital 26% HL / 54% HW; upper jaw length 51% HL; pre-anal about 145% HL; pre-dorsal to 1D about 95% HL; pre-dorsal to 2D about 165% HL; distance base 1D to 2D about 70% HL; 1st dorsal fin length about 40% HL; ventral fin length at least 30% HL; supraorbital canal width 15.5% HL; infraorbital width 20% HL; minimal infraorbital canal width 13% HL.

The following description is based on the holotype (Fig. 15A). Body stout with massive head, highest and widest just behind orbit, tapering rather abruptly between first dorsal and second dorsal into the usual whip-like tail. Origin of first dorsal, pectoral and ventral fins about on same vertical. Pectoral and ventral incomplete, probably rather short. Second dorsal rudimentary; anal well developed.

Teeth all small, on narrow bands of both jaws.

Luminescent tissue (striae) silvery and well visible as a broad band along both sides of isthmus below gill covers, reaching up to bases of pectoral fins, then turning darker and less clearly visible behind ventral fin bases, where they join along medial line, and expanding to about $\frac{2}{3}$ from ventral fin bases to periproct region. Several distinct, broad dark striae on gular region. Anterior lens of ventral luminescent organ small; posterior lens before periproct about two times larger, tear-drop shaped, anteriorly with triangular stretch of dark tissue.

Axial skeleton (based on radiographs). Number of precaudal vertebrae 10; vertebrae 1 to 3 much shorter than subsequent vertebrae. Neural spines of vertebrae 1 and 2 about 30% longer than vertebra 3; neural spines 3 to 7 or 8 depressed and with blunt tips; neural spines 3 to 6 short and of equal length, spines 7 to 8 increasing in length. Bases of neural spines 4 to 8 enlarged. Parapophyses on vertebrae 6 or 7 to 10. Pleural ribs on vertebrae 4 or 5 to 8. First fin ray of 1D supported by two pterygiophores, both inserted behind neural spine 2. Last pterygiophore of 1D inserted behind neural spine 7 or 8. First pterygiophore of 2D above vertebra 18 to 20. First pterygiophore of anal fin not prolonged, inserted in front of first haemal spine on first caudal vertebrae (11).

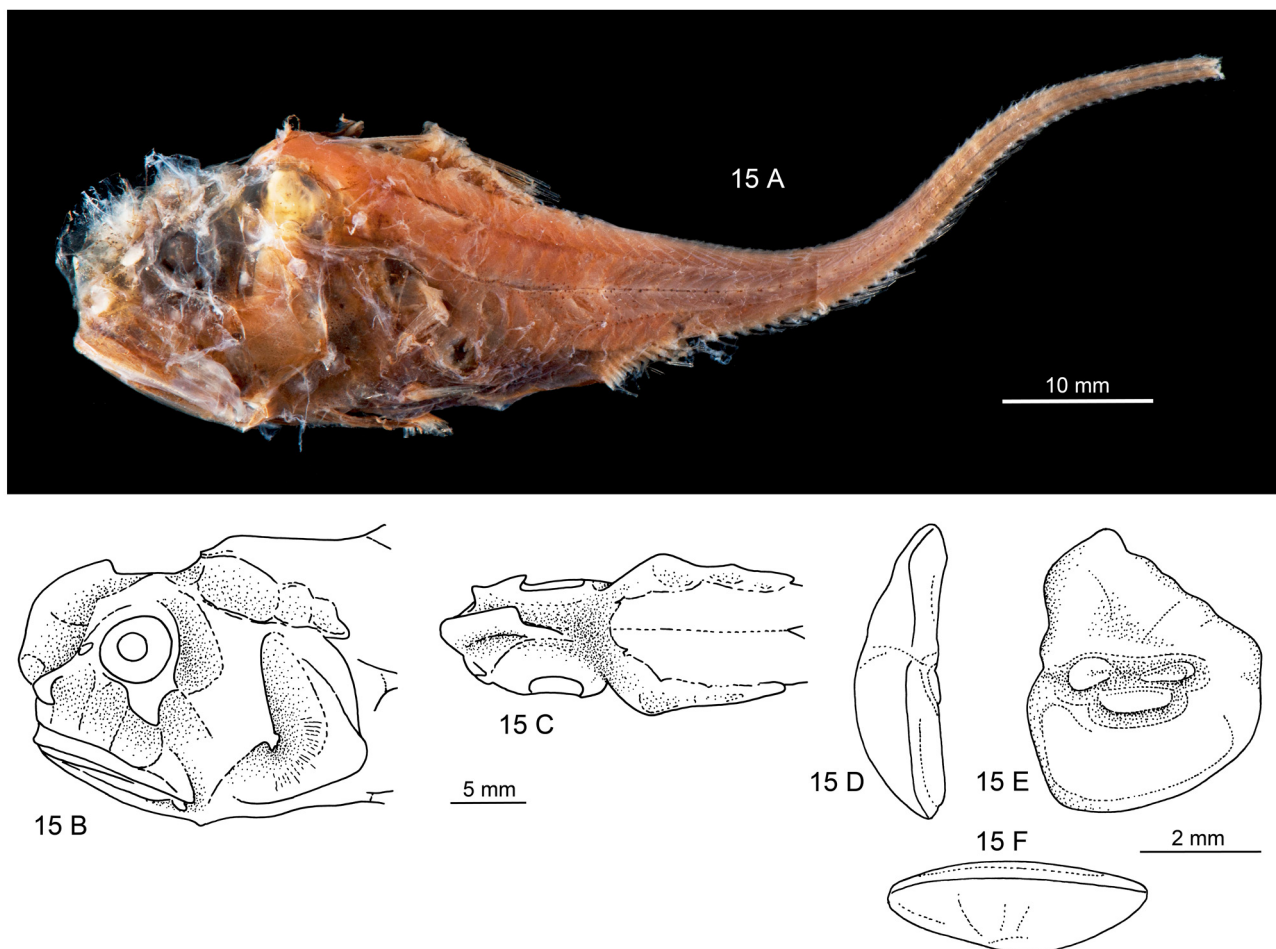


FIGURE 15. *Hymenocephalus sazonovi*: A–F—Holotype, ZMMGU-P 18128, TL 84+ mm, A—Photo (by M. Krag), B—Lateral view of head, C—Dorsal view of head, D—Anterior view of otolith, E—Inner face of otolith, F—Ventral view of otolith.

Head morphology (Fig. 15B–C): Head stout, with blunt anterior profile, snout barely protruding beyond mouth, with high frontal ridge. Bones very thin and fragile; eyes very small; barbel absent. Head canals well developed, covering integument not preserved in any of the studied specimens. Infraorbital canal wider than all other canal systems (20–22% HL), supraorbital canal with 4 segments, width 13–14% HL, supratemporal canal not identified, preopercular canal 15% HL, postorbital-preopercular interspace 11–12% HL. Infranasal supporter small; infraorbital supporter expanded only below rear part of orbit, about 50% OD; preopercular supporter very small (about 3% HL), forked; mandibular hook small.

Otolith morphology (Fig. 15D–F): Otolith high bodied; OL:OH = 0.8; OL:OT about 2.5. Predorsal lobe

massive, regularly dropping down distally to broadly rounded posterior tip. Anterior rim irregular, nearly vertical; ventral rim deep, smooth and regularly curved, deepest anterior of middle. Inner face slightly convex along horizontal axis, with narrow, slightly suprmedian sulcus. Ostial and caudal colliculi small, narrow, particularly the caudal colliculum; pseudocolliculum moderately enlarged. CCL:OCL = 1.2; TCL:PCL = 1.8. Dorsal depression indistinct; ventral furrow distinct, moderately close to ventral rim.

Coloration (in alcohol) (Fig. 15A): Dark brown to black, darkest over trunk and ventral region in front of periproct; tail dark brown. Some black melanophores on head, particularly opercle and along a midlateral band beginning above and behind pectoral fin base.

Distribution (Fig. 16). Probably endemic to the Nazca and Sala y Gomez ridges.

Etymology. The new species is named in memory of the late Yuri I. Sazonov (Moscow, Russia) in recognition of his many contributions to the knowledge of the family Macrouridae. He was also the one first to record the specimens, together with T. Iwamoto, in 1992.

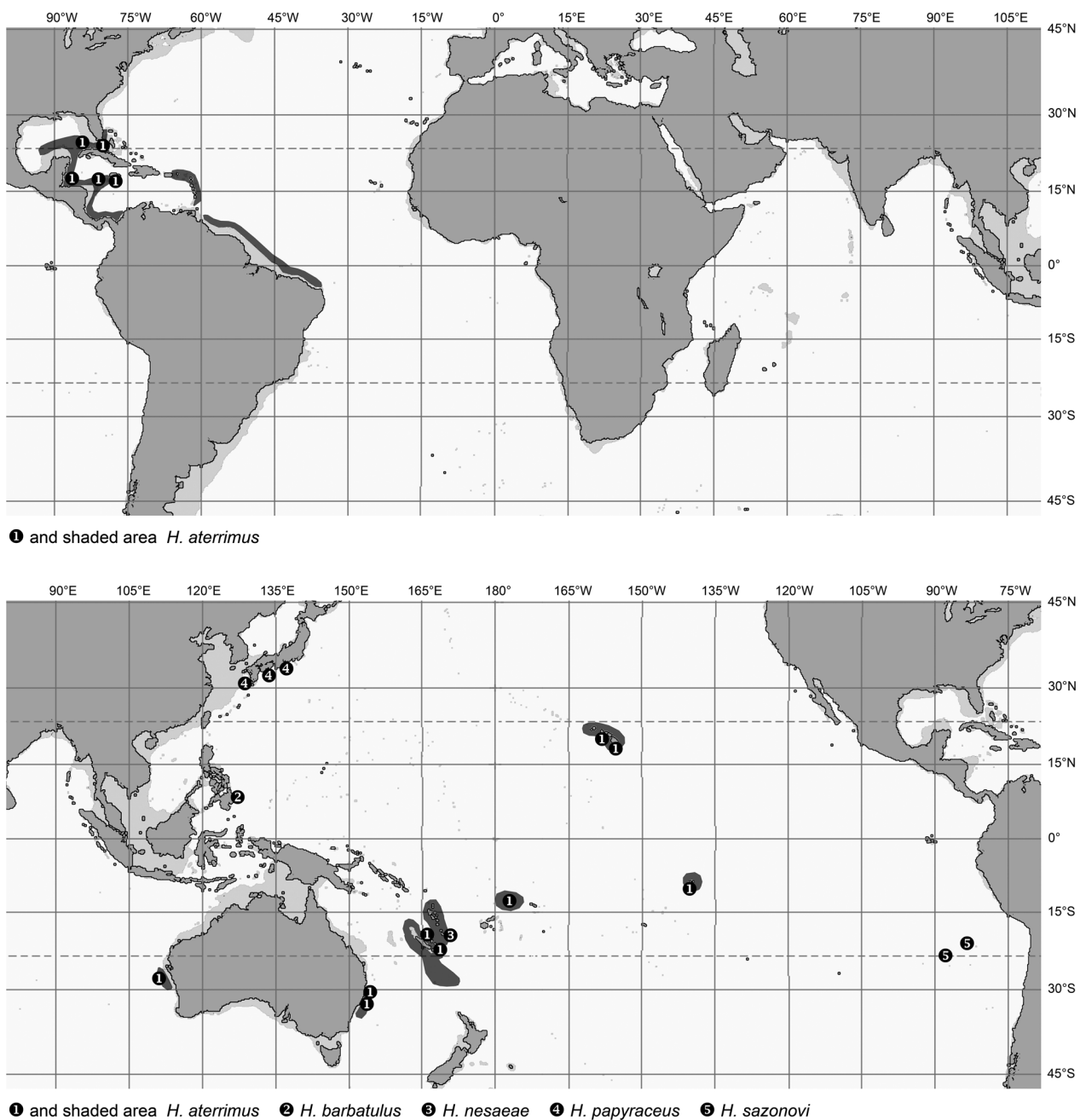


FIGURE 16. Geographical distribution of *Hymenocephalus aterrimus*, *H. barbatulus*, *H. nesaeae*, *H. papyraceus* and *H. sazonovi*.

Hymenocephalus striatulus Group

Hymenocephalus billsam Marshall & Iwamoto, 1973

Figs. 17A–H, 21

Hymenocephalus billsam Marshall & Iwamoto, 1973: 610 (type locality: off Puerto Rico, 17°49'N, 66°11'W).

Hymenocephalus billsam: Prokofiev & Kukuiev, 2009: 165.

Hymenocephalus billsamorum (name change): Iwamoto in Cohen *et al.*, 1990: 230.

Material examined. 21 specimens; 7 specimens MCZ 43045, 85+–114 mm TL, 12°26'N, 82°24'W; 6 specimens MCZ 43047, 85+–122 mm TL, 10°10'N, 59°54'W, 640 m; 5 specimens MCZ 43048, 116–138 mm TL, 16°58'N, 87°53'W, 457–731 m; 1 specimen USNM 198181 (holotype), 140 mm TL, 17°49'N, 66°11'W, 805 m; 1 specimen (otolith only) USNM 209262 (paratype #4), 15°38'N, 61°12'W, 585 m; 1 specimen (otolith only) USNM (not catalogued), R/V Oregon St. 3561.

Diagnosis. Pelvic fin rays 12–14, mostly 13–14; pectoral fin rays 14–17; snout projecting, 20–25% HL; barbel short, 4–5% HL, not reaching vertical through anterior margin of orbit; orbit diameter moderate, 28–35% HL; infraorbital width 12–15% HL; preopercular supporter moderately long, with angle at rear margin, 5–6% HL; gill rakers 23–28; ventral striae reaching to $\frac{1}{2}$ to $\frac{2}{3}$ distance from pelvic fin bases to periproct; otolith with moderately high predorsal lobe, colliculi separated, closely placed across collum, terminating at some distance from anterior and posterior rims of otolith; OL:OH = 1.05; TCL:PCL = 2.6–2.8.

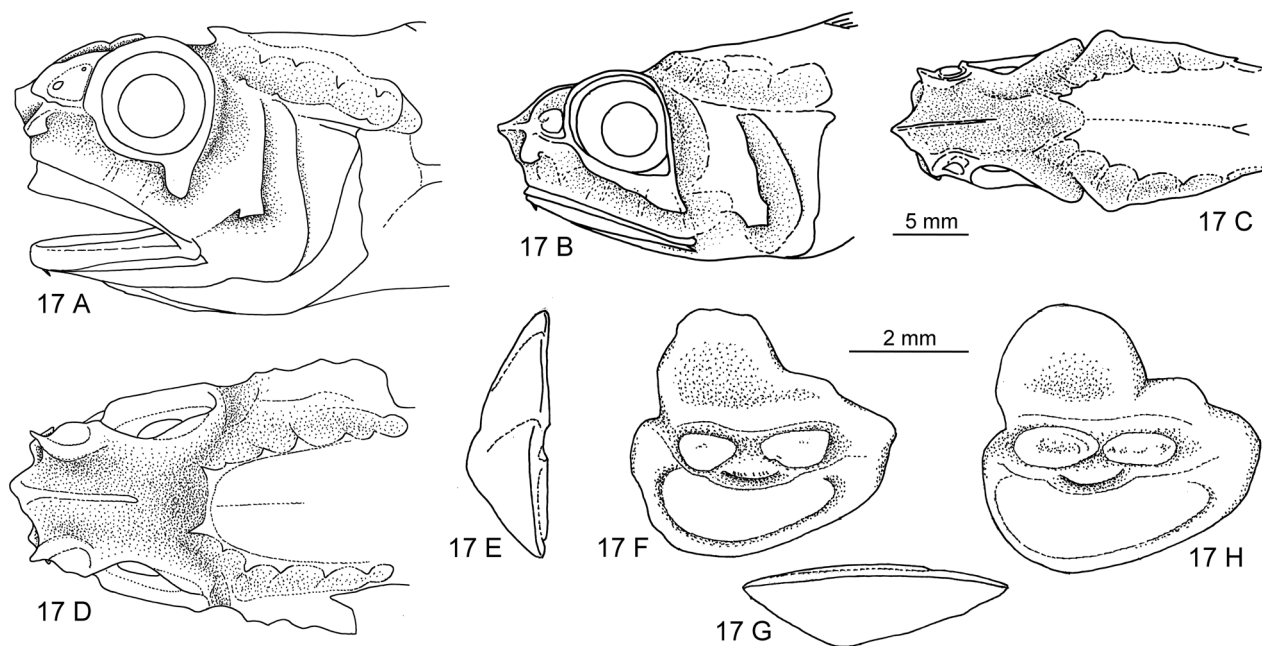


FIGURE 17. *Hymenocephalus billsam*: A, D—Holotype, USNM 198181, A—Lateral view of head, D—Dorsal view of head. B–C—MCZ 43048, B—Lateral view of head, C—Dorsal view of head. E–G—Paratype, USNM 209262, E—Anterior view of otolith, F—Inner face of otolith, G—Ventral view of otolith. H—MCZ 43048, inner face of otolith.

Comparison. *Hymenocephalus billsam* is very similar to *H. striatulus* with which it shares the presence of a small barbel. It differs in the smaller number of fin rays (12–14 vs 14–15) and somewhat smaller orbit (28–35% HL, mostly smaller 33% HL vs 32–39% HL, mostly 33–38% HL), both apparently with a certain degree of overlap. Otoliths provide for further characters for distinction, with *H. billsam* showing a more elongate otolith with a relatively short pseudocolliculum compared to *H. striatulus* (OL:OH = 1.05 vs 0.95–1.0 and TCL:PCL = 2.6–2.8 vs 1.7–2.0). From the other two species in the *striatulus* group, it differs in the presence of a small barbel (vs no barbel) and from *H. lethoneus*, also in the higher number of pelvic fin rays (mostly 13–14 vs mostly 11).

Description. Head morphology (n = 3) (Fig. 17A–D): Snout projecting, long, 20–25% HL, orbit diameter 28–35% HL (mostly 28–33% HL according to Marshall & Iwamoto, 1973), interorbital width 50–60% HW. Barbel short, 4–5% HL, not reaching vertical through anterior margin of orbit. Head canals well developed, moderately

large, infraorbital width 12–15% HL, supraorbital canal with 5 segments, width 12–15% HL, supratemporal canal narrow, above segment 3 of supraorbital canal, preopercular canal width 10–12% HL, postorbital-preopercular interspace very variable, 5–11% HL. Infranasal supporter small; infraorbital supporter short, expanding only beyond rear part of orbit, 20–50% OD; preopercular supporter moderately long, 5–6% HL, rear margin with bulge or obtuse angle, a feature typical for the *striatulus* group and first recognized in *H. billsam* by Marshall & Iwamoto (1973).

Otolith morphology (n = 6) (Fig. 17E–H): Otolith large; OL:OH = 1.05; OH:OT = 3.0. Dorsal rim with a distinct predorsal lobe, postdorsally somewhat undulating and regularly inclined towards rounded posterior tip; posterior tip shifted above sulcus termination; ventral rim regularly curved, smooth, deepest anterior of the middle; anterior rim high, nearly vertical. Inner face slightly convex, with median sulcus. Ostial and caudal colliculi small, rather narrowly placed across collum, terminating at some distance from anterior and posterior tips of otolith; pseudocolliculum short. CCL:OCL = 0.9–1.2; TCL:PCL = 2.6–2.8. Dorsal depression small; ventral furrow distinct, close to ventral rim, anteriorly and posteriorly turning upwards to the sulcus.

Distribution (Fig. 21). *Hymenocephalus billsam* is common and rather widely distributed in the Caribbean and along the east coast of the USA off North Carolina. Also known from apparently disjunct distribution off southern Brazil from 11°–24°S and over the Rio Grande Rise.

Isolated otoliths of *H. billsam* have also been obtained from sea bottom dredges off southern Azores by Schwarzhans (2013). In the same paper, other otoliths dredged from off Guinea and Ghana were also tentatively associated as *H. aff. billsam*, but these are less well-preserved and differ somewhat in their more compressed shape, a narrow collum and long pseudocolliculum. They could potentially represent another species not yet recorded from the Atlantic. All these dredged samples are supposed to be of Holocene age and indicate that *H. billsam* was distributed across a larger area in the recent past.

***Hymenocephalus lethonemus* Jordan & Gilbert, 1904**

Figs. 18A–G, 21

Hymenocephalus lethonemus Jordan & Gilbert, 1904: 615 (type locality: Sagami Bay, Japan).

Hymenocephalus lethonemus: Gilbert & Hubbs, 1916: 188; Okamura, 1970: 54.

Material examined. 26 specimens; 1 specimen BSKU 109012, 105+ mm TL, 28°33'N, 127°02'E, 621 m; 10 specimens NSMT-P 46740, 82+ –145 mm TL, 34°57'N, 138°43'E; 5 specimens NSMT-P 93138, 89+ –130+ mm TL, off Izu Island, Japan; 5 specimens NSMT-P 94418, 132+ –170 mm TL, off Yakushima, Japan; 2 specimens NMST-P 97214, 128+ –63 mm TL, 34°45'N, 138°40'E; 3 specimens USNM 51455 (1658, 1670, 1697), Suruga Bay, Japan, 128–183 m.

Diagnosis. Pelvic fin rays 11, rarely 12 on one side only; pectoral fin rays 13–15; snout projecting, 20–25% HL; barbel absent; orbit diameter moderate, 30–33% HL; infraorbital width 13–15% HL; preopercular supporter moderately long, with obtuse angle at rear margin, 3–5% HL; gill rakers 20–26; ventral striae reaching to ½ distance from pelvic fin bases to periproct; otolith with moderately high predorsal lobe, colliculi separated, widely placed across collum, terminating at some distance from anterior and posterior rims of otolith; OL:OH = 1.05–1.1; TCL:PCL = 2.4–2.6.

Comparison. *Hymenocephalus lethonemus* is very similar to *H. nascens*, with the species differentiated by Gilbert & Hubbs (1920) when they described *H. nascens*, only by the pelvic fin ray count (11 vs 12–13). The low pelvic fin ray count also defines this species best from other members of the *striatulus* group, *H. billsam* and *H. striatulus*, from which it further differs in the absence of a barbel and the generally lower pectoral fin ray count (13–15 vs 14–18). The wide collum and the short pseudocolliculum of the otoliths add further potentially useful characters for distinguishing *H. lethonemus* from *H. nascens*. (TCL:PCL = 2.4–2.6 vs 1.8–2.4). Both species are here tentatively kept separate because of the differences in pelvic fin ray counts and otolith morphology, which appear to be stable.

Description. Head morphology (n = 3) (Fig. 18A–B): Snout projecting, long, 20–25% HL, orbit diameter 30–33% HL, interorbital width 50–60% HW. Barbel absent. Head canals well developed, moderately large, infraorbital width 13–15% HL, supraorbital canal with 5 segments, width 10–13% HL, supratemporal canal narrow, above segment 4 of supraorbital canal, preopercular canal width 10–14% HL, postorbital-preopercular

interspace 6–7% HL. Infranasal supporter moderately large; infraorbital supporter short, expanding only beyond rear part of orbit, 50–70% OD; preopercular supporter moderately long, 3–5% HL, rear margin with obtuse angle.

Otolith morphology (n = 6) (Fig. 18C–G): Otolith moderately large; OL:OH = 1.05–1.1; OH:OT = 3.5. Dorsal rim with a distinct, broad predorsal lobe, entire dorsal rim undulating, with incision behind predorsal lobe; posterior tip shifted above sulcus termination; ventral rim regularly curved, smooth, deepest anterior of the middle; anterior rim high, subvertical to nearly vertical. Inner face slightly convex, with median sulcus. Ostial and caudal colliculi small, widely placed across collum, terminating at some distance from anterior and posterior tips of otolith; pseudocolliculum short. CCL:OCL = 0.8–1.1; TCL:PCL = 2.4–2.6. Dorsal depression small; ventral furrow distinct, close to ventral rim, anteriorly and posteriorly turning upwards to the sulcus.

Distribution (Fig. 21). *Hymenocephalus lethonemus* is common off southern Japan from Sagami Bay to the Ryukyu Islands.

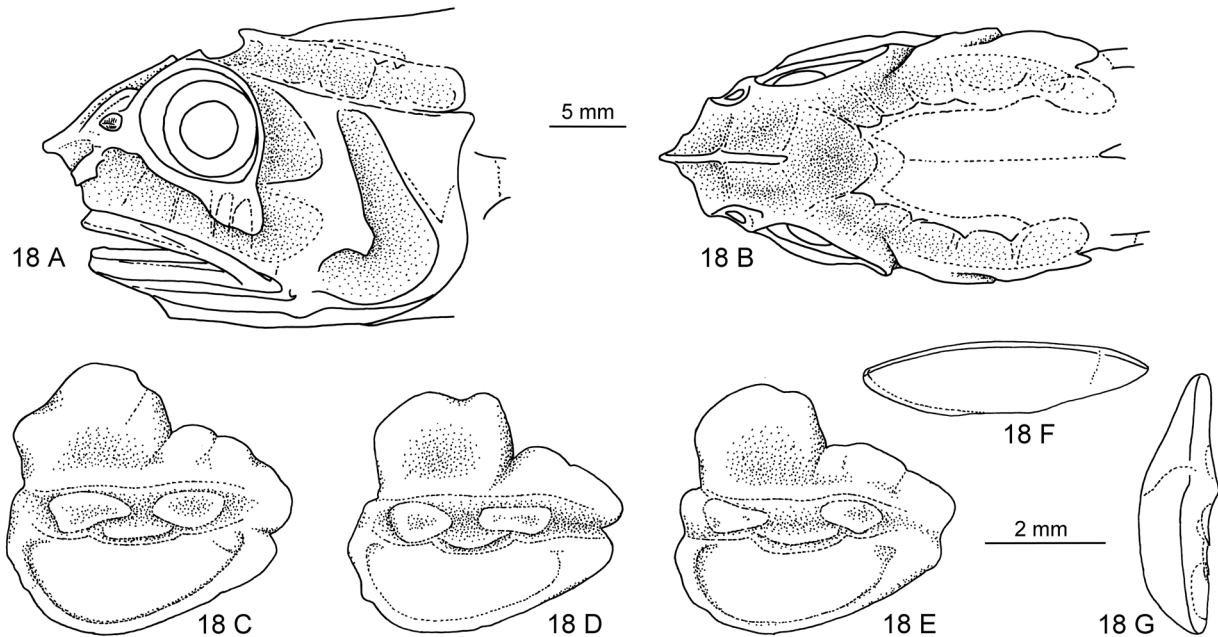


FIGURE 18. *Hymenocephalus lethonemus*: A–B—BSKU 94418, A—Lateral view of head, B—Dorsal view of head. C–G—Otoliths, C–E—Inner faces, F—Ventral view, G—Anterior view, C—NSMT P 46740, D—NSMT P 93138, E–G—BSKU 109012.

Hymenocephalus nascens Jordan & Hubbs, 1920

Figs. 19A–P, 21

Hymenocephalus nascens Jordan & Hubbs, 1920: 535 (type locality: 04°10'N, 118°37'E).

Hymenocephalus nascens: Iwamoto & Merrett, 1997: 523; Iwamoto & Williams, 1999: 177; Merrett & Iwamoto 2000: 759; Iwamoto & McCosker, 2014: 281.

Hymenocephalus lethonemus: Weber, 1913: 167.

Material examined. 24 specimens; 1 specimen AMS I.17813-009, 121+ mm TL, 22°05'S, 165°50'E, 880 m; 4 specimens BSKU 98184-98187, 99–125 mm TL, 05°56'S, 119°29'E, 630–657 m; 3 specimens (otoliths only) MNHN 1995-0873, 18°46'S, 168°55'E, 641–649 m; 3 specimens (otoliths only) MNHN 2008-2442, 16°16'S, 167°18'E, 630–690 m; 2 specimens (otoliths only) MNHN 2011-0216, 16°16'S, 167°18'E, 630–690 m; 3 specimens (otoliths only) USNM 99451, 04°06'N, 118°47'E; 1 specimen WAM P.31799-003, 135 mm TL, 21°39'S, 113°51'E; 2 specimens WAM P.32344-001, 47+–101+ mm TL, 21°29'S, 113°58'E; 1 specimen ZMUC 375859, 08°36'S, 114°34'E, 300 m; 1 specimen ZMUC 375861, off Zamboango, Philippines.

Diagnosis. Pelvic fin rays 12–13, rarely 11 on one side only; pectoral fin rays 13–16; snout projecting, 20–26% HL; barbel absent; orbit diameter moderate, 30–33% HL; infraorbital width 11–16% HL; preopercular supporter moderately long, with obtuse angle at rear margin, 4–9% HL; gill rakers 22–27; ventral striae reaching to

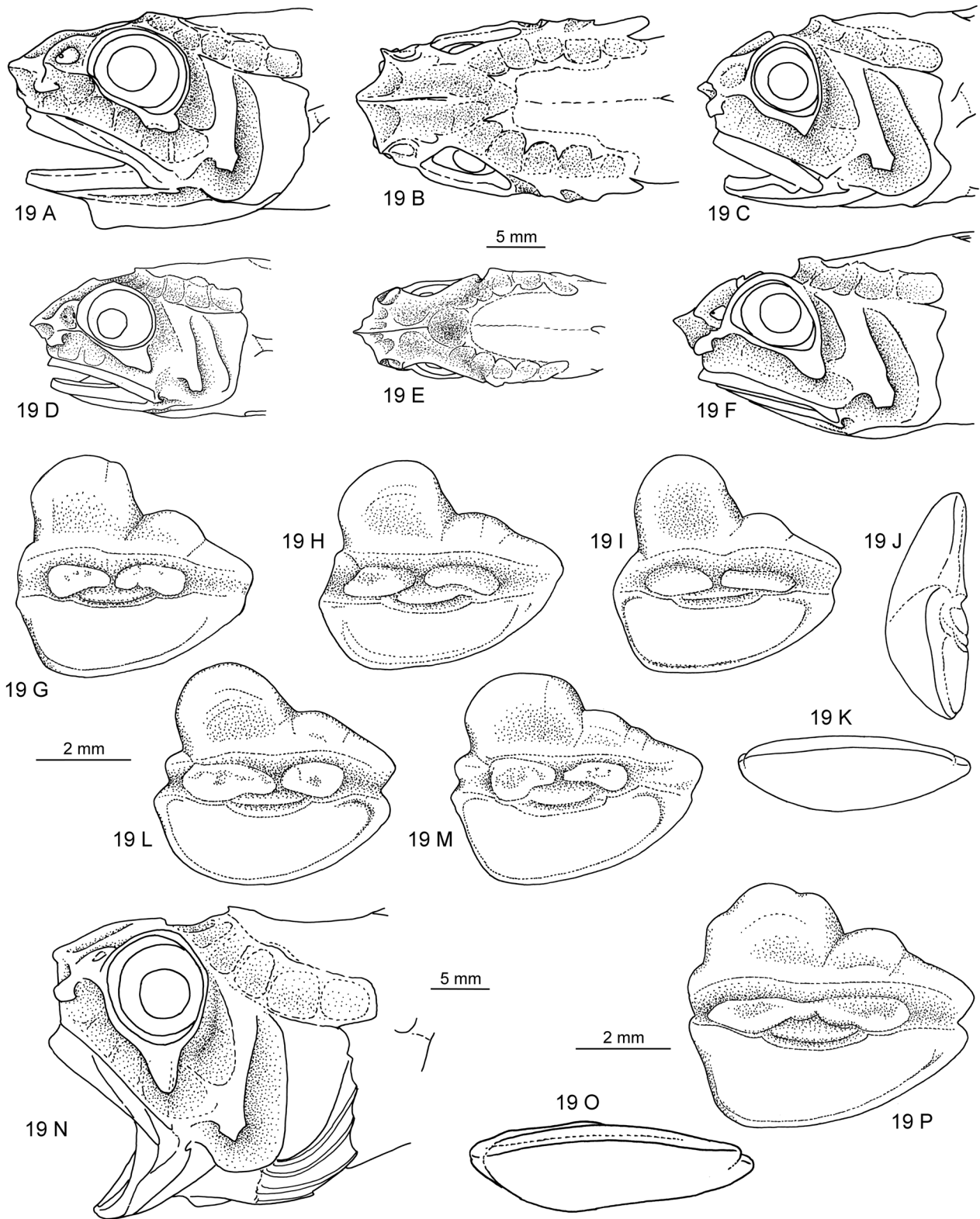


FIGURE 19. *Hymenocephalus nascens*: A–B—MNHN 1995-0873, A—Lateral view of head, B—Dorsal view of head. C—BSKU 098184, lateral view of head. D–E—WAM P.32344-001, D—Lateral view of head, E—Dorsal view of head. F—AMS I.17813-009, lateral view of head. G–M, O–P—Otoliths, G–I, L–M, P—Inner faces, J—Anterior view, K, O—Ventral views, G—WAM P.32344-001, H—BSKU 98184, I–K—BSKU 98187, L–M—USNM 99451, O–P—WAM P.31799-003. N—WAM P.31799-003, lateral view of head.

½ distance from pelvic fin bases to periproct; otolith with moderately high predorsal lobe, colliculi separated, narrowly placed across collum with a tendency to joining in large specimens, terminating at some distance from anterior and posterior rims of otolith; OL:OH = 1.1–1.2; TCL:PCL = 1.8–2.4.

Comparison. *Hymenocephalus nascens* is very similar to *H. lethonemus* (see above). Gilbert & Hubbs (1920) mentioned a single difference between the two species being the pelvic fin ray count with dominantly 12–13 in *H. nascens* and 11 in *H. lethonemus*, however, with a number of specimens in both species exhibiting 11 fin rays on one fin and 12 on the other. Since otoliths also exhibit some subtle difference in proportions and collum width (see above), I am tentatively regarding both nominal species valid subject to later investigations.

Description. Head morphology (n = 5) (Fig. 19A–F, N): Snout projecting, long, 20–26% HL, orbit diameter 30–33% HL, interorbital width 50–60% HW. Barbel absent. Head canals well developed, moderately large, infraorbital width 11–16% HL, supraorbital canal with 5 segments, width 10–16% HL, supratemporal canal narrow, above segment 4 of supraorbital canal, preopercular canal width 9–15% HL, postorbital-preopercular interspace 4–10% HL. Infranasal supporter moderately large; infraorbital supporter short, expanding only beyond rear part of orbit, 30–50% OD; preopercular supporter moderately long, 4–9% HL, rear margin with obtuse angle. *Hymenocephalus nascens* was represented in collections by a relatively large number of well-preserved specimens from a variety of locations. This allowed mapping a larger degree the variability in morphometric characters of the head than was possible with most other species investigated.

Otolith morphology (n = 13) (Fig. 19G–M, O–P): Otolith moderately large; OL:OH = 1.1–1.2; OH:OT = 3.0. Dorsal rim with a distinct, narrow, slightly forward inclined predorsal lobe with rounded tip, distally marked by incision; posterior tip shifted above sulcus termination; ventral rim regularly curved, smooth, deepest anterior of the middle; anterior rim high, subvertical to nearly vertical. Inner face slightly convex, with median sulcus. Ostial and caudal colliculi moderately small, narrowly placed across collum, terminating at some distance from anterior and posterior tips of otolith; pseudocolliculum moderately long. CCL:OCL = 0.7–1.1; TCL:PCL = 1.8–2.4. Dorsal depression small; ventral furrow distinct, close to ventral rim. Otoliths of the largest specimen available (Fig. 19O–P) show a reduced height of the predorsal lobe and an incipient joining of the colliculi. All other characters including detailed head morphology (Fig. 19N) are within the range of *H. nascens*. It is therefore assumed that these changes in otolith morphology reflect late-stage ontogenetic changes, something which otherwise has not been observed much in *Hymenocephalus* otoliths.

Distribution (Fig. 21). *Hymenocephalus nascens* is common and widespread in the West Pacific, from the Philippines off Luzon to the Flores and Halmahera Seas, around the island chains of the Solomons, Vanuatu, Fiji, Wallis and Futuna, New Caledonia and Norfolk Ridge, Chesterfield Plateau and Lord Howe Rise, and the eastern coast of Australia off New South Wales and Western Australia from the Dampier Archipelago to off Northwest Cape.

Hymenocephalus striatulus Gilbert, 1905

Figs. 20A–G, 21

Hymenocephalus striatulus Gilbert, 1905: 665 (type locality: off south coast of Oahu, Hawaii).

Hymenocephalus striatulus: Sazonov & Iwamoto, 1992: 63.

Material examined. 14 specimens; 1 specimen USNM 51611 (holotype), 114 mm TL, off southern coast of Oahu, 350–643 m; 2 specimens USNM 406680, 75+ and 120+ mm TL, 21°13'N, 157°43'W, 567 m; 3 specimens (otoliths only) USNM 51683, off Hawaii (no further details); 4 specimens ZMMGU P-17720, 63+–165 mm TL, 25°07'S, 99°26'W, 730–790 m; 4 specimens ZMMGU P-22382, 24°59'S, 88°25'W, 550–560 m.

Diagnosis. Pelvic fin rays 14–15; pectoral fin rays 15–18; snout projecting, 20–25% HL; barbel rudimentary or very short, 0–3% HL, not reaching vertical through anterior margin of orbit; orbit diameter moderate, 32–39% HL (mostly 33–38% HL); infraorbital width 10–12% HL; preopercular supporter moderately long, with obtuse angle at rear margin, 3–4% HL; gill rakers 25–29; ventral striae reaching to ½ from pelvic fin bases to periproct; otolith with moderately high predorsal lobe, colliculi separated, closely placed across collum, terminating far from anterior and posterior rims of otolith; OL:OH = 0.9–1.0; TCL:PCL = 1.7–2.0.

Comparison. *Hymenocephalus striatulus* is very similar to *H. billsam* with which it shares the presence of a

small, sometimes only rudimentary barbel. For differences see *H. billsam*. The presence of a barbel, the slightly larger orbit size (33–38% HL vs 30–33% HL), and the higher pelvic fin ray count (14–15 vs 11–13) distinguishes *H. striatulus* from *H. lethoneus* and *H. nascens*.

Description. Head morphology (n = 2) (Fig. 20A–B): Snout projecting, long, 20–25% HL, orbit diameter 32–39% HL (mostly 33–38% HL according to Marshall & Iwamoto, 1973), interorbital width 50–60% HW. Barbel rudimentary or short, 0–3% HL. Head canals well developed, moderately large, infraorbital width 10–12% HL, supraorbital canal with 4–5 segments, width 14–16% HL, supratemporal canal not identified, preopercular canal width 12–14% HL, postorbital-preopercular interspace about 10% HL. Infranasal supporter rather large; infraorbital supporter short, expanding only beyond rear part of orbit, 40–50% OD; preopercular supporter moderately long, 3–4% HL, rear margin with indistinct bulge.

Otolith morphology (n = 9) (Fig. 20C–G): Otolith moderately large; OL:OH = 0.9–1.0; OH:OT = 3.0–3.5. Dorsal rim with a distinct, high and broad predorsal lobe, distally marked by indentation; posterior tip shifted above sulcus termination; ventral rim deep and regularly curved, deepest slightly anterior of the middle; anterior rim high; all rims more or less intensely crenulated. Inner face slightly convex, with median sulcus. Ostial and caudal colliculi very small, rather narrowly placed across collum, terminating far from anterior and posterior tips of otolith; pseudocolliculum moderately long. CCL:OCL = 0.7–1.1; TCL:PCL = 1.7–2.0. Dorsal depression small; ventral furrow rather indistinct, running at some distance from ventral rim of otolith.—Otoliths from larger specimens from USNM 406680 and ZMMGU P-17720 show a slightly more elongate shape in the range of OL:OH = 1.0–1.1, which I consider to reflect allometric ontogenetic growth. However, all these specimens are too poorly preserved to warrant figuring.

Discussion. When Sazonov & Iwamoto (1992) described *H. striatulus* from the Sala y Gomez Ridge in the SE Pacific, they noticed that those specimens only differ from the ones of the type locality, Hawaii, in the more distinct development of the barbel. They concluded that they “did not feel this single difference to be sufficient to recognize the species as distinct from *H. striatulus*”. My investigations of the head morphology and the otoliths, the latter however hampered by poor preservation of the otoliths from the specimens from Sala y Gomez, do not add any further aspects and hence support their view of a single valid species, despite the considerable geographical distance between the two areas.

Distribution (Fig. 21). Known from off Hawaii and Sala y Gomez.

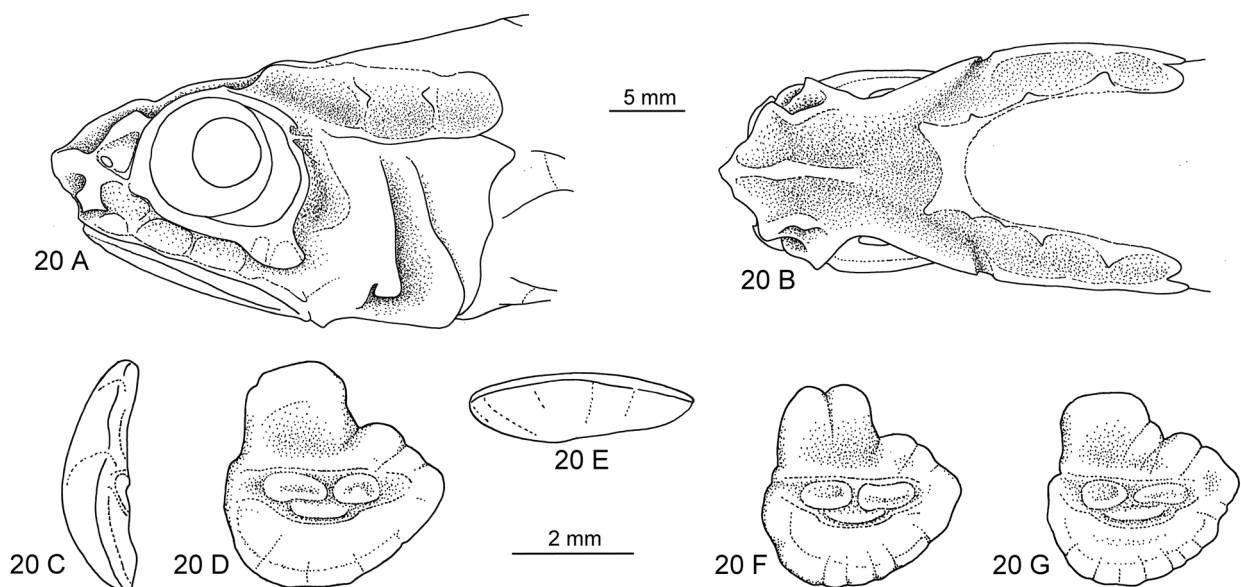


FIGURE 20. *Hymenocephalus striatulus*: A–B—Holotype, USNM 51611, A—Lateral view of head, B—Dorsal view of head. C–G—Otoliths, USNM 51683, C—Anterior view, D, F, G—Inner faces, E—Ventral view.

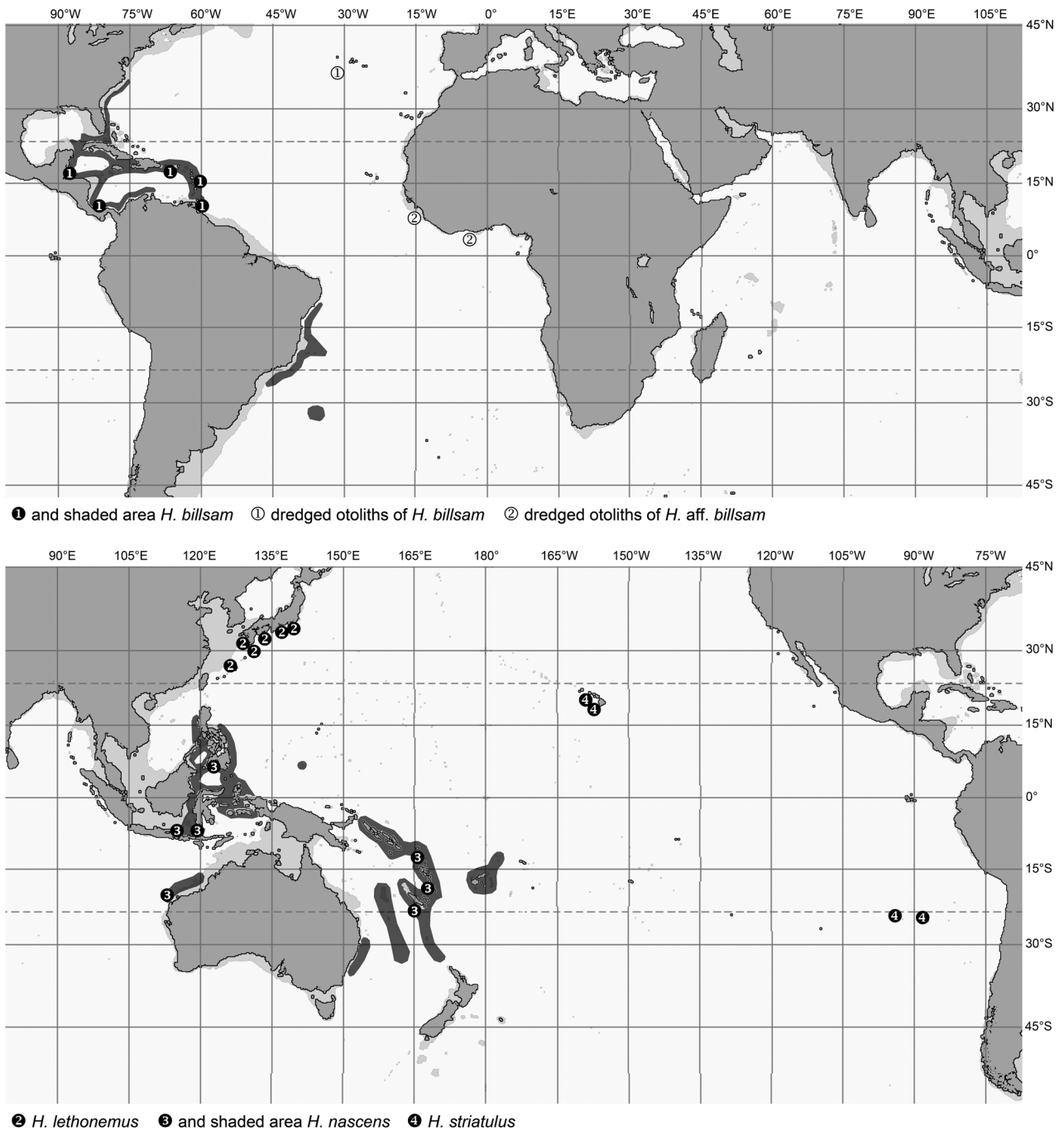


FIGURE 21. Geographical distribution of *Hymenocephalus billsam*, *H. lethonemus*, *H. nascens* and *H. striatulus*.

Hymenocephalus antraeus Group

Hymenocephalus antraeus Gilbert & Cramer, 1897

Figs. 22A–G, 27

Hymenocephalus antraeus Gilbert & Cramer, 1897: 428 (type locality: 21°08'N, 157°49'W).

Material examined. 9 specimens; 6 specimens LACM 57119, 120+ –171 mm TL, off Hawaii, R/V Townsend Cromwell TC 52–88; 3 specimens USNM 47735 (syntypes), 130–145 mm TL, 21°08'N, 157°49'W, 627 m.

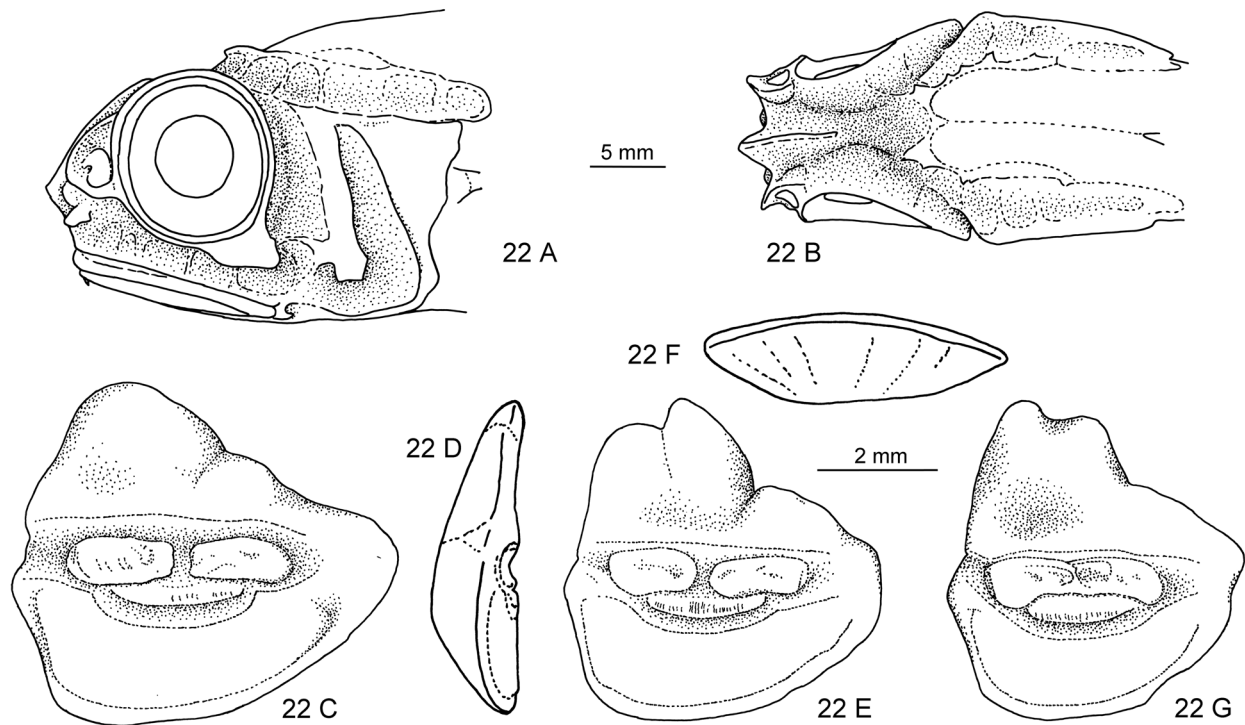


FIGURE 22. *Hymenocephalus antraeus*: A–B—LACM 57119-1, A—Lateral view of head, B—Dorsal view of head. C–G—Otoliths, USNM 47735, C, E, G—Inner faces, D—Anterior view, F—Ventral view.

Diagnosis. Pelvic fin rays 11–12, mostly 12; pectoral fin rays 13–15, rarely 16; snout barely projecting, short, 15–18% HL; barbel short, 3–4% HL; orbit diameter large, 35–40% HL; infraorbital width 8–10% HL; preopercular supporter moderately long, with obtuse angle at rear margin, 5–7% HL; gill rakers 21–24; ventral striae reaching to $\frac{1}{2}$ from pelvic fin bases to periproct; otolith with high predorsal lobe, colliculi separated, narrowly placed across collum with occasional tendency to partly join, terminating at some distance from anterior and posterior rims of otolith; OL:OH = 0.95–1.1; TCL:PCL = 1.6–1.7.

Comparison. *Hymenocephalus antraeus* differs from other members in the *antraeus* Group primarily in the larger orbit (35–40% HL vs 30–35% HL), higher number of pelvic fin rays (11 to mostly 12 vs 7–11), narrow infraorbital width (8–10% HL vs 10–16% HL), and presence of an obtuse angle at the rear margin of the preopercular supporter (vs. straight in all other members of the group). The last character is shared with species of the *striatulus* Group, from which *H. antraeus* differs in its short, barely projecting snout (15–18% HL vs 20–25% HL), large orbit (except for *H. striatulus*), and long pseudocolliculum (TCL:PCL = 1.6–1.7 vs 1.7–2.8).

Description. Head morphology (n = 2) (Fig. 22A–B): Snout short, rounded, barely projecting, 15–18% HL, orbit diameter large, 35–40% HL, interorbital width 50–60% HW. Barbel short, 3–4% HL, not reaching vertical through anterior edge of orbit. Head canals well developed, variably large, infraorbital width narrow, 8–10% HL, supraorbital canal with 6 segments, width 11–13% HL, supratemporal canal moderately developed, above segment 4 of supratemporal canal, preopercular canal width 11–13% HL, postorbital-preopercular interspace 7–8% HL. Infranasal supporter small; infraorbital supporter short, expanding only beyond rear part of orbit, 40–50% OD; preopercular supporter moderately long, 5–7% HL, rear margin with obtuse angle.

Otolith morphology (n = 4) (Fig. 22C–G): Otolith large; OL:OH = 0.95–1.1; OH:OT = 3.5. Dorsal rim with a distinct, broad, somewhat irregularly formed predorsal lobe with pointed tip, distally marked by small incision; posterior tip shifted above sulcus termination; ventral rim deep, regularly curved, smooth, deepest anterior of the middle; anterior rim high, subvertical to nearly vertical. Inner face slightly convex, with median sulcus. Ostial and caudal colliculi moderately small, narrowly placed across collum, terminating at some distance from anterior and posterior tips of otolith; pseudocolliculum long. CCL:OCL = 0.95–1.15; TCL:PCL = 1.6–1.7. Dorsal depression small; ventral furrow distinct, moderately close to ventral rim. One otolith was found with nearly joined colliculi

(Fig. 22G). Together with one other case observed in *H. nascens*, this is the only instance of incipient joining of colliculi in the otoliths of species of *Hymenocephalus*.

Distribution (Fig. 27). Apparently endemic to Hawaii.

Hymenocephalus hachijoensis Okamura, 1970

Figs. 23A–D, 27

Hymenocephalus striatissimus hachijoensis Okamura, 1970: 50 (type locality: 33°16'N, 140°03'E).

Hymenocephalus hachijoensis: Okamura, 1984: 93; Sazonov & Iwamoto, 1992: 62.

Material examined. 2 specimens BSKU 14171 (holotype), 195 mm TL, and BSKU 14172 (paratype), 130 mm TL, 33°16'N, 140°03'E, 570 m.

Diagnosis. Pelvic fin rays 7–8; pectoral fin rays 14–15; snout barely projecting, short, 15–17% HL; barbel long, 30–35% HL, reaching vertical through center of orbit; orbit diameter large, 35–38% HL; infraorbital width 10–12% HL; preopercular supporter moderately long, with straight rear margin, 6–7% HL; gill rakers 18–20; ventral striae reaching to ½ distance from pelvic fin bases to periproct; otolith with high predorsal lobe, colliculi separated, narrowly placed across collum; OL:OH = 1.05; TCL:PCL = 1.6.

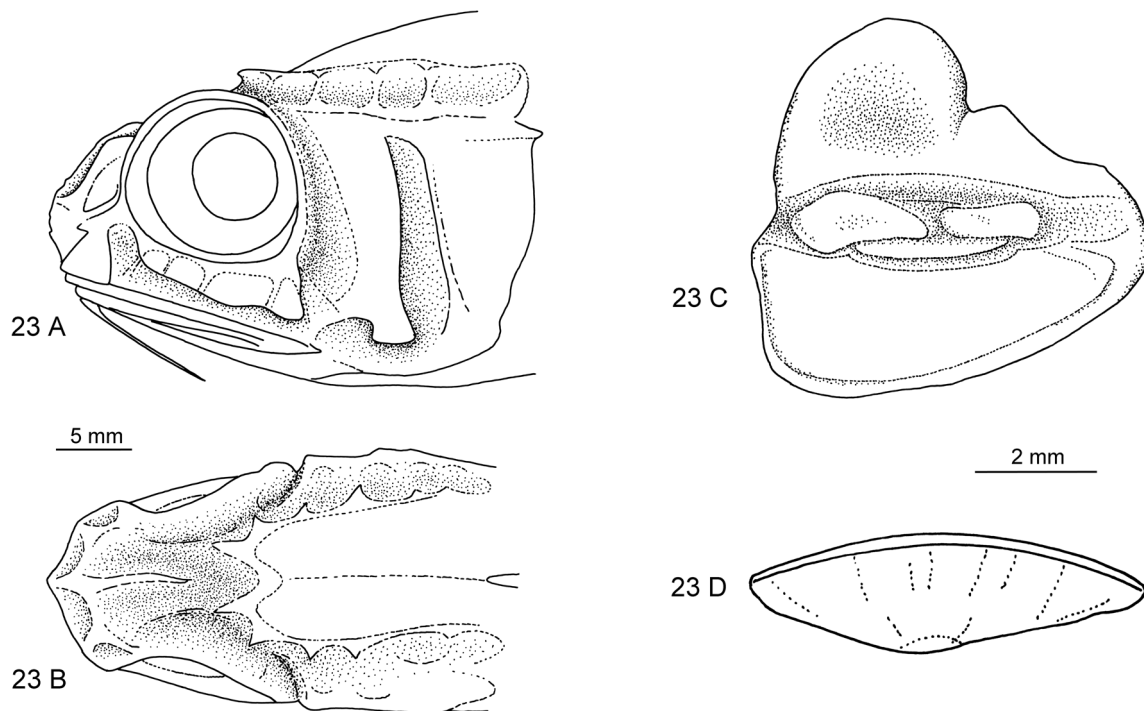


FIGURE 23. *Hymenocephalus hachijoensis*, Holotype, BSKU 14171: A—Lateral view of head, B—Dorsal view of head, C—Inner face of otolith, D—Ventral view of otolith.

Comparison. *Hymenocephalus hachijoensis* is readily recognized by the long barbel, which is shorter than in *H. longibarbis* and *H. iwamotoi*, of about the same length as in *Hymenogadus gracilis*, and longer than in any other species of the genus *Hymenocephalus*, with those of *H. aeger* coming closest at 20–25% HL. The short, rounded snout resembles species in the *striatissimus* Group, like the low number of pelvic fin rays (7–8 vs 10–12 in other members of the *antraeus* Group) and the long infraorbital supporter. The separated colliculi and only moderately enlarged pseudocolliculum easily distinguish *H. hachijoensis* from species of the *H. striatissimus* Group. These observations support the concept first expressed by Okamura (1984) to elevate *H. hachijoensis* to species level.

Description. Head morphology (n = 2) (Fig. 23A–B): Snout short, rounded, barely projecting, 15–17% HL, orbit diameter large, 35–38% HL, interorbital width 50–60% HW. Barbel long, 30–35% HL, reaching vertical through center of orbit. Head canals well developed, infraorbital width 10–12% HL, supraorbital canal with 5

segments, width 9–10% HL, supratemporal canal not identified, preopercular canal width 9–10% HL, postorbital-preopercular interspace 8–10% HL. Infranasal supporter very large, touching upper lip; infraorbital supporter long, expanded beyond entire orbit, 90–100% OD; preopercular supporter moderately long, 6–7% HL, rear margin straight.

Otolith morphology (n = 1) (Fig. 23C–D): Otolith large; OL:OH = 1.05; OH:OT = 3.2. Dorsal rim with a distinct, moderately broad predorsal lobe with rounded tip, distally marked by small incision; posterior tip at about level of sulcus termination; ventral rim deep, regularly curved, smooth, deepest anterior of the middle; anterior rim high, nearly vertical. Inner face slightly convex, with slightly supramedian sulcus. Ostial and caudal colliculi moderately small, narrowly placed across collum, terminating moderately close to anterior rim and at some distance from posterior tip of otolith; pseudocolliculum long. CCL:OCL = 0.75; TCL:PCL = 1.6. Dorsal depression small; ventral furrow distinct, moderately close to ventral rim.

Distribution (Fig. 27). *Hymenocephalus hachijoensis* was originally described only from the type locality off the small Hachijo Island on the Iwo Jima Ridge off southern central Japan. Sazonov & Iwamoto (1992:63) also recorded specimens caught over seamounts of the Emperor Ridge (32°N, 173°E and 41°04'N, 170°32'E) and on the Kyushu-Palau Ridge (no geographic details recorded).

Hymenocephalus heterolepis (Alcock, 1889)

Figs. 24A–M, 27

Macrurus heterolepis Alcock 1889: 396 (syntypes from: Andaman Sea, off Ross Island, and Bay of Bengal, between North and South Sentinel Islands).

Macrurus (Mystaconurus) heterolepis: Alcock 1891: 122 and 309 (figure).

Macrurus (Mystaconurus) cavernosus: Alcock 1899: 117 (records from Andaman Sea only).

Hymenocephalus heterolepis: Iwamoto in Cohen et al. 1990: 231.

Material examined. 114 specimens; 1 specimen BMNH 1890.7.31.6 (syntype), about 120 mm TL, Andaman Sea, off Ross Island; 98 specimens CAS 50132, 83+ –121 mm TL, 10°39'N, 96°34'E, 367–375 m; 15 specimens CAS 50124, 91+ –120+ mm TL, 10°39'N, 97°06'E, 293 m.

Diagnosis. Pelvic fin rays 10–11; pectoral 11–13; gill rakers 22–25. Barbel short, 5–10% HL, not reaching vertical through anterior rim of orbit. Orbit 28–32% HL. Snout pointed, protruding, 17.5–20% HL. Ventral striae extending to about $\frac{2}{3}$ the distance from pelvic fin bases to periproct (Fig. 24F). Otolith compressed, OL:OH = 0.9–0.95; colliculi separated, small, narrowly placed across collum; pseudocolliculum long, TCL:PCL = 1.5–1.7.

Comparison. *Hymenocephalus heterolepis* resembles *H. italicus*, with which it commonly has been synonymized (first synonymized with *H. cavernosus* by Alcock (1899), see below under *H. italicus*) and the new species *H. punt* described in the following. From *H. italicus* it differs in the smaller orbit (28–33 % HL vs 35–40% HL) and the separated colliculi of the otolith (vs joined). The additional distinguishing character of the otoliths supports the recognition of the species. For distinction from *H. punt* n.sp. see below.

Description. Head morphology (n = 4) (Fig. 24A–E): Snout moderately long, pointed, projecting, 17.5–20% HL, orbit diameter small, 28–32% HL, interorbital width 60–65% HW. Barbel short, 5–10% HL, not reaching vertical through anterior rim of orbit. Head canals well developed, infraorbital width 12–16% HL, supraorbital canal with 5 to 6 segments, width 12–15% HL, supratemporal canal rarely observable, above segment 4 of supraorbital canal, preopercular canal width 13–15% HL, postorbital-preopercular interspace 6–8% HL. Infranasal supporter moderately large; infraorbital supporter short, expanding only beyond rear part of orbit, 35–70% OD; preopercular supporter moderately long, 6–8% HL, with straight rear margin.

Otolith morphology (n = 7) (Fig. 24H–M): Otolith large; OL:OH = 0.9–0.95; OH:OT = 3.2–3.5. Dorsal rim with large, very broad, somewhat crenulated predorsal lobe with mostly pointed tip, distally inclining to posterior tip without marked incision; posterior tip at about level of sulcus termination; ventral rim deep, regularly curved, smooth, deepest anterior of the middle; anterior rim high, subvertical to nearly vertical. Inner face slightly convex, with median sulcus. Ostial and caudal colliculi small, narrowly placed across collum, terminating far from anterior and posterior tips of otolith; pseudocolliculum long. CCL:OCL = 0.9–1.3; TCL:PCL = 1.5–1.7. Dorsal depression moderately large, indistinct; ventral furrow distinct, moderately close to ventral rim.

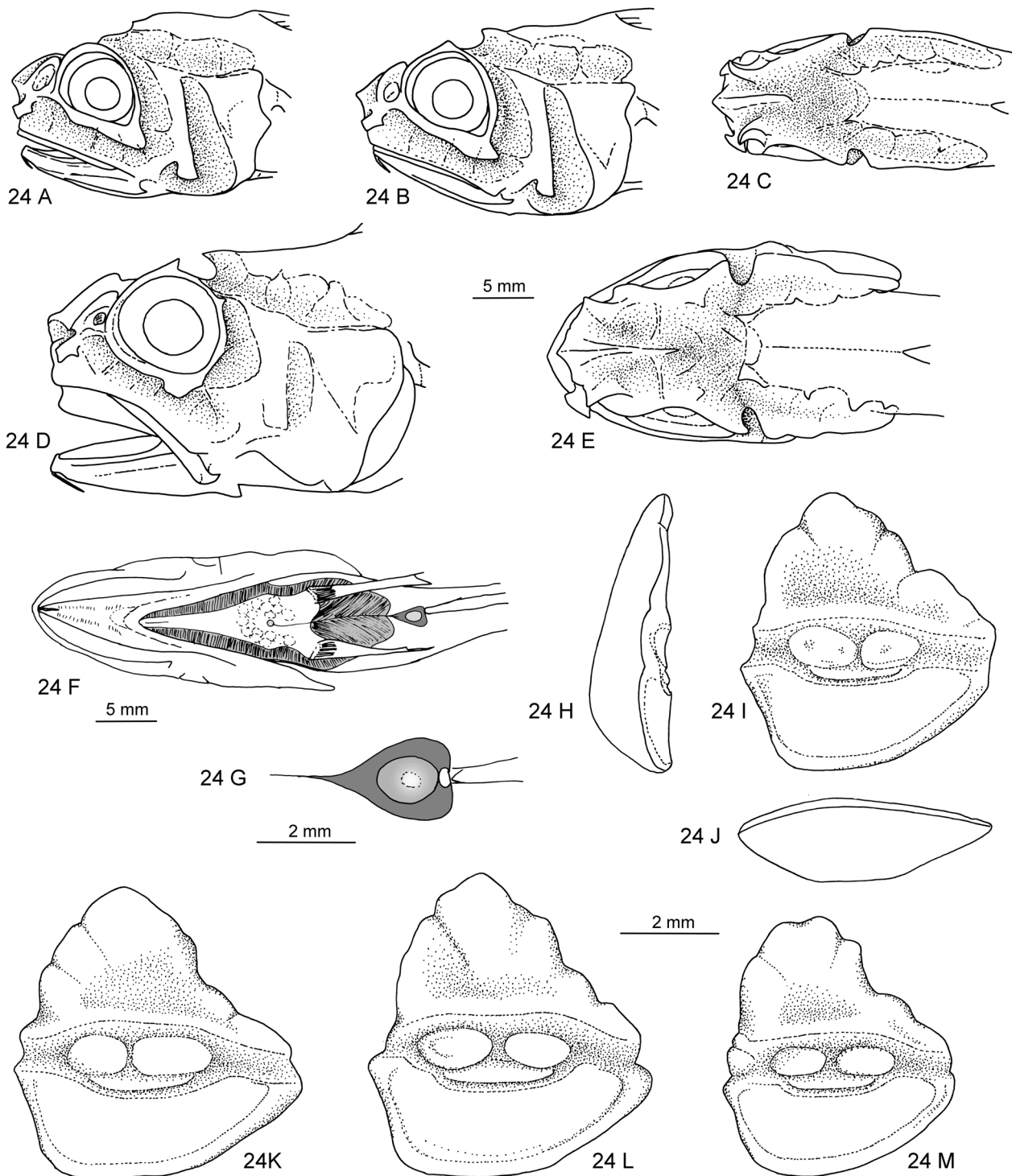


FIGURE 24. *Hymenocephalus heterolepis*: A—CAS 50132, TL 93+ mm, lateral view of head. B—CAS 50132, TL 85+ mm, B—Lateral view of head, C—Dorsal view of head. D—Syntype, BMNH 1890.7.31.6, D—Lateral view of head, E—Dorsal view of head. F—CAS 50132, TL 85+ mm, F—Ventral view of head and trunk, G—detail view of posterior lens of ventral luminescent organ. H—M—Otoliths, CAS 50132, H—Anterior view, I, K—M—Inner faces, J—Ventral view.

Discussion. Alcock (1899) stated that he was "satisfied by actual comparison of the specimens with one received from the Smithsonian Institution, that the species described by him as *Mystacomurus heterolepis* is the same as Goode and Bean's *Hymenocephalus cavernosus*", and he believed "that both these names will prove to be synonyms of Giglioli's *Hymenocephalus italicus* from the Mediterranean". After analysis of the specimens available to me, and in particular after investigation of the size of the orbit and the morphology of the otoliths, I

conclude that *H. heterolepis* should be recognized as a valid species, in line with the recommendation made by Iwamoto (in Cohen *et al.*, 1990).

Distribution (Fig. 27). *Hymenocephalus heterolepis* appears to be geographically restricted to the sea around the Andaman Islands and the western coast of the Malay Peninsula.



FIGURE 25. *Hymenocephalus punt*: A—Paratype, ZMMGU-P 23600, TL 140 mm (photo M. Krag). B—Holotype ZMMGU-P 23599, TL 106+ mm (photo M. Krag).

***Hymenocephalus punt* n.sp.**

Figs. 1D–F, 25A–B, 26A–K, 27

Material examined. (30 specimens, 87–168 mm TL.) Holotype ZMMGU P-23599, 106+ mm TL, off western Socotra, Yemen, 12°18' to 12°14'N, 53°09' to 53°06'E, 375–380 m, bottom shrimp trawl, Vityaz cruise 17, station 2560, 27 October 1988; Paratypes: ZMMGU P-23600 (ex IORAS 00222), 5 specimens, 99–140 mm, same data as holotype (further 16 specimens not studied). ZMMGU P-23601 (ex IORAS 00223), 6 specimens, 87–146 mm TL (further 3 specimens not studied), 12°20' to 12°13'N, 53°11' to 53°06'E, 384–390 m, bottom trawl, Vityaz cruise 17, station 2566, 28 October 1988. ZMMGU P-23602 (ex IORAS 00229), 1 specimen, 125 mm TL (further 1 specimen not studied), 12°19' to 12°13'N, 53°09' to 53°05'E, 395–420 m, bottom shrimp trawl, Vityaz cruise 17, station 2830, 16 January 1989. ZMMGU P-23603, 2 specimens, 155–168 mm TL, 16°14'N, 52°41'E, 490–530 m, Dm. Stefanov cruise 3, trawl 143, 15 February 1989. USNM 301271, 3 specimens, 81+–130 mm TL, 12°01'N, 51°16'E, 375–393 m, bottom trawl, Beinta cruise 20, haul 18, 12 March 1987, G. and J. Small. BMNH 1939.5.24.691–702, 12 specimens, 13°41' to 13°13' N, 46°14' to 46°10'E, 441 m, Murray Expedition station 35, 16 October 1933.

Diagnosis. Pelvic fin rays 10–11; pectoral (13) 14–15; gill rakers 20–24. Barbel moderately long 11–15% HL, reaching vertical through anterior rim of orbit. Orbit 28–30% HL. Snout pointed, protruding, 17.5–20% HL. Ventral striae extending to about 1/3 to 1/2 the distance from pelvic fin bases to periproct. Otolith moderately compressed (OL:OH = 1.0–1.05); colliculi separated, small; pseudocolliculum small (TCL:PCL = 1.9–2.2).

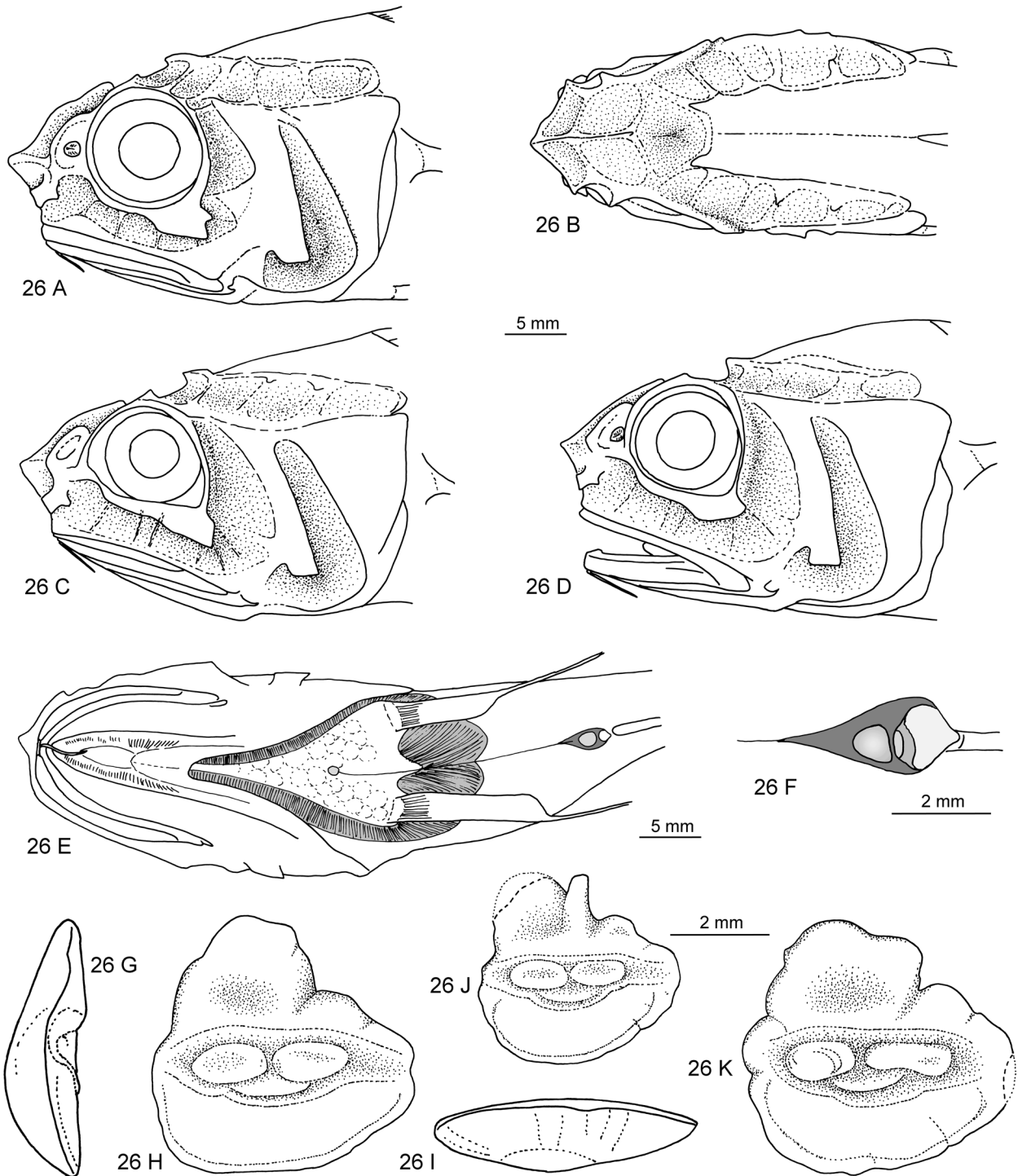


FIGURE 26. *Hymenocephalus punt*: A–B—Holotype, ZMMGU-P 23599, TL 106+ mm, A—Lateral view of head, B—Dorsal view of head. C—Paratype, ZMMGU-P 23602, TL 125+ mm, lateral view of head. D—Paratype, ZMMGU-P 23603, TL 168 mm, lateral view of head. E–F—Paratype, ZMMGU-P 23600, TL 99+ mm, E—Ventral view of head and trunk, F—detail view of posterior lens of ventral luminescent organ. G–K—Otoliths, G—Anterior view, H, J, K—inner faces, I—Ventral view, G–I—Paratype, ZMMGU-P 23600, TL 140 mm, J—Paratype, USNM 301271, TL 130 mm, K—Paratype ZMMGU-P 23600, TL 99+mm.

Comparison. *Hymenocephalus punt* is related to *H. heterolepis* from which it differs in a number of rather subtle characters as follows: pectoral fin rays 14–16, rarely 13 seen on one side only (vs 11–13), luminescent striae reaching about one third to half the distance from ventral fin bases to periproct (vs two thirds the distance to nearly

reaching the periproct), barbel reaching vertical through anterior rim of orbit / 11–15% HL (vs not reaching vertical through anterior rim of orbit / 6–9% HL), OL:OH = 1.0–1.1 (vs 0.9–0.95) and TCL:PCL = 1.9–2.2 (vs 1.5–1.7).

Description. Counts (from 28 specimens): 1D. II,8 (II,8–10); P. 14 (14–15, occasionally 13 on one side); V. 11 (10–11); first gill raker inner side 22 (20–24); second gill raker outer side 23 (20–24).

Measurements (from holotype and two best-preserved paratypes): head length 32.8–33.7 mm, about 20% TL (from PT ZMMGU P-23603, 168 mm TL); head height 72–76% HL; head width 52% HL (holotype only); barbel 11–15% HL; snout 17.5–20% HL; orbit 28–30% HL; postorbital 50–54%HL; interorbital 32% HL / 61% HW (holotype only); upper jaw length 47–49% HL; pre-anal about 150% HL; pre-dorsal to 1D about 90–100% HL; pre-dorsal to 2D about 180–190% HL; distance base 1D to 2D about 90–100% HL; 1st dorsal fin length about 70% HL, the first fin ray being slightly longer than the subsequent ones; pectoral fin length 70–75% HL, the first fin ray being markedly longer than the subsequent ones; ventral fin length, 1st ray 95% HL, 2nd ray 50–55% HL; supraorbital canal width 10–13% HL; infraorbital width 9.5–12% HL; minimal infraorbital canal width 6.0–7.5% HL.

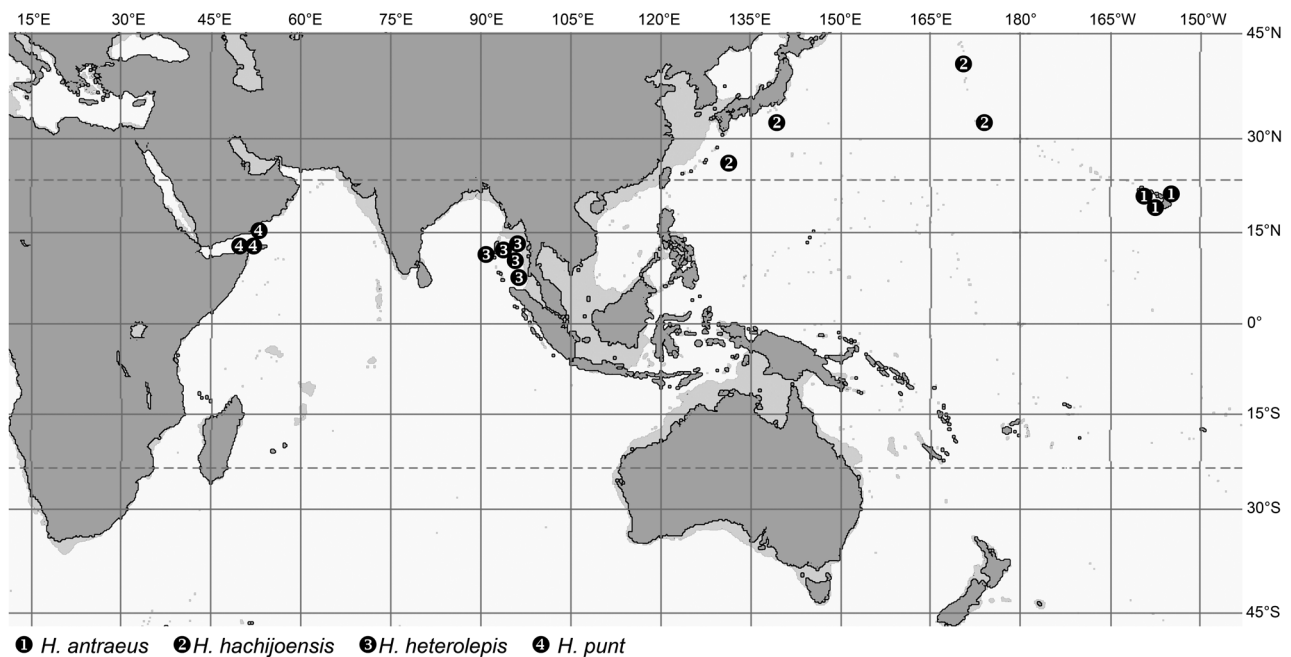


FIGURE 27. Geographical distribution of *Hymenocephalus antraeus*, *H. hachijoensis*, *H. heterolepis* and *H. punt*.

The following description is based on the holotype. Body moderately slender with large head, highest and widest at rear part of head just behind orbit, tapering rather regularly behind first dorsal into the usual whip-like tail. Origin of pectoral and ventral fins about on same vertical, origin of first dorsal more anteriorly positioned. First ray of ventral nearly twice the length of subsequent rays; first rays of first dorsal and pectoral also somewhat longer than subsequent rays. Second dorsal rudimentary; anal well developed.

Teeth all small in narrow bands in both jaws.

Luminescent tissue (striae) dark, dominantly black with few silver stripes, extending as a narrow band along both sides of isthmus below gill covers, reaching to bases of pectoral fins and behind ventral fin bases, where they join along medial line, and extend to about 30–50% of the distance from ventral fin bases to periproct region. Gular region dark, with some black lines. Anterior lens of ventral luminescent organ small; posterior lens before periproct about two times larger, tear-drop shaped, anteriorly with triangular stretch of dark tissue and broad dark tissue to sides of lens as well.

Axial skeleton (based on radiographs). Number of precaudal vertebrae 10; vertebrae 1–3 much shorter than subsequent vertebrae. Neural spines of vertebrae 1 and 2 about twice as long as vertebra 3, forwardly inclined, neural spine 1 stronger than 2; neural spines 3 to 8 depressed, spines 3 to 7 with blunt tips; neural spines 3 to 6 short and of equal length, spines 7 to 8 increasing in length. Bases of neural spines 4 to 8 enlarged. Parapophyses on vertebrae 6 to 10. Pleural ribs on vertebrae 5 to 8 or 9. First fin ray of 1D supported by two pterygiophores, both inserted behind neural spine 2. Last pterygiophore of 1D inserted behind neural spine 8. First pterygiophore of 2D

above vertebra 17 to 18. First pterygiophore of anal fin not prolonged, inserted in front of first haemal spine on first caudal vertebrae (11).

Head morphology (n = 4): Head massive, with pointed anterior profile and snout protruding well beyond mouth. Bones moderately thin and fragile; eyes moderately large; barbel moderately long, reaching vertical through anterior rim of orbit. Head canals well developed, covered with very thin, mostly fragmented integument. Infraorbital width 10–15%HL, supraorbital canal with 5–6 segments, width 7–12% HL, supratemporal canal narrow, above segment 4 of supraorbital canal, preopercular canal width 10–12% HL, postorbital-preopercular interspace 7–10% HL. Neuromasts exceptionally clearly visible in several specimens because of overall dusty dark pigmentation and good overall preservation (Fig. 1D–F). Infranasal supporter well developed; infraorbital supporter expanded only below rear part of orbit, 40–60% OD; preopercular supporter moderately long (4–6% HL), with straight rear margin; mandibular hook distinct.

Otolith morphology (n = 10): Otolith high bodied, slightly longer than high; OL:OH = 1.0–1.1; OL:OT about 3.5. Predorsal lobe massive, marked posteriorly by an incision located slightly behind middle of otolith. Anterior rim irregularly curved, high; posterior tip rounded. Ventral rim moderately deep and regularly curved, deepest slightly anterior of middle. Inner face slightly convex along horizontal axis, with narrow, median to slightly inframedian sulcus. Ostial and caudal colliculi small, well separated (nearly joined in one specimen), of nearly equal size; pseudocolliculum moderately enlarged. CCL:OCL = 1.0–1.2; TCL:PCL = 1.9–2.2. Dorsal depression indistinct; ventral furrow distinct, moderately close to ventral rim.

Coloration (in alcohol): Medium to dark brown; opercle, premaxilla and ventral region from tip of mandible to periproct particularly dark; numerous small melanophores on preopercle, upper lip, anterior rim of nape and along sides of nasal flap; first dorsal, ventral and pectoral fins with small melanophores, pectoral fin with dark area on central part, when well preserved; melanophores at bases of second dorsal and anal fin rays; body above median line and behind opercle darker brown than below; entire body behind head with irregularly distributed star-like large melanophores.

Distribution. Probably endemic off the shores of northern Somalia, Yemen and southern Oman.

Etymology. The new species is named after the mythic kingdom of Punt, thought to have been historically located in northern Somalia. The name is used as a noun in apposition.

Hymenocephalus italicus Group

Hymenocephalus italicus Giglioli, 1884

Figs. 28A–P, 29

Hymenocephalus italicus Giglioli, 1884: 228 (type locality: off Genoa, Italy).

Hymenocephalus italicus: Vaillant, 1888: 211; Marshall & Iwamoto, 1973: 605; Iwamoto in Cohen *et al.*, 1990: 230.

Bathygadus cavernosus Goode & Bean 1885: 598.

Hymenocephalus cavernosus: Goode & Bean, 1896: 408.

Macrurus (Mystaconurus) cavernosus: Alcock, 1899: 117 (Gulf of Mexico only).

Material examined. 63 specimens; 12 specimens BMNH 1939.5.24.705–716, 04°58'N, 73°16'E; 4 specimens IORAS 00224, 88–135 mm TL, 25°28'S, 35°14'E; 1 specimen IORAS 00225, 171 mm TL, 09°28'S, 60°08'E; 8 specimens IORAS 00226, 104–160 mm TL, 08°47'S, 59°55'E; 2 specimens MCZ 43020, 125+–127+ mm TL, 07°40'N, 54°47'W, 548 m; 7 specimens MCZ 43049, 29°08'N, 88°13'W, 457 m; 1 specimen (otolith only) MCZ 51404, 23°22'N, 79°56'W, 521–548 m; 3 specimens (otoliths only) MVZ 52949, 21°21'N, 17°37'W, 400 m; 1 specimen MCZ 57926, 11°36'N, 62°46'W, 530 m; 2 specimens USNM 109502, 123 and 152 mm TL, Maldives, Kardiva channel, 5°N, 73°E, John Murray Expedition; 1 specimen ZMB 17646, 165 mm TL, 00°27'N, 42°47'E; 1 specimen ZMB 22336, 137+ mm TL, 01°40'N, 41°47'E; 1 specimen ZMB 22337, 144+ mm TL, 00°27'N, 42°47'E; 1 specimen ZMB 34033, 166 mm TL, off Mauritania; 1 specimen ZMB 34055, 158 mm TL, off Mauritania; 3 specimens ZMB 34063, 125–146 mm TL, off Mauritania; 3 specimens ZMUC 23.8.1890, journal 52.53.57, 95–105 mm TL, off Morocco; 2 specimens ZMUC 1.11.1892, 81–114 mm TL, off Messina, Italy; 8 specimens ZMUC 373411–373418, 74+–178 mm TL, 29°55'S, 31°20'E; 1 specimen (otolith only) leg. John Fitch, Mediterranean (no further data).

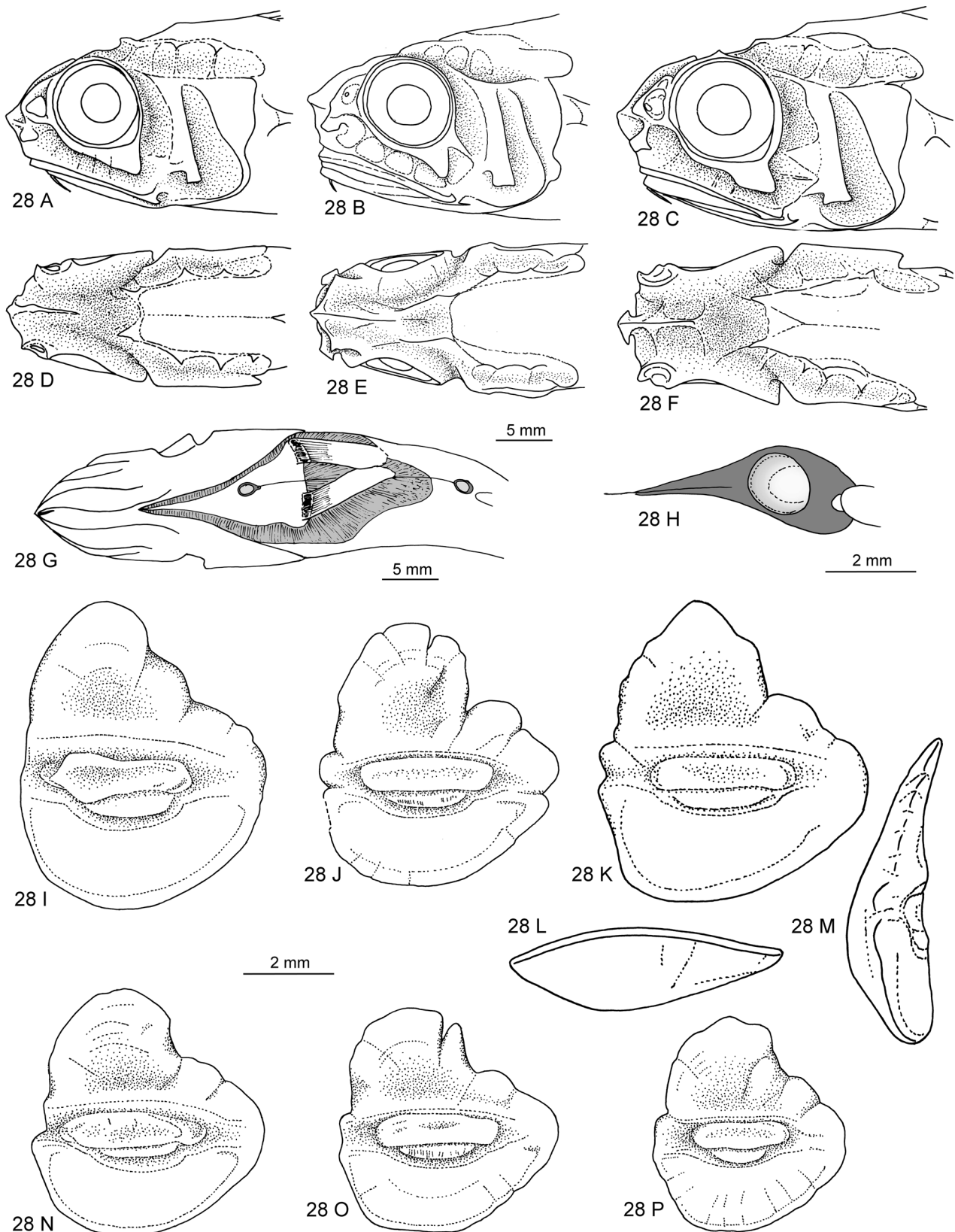


FIGURE 28. *Hymenocephalus italicus*: A, D—MCZ 43049, A—Lateral view of head, D—Dorsal view of head. B, E—ZMUC P373417, B—Lateral view of head, E—Dorsal view of head. C, F—IORAS 00225, C—Lateral view of head, F—Dorsal view of head. G—H—USNM 109502, G—Ventral view of head and trunk, H—detail view of posterior lens of ventral luminescent organ. I—P—Otoliths, I—K, N—P—Inner faces, L—Ventral view, M—Anterior view, I—MCZ 43020, J—MCZ 52949, K—M—IORAS 00226, N—MCZ 51404, O—ZMUC P.23-8-1890, P—USNM 109502.

Diagnosis. Pelvic fin rays 11, rarely 10 or 12; pectoral 12–14; gill rakers 20–25. Barbel short 7–12% HL, not or just reaching vertical through anterior rim of orbit. Orbit 34–38% HL. Snout pointed, protruding, 18–20% HL. Ventral striae extending to about $\frac{1}{2}$ to $\frac{2}{3}$ the distance from pelvic fin bases to periproct (Fig. 28G). Otolith compressed, OL:OH = 0.8–0.95; colliculi fused; pseudocolliculum long, TCL:PCL = 1.5–1.7.

Comparison. *Hymenocephalus italicus* resembles *H. heterolepis* and *H. punt* but differs from both in having a larger orbit (34–38% HL vs 28–32% HL) and a compressed otolith with fused colliculi (vs. separated colliculi). The latter is also the best character to distinguish it from the otherwise closely similar *H. antraeus*, which further differs in having a shorter barbel (3–4% HL vs. 7–12% HL) and the more rounded and less protruding snout.

Description. Head morphology (n = 4) (Fig. 28A–F): Snout moderately long, pointed, projecting, 18–20% HL, orbit diameter large, 34–38% HL, interorbital width 55–70% HW. Barbel short, 7–12% HL, mostly reaching vertical through anterior rim of orbit. Head canals well developed, infraorbital width 9–14% HL, supraorbital canal with 5–6 segments, width 12–15% HL, supratemporal canal moderately wide, above segment 4 of supraorbital canal, preopercular canal width 12–16% HL, postorbital-preopercular interspace 5–7% HL. Infranasal supporter moderately large; infraorbital supporter short, expanding only beyond rear part of orbit, 30–50% OD; preopercular supporter moderately long, 4–7% HL, with straight rear margin.

Otolith morphology (n = 9) (Fig. 28I–P): Otolith large; OL:OH = 0.8–0.95; OH:OT = 3.5. Dorsal rim with very large and broad, often crenulated predorsal lobe, distally inclining to posterior tip with small incision; posterior tip at about level of sulcus termination; ventral rim deep, regularly curved, mostly smooth, deepest anterior of the middle; anterior rim high, subvertical to nearly vertical. Inner face slightly convex, with median sulcus. Colliculi completely fused, terminating far from anterior and posterior tips of otolith; pseudocolliculum very long. TCL:PCL = 1.5–1.7. Dorsal depression moderately large, indistinct; ventral furrow moderately distinct, close to ventral rim.

Discussion. *Hymenocephalus italicus* is one of the more widespread species of the genus and specimens were examined from a variety of geographic origins. Specimens from the western Atlantic (Fig. 28A, D) and Indian Ocean (Fig. 28C, F) generally seem to have slightly longer barbels than those from the eastern Atlantic (Fig. 28B, E). Otoliths from specimens from the western Atlantic (Fig. 28I, N) are generally more compressed and have a smoother outline than those from specimens from the eastern Atlantic (Fig. 28J, O) or the Indian Ocean (Fig. 28K–M, P). However, none of these subtle differences appear to be stable enough to warrant distinction at the species or even the subspecies level. Larger statistical series would have to be analyzed or DNA-methods applied for confirmation of any distinction between them.

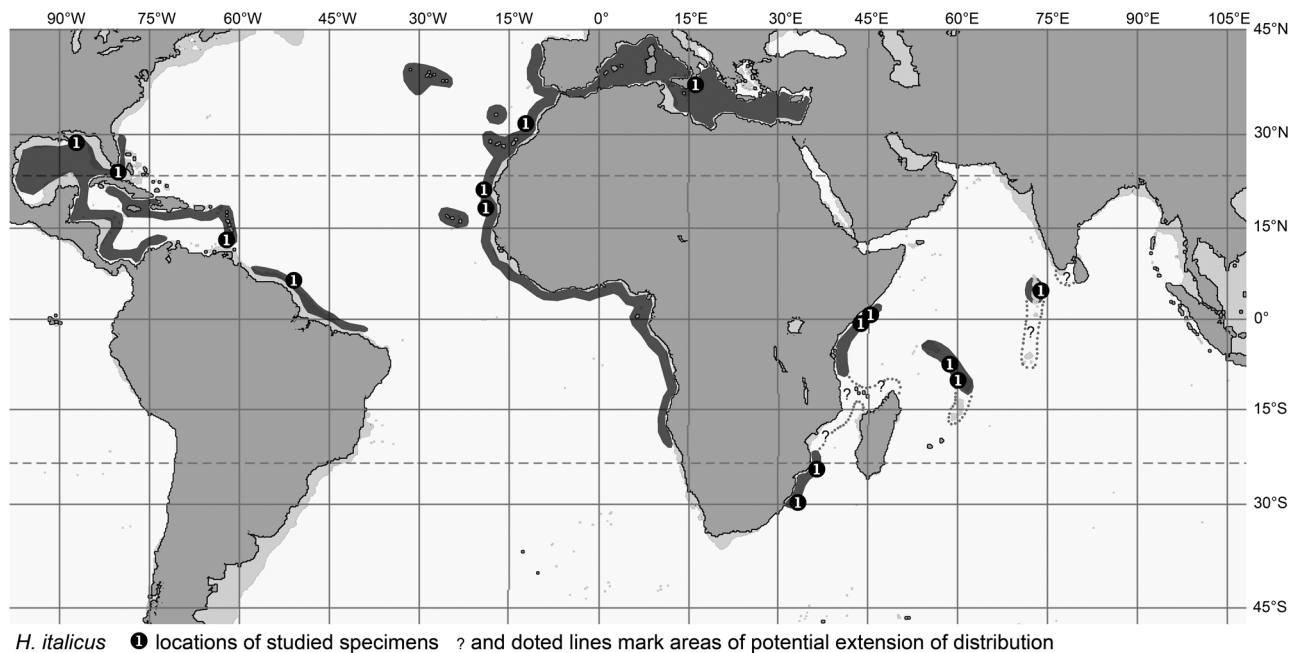


FIGURE 29. Geographical distribution of *Hymenocephalus italicus*.

Distribution (Fig. 29). *Hymenocephalus italicus* is common in the tropical western Atlantic, in the eastern Atlantic from Portugal to Angola, the Mediterranean and the western Indian Ocean so far recorded from off southern Somalia to Zanzibar, off Mozambique to Durban, along the Mascarene Ridge and off Maldives. Reports from the eastern Indian Ocean (Bay of Bengal and Andaman Sea) represent *H. heterolepis* and records from the Gulf of Aden represent *H. punt*.

Hymenocephalus striatissimus Group

Hymenocephalus aeger Gilbert & Hubbs, 1920

Figs. 30A–G, 37

Hymenocephalus striatissimus aeger Gilbert & Hubbs, 1920: 531 (type locality: 00°15'N, 127°24'E).

Hymenocephalus striatissimus aeger: Iwamoto & Williams, 1999: 178.

Material examined. 11 specimens; 1 specimen MNHN 2006-0159, 07°44'S, 156°29'E, 518–527 m; 1 specimen MNHN 2006-0218, 08°09'S, 157°01'E, 460–487 m; 3 specimens MNHN 2006-0556, 91+–140 mm TL, 08°16'S, 160°04'E, 430 m; 1 specimen WAM P.30578-002, 121 mm TL, 17°57'S, 118°17'E; 1 specimen ZMUC P375844, 84+ mm TL, Kai Islands; 1 specimen ZMUC P375854, 127 mm TL, Kai Islands; 1 specimen ZMUC P375856, 91+ mm TL, Kai Islands; 1 specimen ZMUC P 375857, 126 mm TL, Kai Islands; 1 specimen ZMUC unregistered, 05°46'S, 132°52'E.

Diagnosis. Pelvic fin rays 8; pectoral fin rays 13–15; gill rakers 19–23. Barbel long, 20–25% HL, reaching beyond a vertical through anterior rim of orbit. Orbit 35–40% HL. Snout obtuse, slightly protruding, 15–18% HL. Ventral striae extending to about $\frac{2}{3}$ the distance from pelvic fin bases to periproct. Infraorbital supporter long, 70–90% OD. Otolith compressed, OL:OH = 0.9–1.0; colliculi fused; pseudocolliculum long, TCL:PCL = 1.25–1.45.

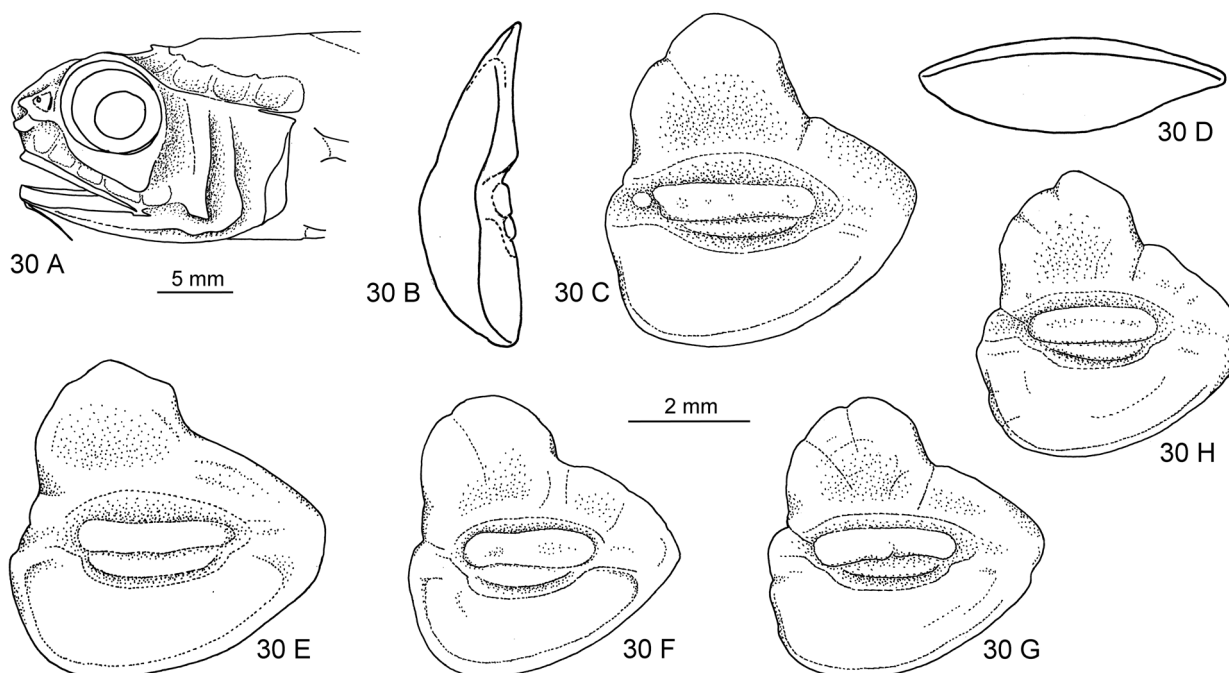


FIGURE 30. *Hymenocephalus aeger*: A—ZMUC P375844, lateral view of head. B–H—Otoliths, B—Anterior view, C, E–H—Inner faces, D—Ventral View, B–D—ZMUC P375844, E—ZMUC unregistered, 05°46'S, 132°52'E, F—MNHN 2006-0218, G—ZMUC P375857, H—ZMUC P375856.

Comparison. *Hymenocephalus aeger* was established by Gilbert & Hubbs (1920) as a subspecies of *H. striatissimus* on the basis of a longer barbel and a smaller eye. The difference in the eye (orbit) size was not verified from the specimens examined, but the longer barbel is quite distinct. In addition, the otoliths are slightly less

compressed than those of the other species of the *striatissimus* Group (OL:OH = 0.9–1.0 vs 0.75–0.9). This subtle difference in otolith proportions further supports the recognition of a separate taxonomic entity.

Description. Head morphology (n = 2) (Fig. 30A): Snout rather short and obtuse, only slightly projecting, 15–18% HL, orbit diameter large, 35–40% HL, interorbital width 60–70% HW. Barbel long, 20–25% HL, reaching slightly beyond a vertical through anterior rim of orbit. Head canals well developed, infraorbital width 11–14% HL, supraorbital canal with 4 to 5 segments, width 10–15% HL, supratemporal canal rarely identifiable, above segment 3 or 4 of supraorbital canal, preopercular canal width 12–16% HL, postorbital-preopercular interspace 4–7% HL. Infranasal supporter moderately large; infraorbital supporter long, extended below almost entire length of orbit, 70–90% OD; preopercular supporter moderately long, 5–8% HL, with straight rear margin.

Otolith morphology (n = 10) (Fig. 30B–H): Otolith large; OL:OH = 0.9–1.0; OH:OT = 3.5. Dorsal rim with very large, moderately broad, smooth predorsal lobe, distally marked by small concavity, inclining to posterior tip; posterior tip slightly expanded, positioned at about level of sulcus termination; ventral rim deep, regularly curved, smooth, deepest anterior of the middle; anterior rim high, subvertical to nearly vertical. Inner face slightly convex, with median sulcus. Colliculi completely fused, terminating far from anterior and posterior tips of otolith; pseudocolliculum very long. TCL:PCL = 1.25–1.45. Dorsal depression small, indistinct; ventral furrow distinct, close to ventral rim.

Discussion. Gilbert & Hubbs (1920) studied a large number of specimens of the three nominal subspecies of *H. striatissimus*, and recorded that they found intergrades between *H. striatissimus aeger* and *H. s. torvus* along the Tawi Tawi Archipelago of the Philippines, which led them to establish this form as a subspecies of *H. striatissimus*. I was unable to verify their observation of intergrades, but found a specimen from off the nearby Jolo Island in the collection of ZMUC (P375860), which I consider as *H. striatissimus* (Fig. 32B–C). Since otoliths seem to present a further character helpful to identify *H. s. aeger*, I now tentatively propose full species rank for *H. aeger*, subject however to verification of a more detailed and possibly statistical assessment of this difficult species group.

Distribution (Fig. 37). Specimens studied and considered valid for *H. aeger* are from off NW-Australia, off southern New Guinea and off the Solomon Islands.

Hymenocephalus megalops Iwamoto & Merrett, 1997

Figs. 31A–H, 37

Hymenocephalus megalops Iwamoto & Merrett, 1997: 521 (type locality: 19°36'S, 158°49'E).

Hymenocephalus megalops: Merrett & Iwamoto, 2000: 758.

Material examined. 35 specimens; 24 specimens AMS I.32433-002, 64–132 mm TL, 10°29'S, 144°01'E, 596–603 m; 1 specimen MNHN 1995-0974, 184 mm TL, 17°45'S, 168°42'E, 690–750 m; 5 specimens MNHN 1995-0989, 91+–135 mm TL, 16°33'S, 167°55'E, 602–620 m; 3 specimens MNHN 1997-0672, 75+–152 mm TL, 14°52'S, 167°03'E; 2 specimens MNHN 2008-2489, 91–124 mm TL, 16°35'S, 167°41'E, 582–614 m.

Diagnosis. Pelvic fin rays 8; pectoral fin rays 14–16; gill rakers 20–23. Barbel short, 10–15% HL. Orbit large, 41–45% HL. Snout obtuse, slightly protruding, 14–18% HL. Ventral striae extending to about $\frac{2}{3}$ to almost the entire distance from pelvic fin bases to periproct. Infraorbital supporter long, 70–90% OD. Otolith very compressed with massive predorsal lobe, OL:OH = 0.75–0.8; colliculi fused; pseudocolliculum long, TCL:PCL = 1.25–1.45.

Comparison. *Hymenocephalus megalops* differs from other members of the *striatissimus* Group primarily through the very large orbit (41–45% HL vs 35–40% HL). The otolith is one of the most high-bodied found in the genus with a very massive and intensely ornamented predorsal lobe, which represents a further character useful for the recognition of the species.

Description. Head morphology (n = 3) (Fig. 31A–C): snout short, blunt, only slightly projecting, 14–18% HL, orbit diameter very large, 41–45% HL (up to 48% according to Iwamoto & Merrett, 1997), interorbital width 45–60% HW. Barbel short, 10–15% HL, reaching to vertical through anterior rim of orbit. Head canals well developed, infraorbital width 10–12% HL, supraorbital canal width 10–16% HL, preopercular canal with mostly 4, rarely 5 segments, width 12–16% HL, supratemporal canal rarely identifiable, above segment 3 of supraorbital canal, postorbital-preopercular interspace 4–7% HL. Infranasal supporter large; infraorbital supporter long, extended below almost entire length of orbit, 70–90% OD; preopercular supporter moderately long, 5–8% HL, with straight rear margin.

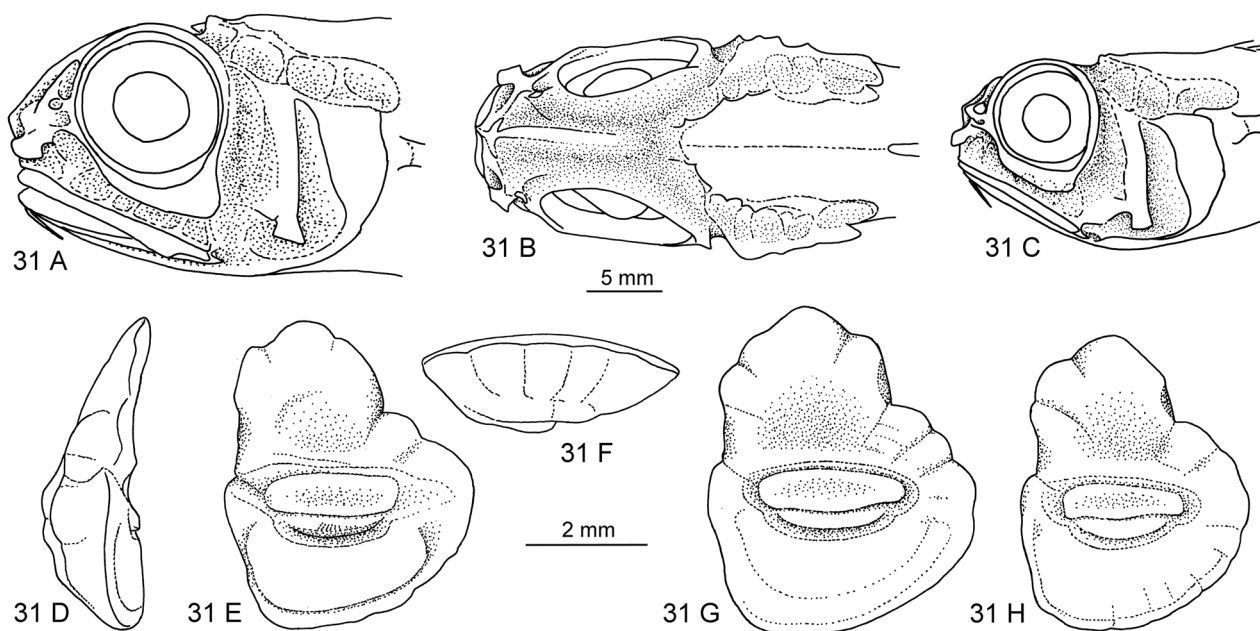


FIGURE 31. *Hymenocephalus megalops*: A–B—MNHN 1995-0989, A—Lateral view of head, B—Dorsal view of head. C—AMS I.32433-002, lateral view of head. D–H—Otoliths, D—Anterior view, E, G, H—Inner faces, F—Ventral view, D–F—MNHN 1997-0672, G–H—AMS I.32433-002.

Otolith morphology ($n = 6$) (Fig. 31D–H): Otolith large; OL:OH = 0.75–0.8; OH:OT = 3.0. Dorsal rim with very large and broad, crenulated predorsal lobe, distally marked by vertical incision; posterior tip broadly rounded, positioned at about level of sulcus termination; ventral rim very deep, regularly curved, smooth, deepest anterior of the middle; anterior rim high, nearly vertical. Inner face slightly convex, with median sulcus. Colliculi completely fused, terminating far from anterior and posterior tips of otolith; pseudocolliculum very long. TCL:PCL = 1.25–1.45. Dorsal depression moderately large, moderately indistinct; ventral furrow distinct, close to ventral rim.

Distribution. (Fig. 37) *Hymenocephalus megalops* is a common species at locations in the Coral Sea off NE-Australia and south of Papua Niugini, Chesterfield Plateau, New Caledonia, Vanuatu to Wallis and Futuna Islands.

Hymenocephalus striatissimus Jordan & Gilbert, 1904

Figs. 32A–F, 37

Hymenocephalus striatissimus Jordan & Gilbert, 1904: 612 (type locality: Suruga Bay, southern Japan).

Hymenocephalus striatissimus striatissimus: Jordan & Gilbert, 1920: 527; Okamura, 1970: 48.

Material examined. 9 specimens; 5 specimens BSKU 110055, 110102, 110103, 110412, 110413, Suruga Bay, Japan; 3 specimens ZMUC unregistered from 13.5.1914, 115–145 mm TL, off Cape Bonomisaki, Kyushu, southern Japan; 1 specimen ZMUC P375860, 125 mm TL, off Jolo Island, Philippines.

Diagnosis. Pelvic fin rays 8; pectoral fin rays 14–17; gill rakers 19–22. Barbel moderately long, 15–20% HL. Orbit 37–42% HL. Snout short, rounded, almost not protruding, 10–14% HL. Ventral striae extending to periproct. Infraorbital supporter long, 80–90% OD. Otolith compressed, OL:OH = 0.8–0.9; colliculi fused; pseudocolliculum long, TCL:PCL = 1.35–1.5.

Comparison. *Hymenocephalus striatissimus* differs from *H. aeger* in the shorter barbel (15–20% HL vs 20–25% HL), the ventral striae reaching the periproct (vs. reaching about $\frac{2}{3}$ distance from pelvic-fin bases to periproct) and the more compressed otoliths (OL:OH = 0.8–0.9 vs 0.9–1.0). From *H. torvus* it differs in the higher number of pelvic fin rays (8 vs 7). From both species it appears to differ in the higher number of pectoral fin rays (14–17 vs 12–14) and also in the more blunt snout profile expressed in an unusually low snout length ratio (10–14% HL vs 15–18% HL). This latter character, however, is strongly affected by preservation and requires verification by a statistically meaningful number of well preserved specimens.

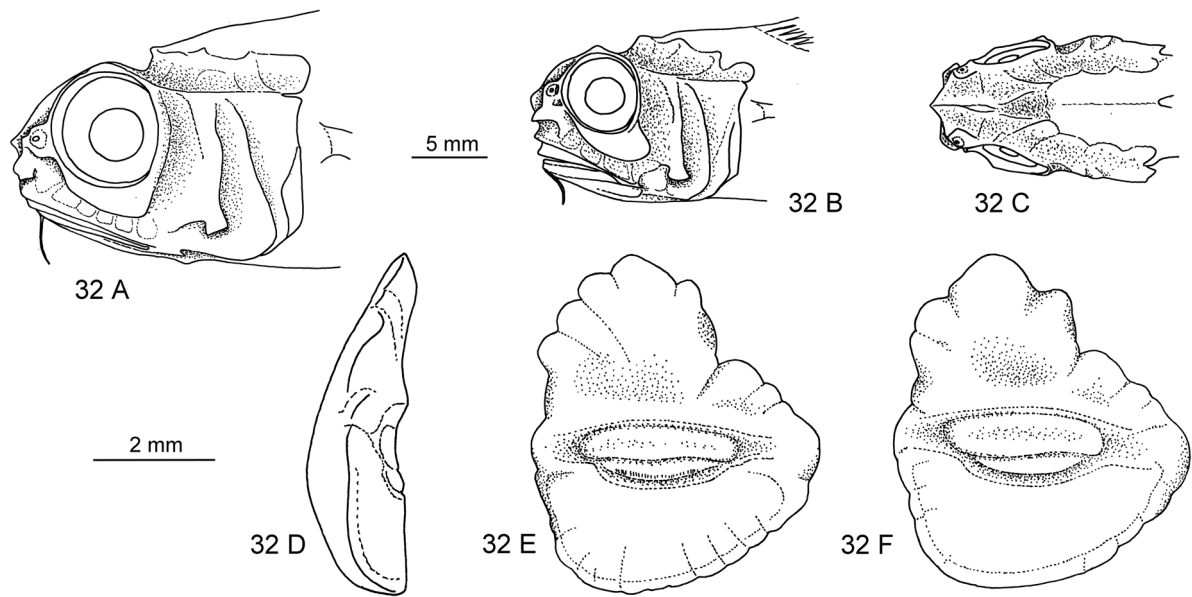


FIGURE 32. *Hymenocephalus striatissimus*: A—ZMUC P15-5-1914, lateral view of head. B—C—ZMUC P375860, B—Lateral view of head, C—Dorsal view of head. D—F—Otoliths, E—F—Inner faces, D—Ventral view, D—E—BSKU 110412, F—BSKU 110102.

Description. Head morphology ($n = 2$) (Fig. 32A–C): Snout short, blunt, barely projecting, 10–14% HL, orbit diameter large, 37–42% HL, interorbital width 60–70% HW. Barbel moderately long, 15–20% HL, reaching slightly beyond vertical through anterior rim of orbit. Head canals well developed, infraorbital width 12–15% HL, supraorbital canal with 4 to 5 segments, width 13–15% HL, supratemporal canal rarely identifiable, above segment 3 or 4 of supraorbital canal, preopercular canal width 12–16% HL, postorbital-preopercular interspace 4–7% HL. Infranasal supporter moderately large; infraorbital supporter long, extended beyond almost entire length of orbit, 80–90% OD; preopercular supporter moderately long, 5–8% HL, with straight rear margin.

Otolith morphology ($n = 10$) (Fig. 32D–F): Otolith large; OL:OH = 0.8–0.9; OH:OT = 3.5. Dorsal rim with very large, broad, crenulated predorsal lobe, distally marked by indentation; posterior tip rounded, positioned at about level of sulcus termination; ventral rim deep, regularly curved, smooth or slightly crenulated, deepest anterior of the middle; anterior rim high, nearly vertical. Inner face slightly convex, with median sulcus. Colliculi completely fused, terminating far from anterior and posterior tips of otolith; pseudocolliculum very long. TCL:PCL = 1.35–1.5. Dorsal depression moderately large, moderately indistinct; ventral furrow moderately distinct, close to ventral rim.

Discussion. Gilbert & Hubbs (1920) studied a large number of specimens and observed intergrades between *H. striatissimus striatissimus* and *H. s. torvus* off the northwestern coast of Luzon, Philippines. I did not study these particular specimens, but a specimen from off Jolo Island, much further south, and where they had observed intergrades between *H. aeger* and *H. torvus*, in the collection of ZMUC (P375860), which I consider as representing *H. striatissimus* (Fig. 32B–C) based on the short snout and the presence of 8 rays in the pelvic fin.

Distribution (Fig. 37). Gilbert & Hubbs (1920) reported *H. striatissimus* from Japan, Taiwan and southwards to northern Luzon. The single specimen studied from Jolo extends the distribution further southwards.

Hymenocephalus torvus Smith & Radcliffe, 1912

Figs. 33A–G, 37

Hymenocephalus torvus Smith & Radcliffe, 1912: 110 (type locality: off Jolo, 06°00'N, 120°45'E; location corrected by Jordan & Gilbert, 1920).

Hymenocephalus torvus: Iwamoto & McCosker, 2014: 281.

Hymenocephalus striatissimus torvus: Jordan & Gilbert, 1920: 530.

Material examined. 15 specimens; 2 specimens (otoliths only) USNM 148995, 13°47'N, 121°35'E, 347 m; 5 specimens USNM 149032, 96+ –143 mm TL, Albatross Philippines Expedition (no further details); 1 specimen USNM 149465, 160 mm TL, 08°37'N, 124°36'E, 402 m; 1 specimen USNM 149468, 162 mm TL, 08°35'N, 124°36'E, 366 m; 1 specimen (otolith only) USNM 149471, 13°32'N, 121°01'E, 446 m; 2 specimens ZMUC unregistered 09.03.1914, 117–136 mm TL, 07°25'N, 123°14'E.

Diagnosis. Pelvic fin rays 7 (rarely 8 on one side); pectoral fin rays 12–14; gill rakers 19–22. Barbel short, 10–15% HL. Orbit 34–40% HL. Snout short, only slightly protruding, 15–20% HL. Ventral striae extending to periproct. Infraorbital supporter long, 80–90% OD. Otolith compressed, OL:OH = 0.8–0.9; colliculi fused; pseudocolliculum long, TCL:PCL = 1.35–1.5.

Comparison. For differences see discussion to *H. aeger* and *H. striatissimus*.

Description. Head morphology (n = 2) (Fig. 33A–B): Snout short, slightly projecting, 15–20% HL, orbit diameter large, 34–40% HL, interorbital width 60–70% HW. Barbel short, 10–15% HL, not or just reaching vertical through anterior rim of orbit. Head canals well developed, infraorbital width 12–15% HL, supraorbital canal with 5 segments, width 13–15% HL, supratemporal canal above segment 4 of supraorbital canal, preopercular canal width 12–16% HL, postorbital-preopercular interspace 4–7% HL. Infranasal supporter moderately large; infraorbital supporter long, extended below almost entire length of orbit, 80–90% OD; preopercular supporter moderately long, 5–8% HL, with straight rear margin.

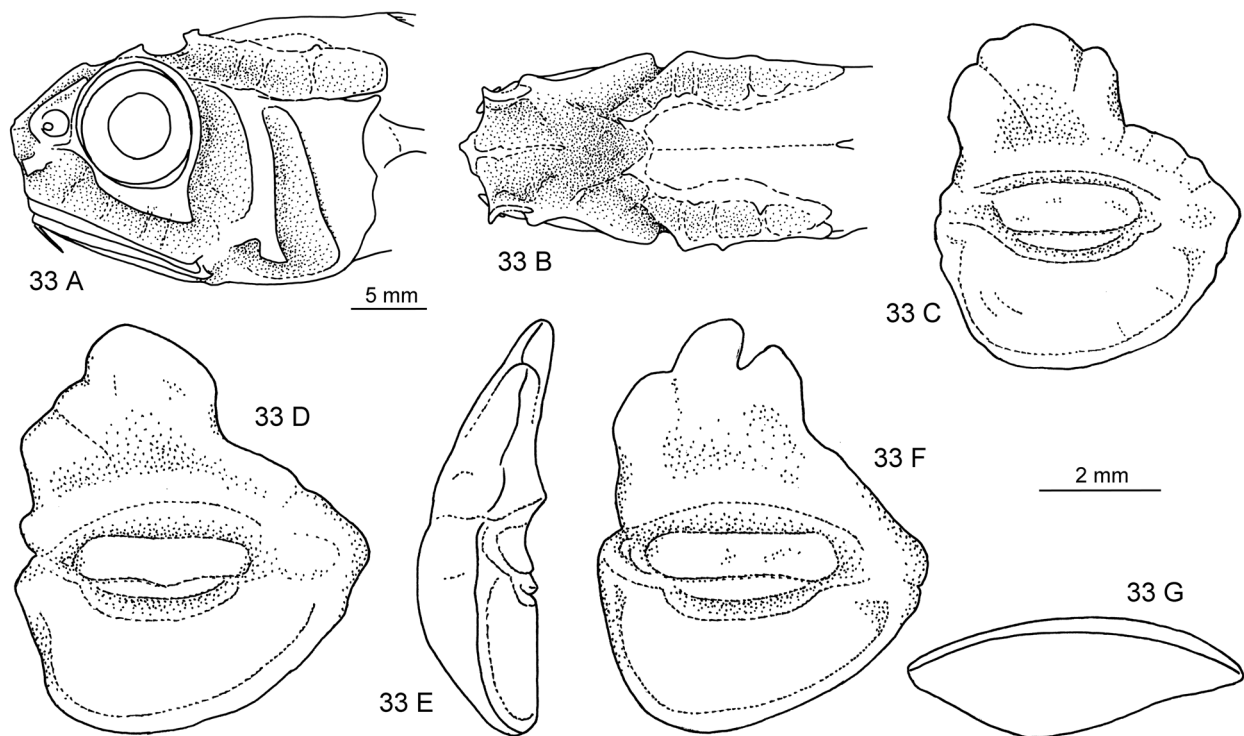


FIGURE 33. *Hymenocephalus torvus*: A–B—USNM 149465, A—Lateral view of head, B—Dorsal view of head. C–G—MNHN 2005-0928, otoliths, C, D, F—Inner faces, E—Anterior view, G—Ventral view.

Otolith morphology (n = 10) (Fig. 33D–G). Otolith large; OL:OH = 0.8–0.9; OH:OT = 3.5. Dorsal rim with very large, broad, undulating or crenulated predorsal lobe, distally marked by indentation; posterior tip rounded, positioned at about level of sulcus termination; ventral rim deep, regularly curved, smooth, deepest anterior of the middle; anterior rim high, nearly vertical. Inner face slightly convex, with median sulcus. Colliculi completely fused, terminating far from anterior and posterior tips of otolith; pseudocolliculum very long. TCL:PCL = 1.4–1.5. Dorsal depression moderately large, moderately indistinct; ventral furrow distinct, close to ventral rim.

Discussion. I follow Iwamoto and McCosker's (2014) rationale in regarding *H. torvus* as a species separate from *H. striatissimus*, with snout profile and pectoral fin counts probably adding further characters for distinction, while otolith morphology does not.

Distribution (Fig. 37). The geographic distribution of *H. torvus* appears to be restricted to the Philippines.

Hymenocephalus grimaldii Group

Hymenocephalus grimaldii Weber, 1913

Figs. 34A–H, 37

Hymenocephalus grimaldii Weber, 1913: 169 (type locality: 07°19'S, 116°49'E).

Material examined. 18 specimens; 4 specimens BSKU 16709–16712, Timor Sea; 7 specimens BSKU 17010–17016, 102+–148 mm TL, 12°42'S, 123°08'E; 1 specimen BSKU 98160, 160 mm TL, 05°54'S, 119°29'E, 558–593 m; 5 specimens BSKU 98162–63, 98167, 98169–70, 05°54'S, 119°29'E, 558–593 m; 1 specimen WAM P.32344-006, 117+ mm TL, 21°29'S, 113°58'E.

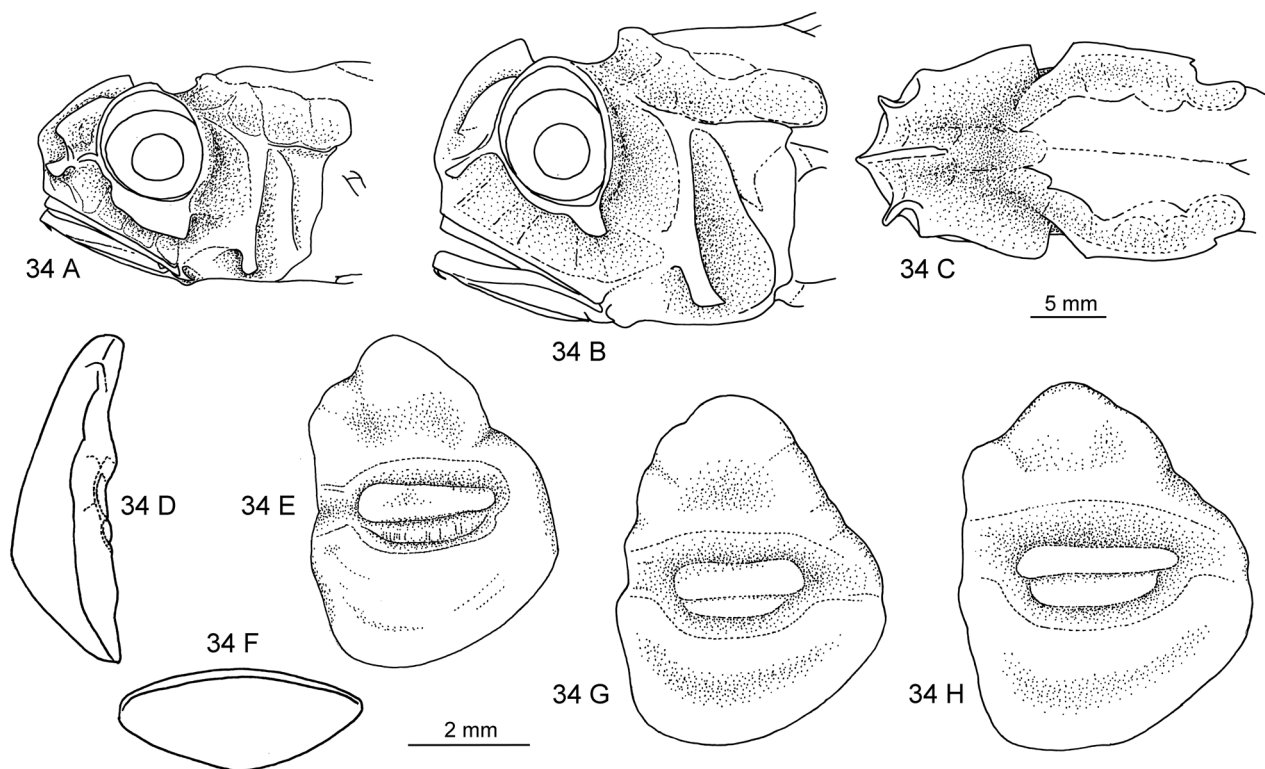


FIGURE 34. *Hymenocephalus grimaldii*: A—WAM P.32344-006, lateral view of head, B–C—BSKU 098160, B—Lateral view of head, C—Dorsal view of head. D–H—Otoliths, D—Anterior view, E—Ventral view, F–H—Inner faces, D–E—WAM P.32344-006, F—BSKU 17010, G—BSKU 17011.

Diagnosis. Pelvic fin rays 8; pectoral fin rays 9–11, rarely 12; gill rakers 17–21. Barbel absent. Orbit moderately large, 34–38% HL, strongly oblique. Snout obtuse, short, barely protruding, 15–20% HL. Ventral striae extending to periproct. Preopercular supporter very long and narrow, 8–13% HL. Otolith very compressed with broad predorsal lobe, OL:OH = 0.75–0.8; colliculi fused; pseudocolliculum very long, TCL:PCL = 1.15–1.25.

Comparison. *Hymenocephalus grimaldii* is readily recognized by the combination of low counts of pelvic and pectoral fin rays, absence of a barbel, strongly obliquely oriented orbit and very long and narrow preopercular supporter. The otolith morphology adds another set of easily recognizable characters such as the broad, but rather shallow predorsal lobe, the very compressed otolith with the longest pseudocolliculum observed in all *Hymenocephalus* species (TCL-PCL = 1.15–1.25).

Description. Head morphology (n = 2) (Fig. 34A–C): Snout short, blunt, high, only slightly projecting, 15–20% HL, orbit diameter large, 34–38% HL, oriented at an angle of 70–80° inclination to long axis of fish, with the longest orbit diameter being 42–45% HL, interorbital width about 80% HW indicating the most advanced lateralization of the eyes. Barbel absent. Head canals well developed, infraorbital width 15–17% HL, supraorbital canal with 4 segments, width 15–18% HL, supratemporal canal above segment 3 of supraorbital canal, preopercular canal width 13–19% HL, postorbital-preopercular interspace 3–5% HL. Infranasal supporter small,

thin; infraorbital supporter variable, extended below almost entire length of orbit (70–80% OD) in specimens from Indonesia (Fig. 34A), but below the rear part of the orbit only in the specimen off NW Australia (30–40% OD) (Fig. 34B–C); preopercular supporter very long and narrow, 8–13% HL, with straight rear margin.

Otolith morphology (n = 8) (Fig. 34D–H): Otolith large; OL:OH = 0.75–0.8; OH:OT = 3.2–3.5. Dorsal rim with moderately large but very broad, mostly smooth predorsal lobe, distally reaching close to the obtuse, broadly rounded posterior tip without indentation mark; ventral rim very deep, regularly curved, smooth, deepest anterior of the middle; anterior rim high, nearly vertical. Inner face slightly convex, with slightly suprmedian sulcus. Colliculi completely fused, terminating far from anterior and posterior tips of otolith, sometimes dorsally reduced and then rather narrow; pseudocolliculum very long. TCL:PCL = 1.15–1.25. Dorsal depression indistinct; no ventral furrow, instead broad, indistinct depression at center of ventral field and parallel to ventral rim of otolith.

Distribution. (Fig. 37) *Hymenocephalus grimaldii* has been collected in the Timor and Java Seas of Indonesia, and one specimen has now been identified from off Northwest Cape, Western Australia.

Hymenocephalus neglectissimus Sazonov & Iwamoto, 1992

Figs. 35A–C, 37

Hymenocephalus neglectissimus Sazonov & Iwamoto, 1992: 56 (type locality: Sala y Gomez Ridge, Prof. Shtokman cr. 18, sta. 1964).

Hymenocephalus neglectissimus: Iwamoto & Merrett, 1997: 523 (reference values only).

Material examined. 2 specimens ZMMGU P-18221, 105 and 112 mm TL, 23°33'S, 89°11'W, 563–590 m.

Diagnosis (after Sazonov & Iwamoto with additions). Pelvic fin rays 8; pectoral fin rays 13–15; gill rakers 16–21. Barbel moderately long, 15–28% HL. Black blotch on dorsum short, with clear-cut outline. Orbit very large, 44–55% HL along the longest diameter, slightly oblique. Snout rounded, not protruding, 10–15% HL. Ventral striae extending to about $\frac{2}{3}$ the distance from pelvic fin bases to periproct. Infraorbital width 5–8% HL. Otolith very compressed with broad, pointed predorsal lobe, OL:OH = 0.8.

Comparison. *Hymenocephalus neglectissimus* is a small species that is characterized by its large orbit size in combination with a long barbel and a narrow infraorbital width and narrow infraorbital supporter. Sazonov & Iwamoto used the sharp edged, short black blotch on the dorsum as a further character to distinguish *H. neglectissimus* from the co-occurring *H. semipellucidus* (long and eroded outline).

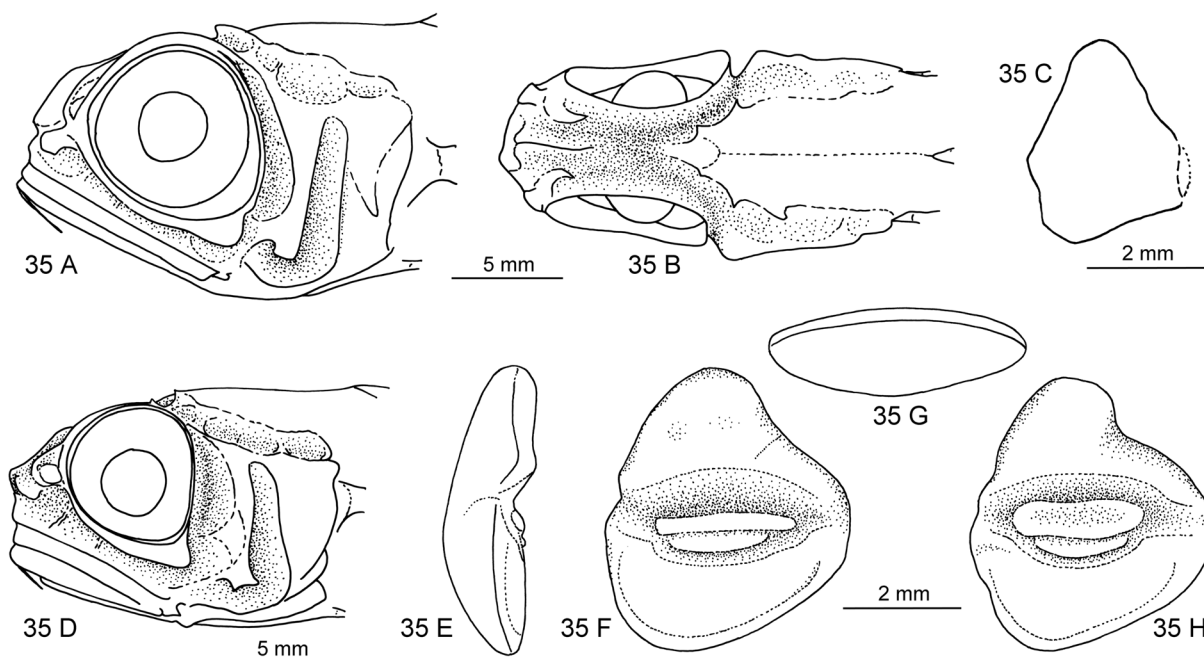


FIGURE 35. A–C: *Hymenocephalus neglectissimus*: A–C—ZMMGU-P 18221, A—Lateral view of head, B—Dorsal view of head, C—Schematic outline drawing of formalin eroded otolith. D–H: *Hymenocephalus semipellucidus*, ZMMGU-P 18205: D—Lateral view of head, E—Anterior view of otolith, F, H—Inner faces of otoliths, G—Ventral view of otolith.

Description. Head morphology (n = 1) (Fig. 35A–B): snout short, rounded, not projecting, 10–15% HL, orbit diameter very large, 42–50% HL, 44–55% HL along the longest diameter, slightly obliquely oriented, interorbital width about 40–50% HW. Barbel moderately long, 15–20% HL (up to 28% HL according to Sazonov & Iwamoto), reaching slightly beyond vertical through anterior margin of orbit. Head canals well developed, infraorbital width 5–8% HL, supraorbital canal with 4 segments, width 6% HL, supratemporal canal indistinct, above segment 3 of supraorbital canal, preopercular canal width 10% HL, postorbital-preopercular interspace 4% HL. Infranasal supporter short; infraorbital very short and narrow, 25% OD; preopercular supporter short, 4% HL, with straight rear margin.

Otolith morphology (n = 1) (Fig. 35C): otolith large; OL:OH = 0.8. No sufficiently well preserved otolith was retrieved from any of the studied specimens. An outline could be reconstructed from one otolith, which has a very compressed shape and a broad, dorsally pointed predorsal lobe.

Distribution (Fig. 37). *Hymenocephalus neglectissimus* is only known from the Sala y Gomez Ridge.

***Hymenocephalus semipellucidus* Sazonov & Iwamoto, 1992**

Figs. 35D–H, 37

Hymenocephalus semipellucidus Sazonov & Iwamoto, 1992: 60 (type locality: Sala y Gomez Ridge, Prof. Shtokman cr. 18, sta. 2019).

Hymenocephalus semipellucidus: Iwamoto & Merrett, 1997: 523 (reference values only).

Material examined. 3 specimens ZMMGU P-18205, 135–150 mm TL, 25°08'S, 99°25'W, 750–800 m.

Diagnosis (after Sazonov & Iwamoto with additions). Pelvic fin rays 8; pectoral fin rays 15–19; gill rakers 15–20. Barbel short, 10–17% HL. Black blotch on dorsum long, with eroded outline. Orbit very large, 40–46% HL (43–50% HL along the longest diameter), slightly oblique. Snout rounded, very slightly protruding, 15–20% HL. Ventral striae extending to about ½ the distance from pelvic fin bases to periproct. Infraorbital width 9–11% HL. Otolith compressed with triangular shaped, not very high, pointed predorsal lobe, OL:OH = 0.8–0.9; colliculi fused, narrowed; pseudocolliculum very long, TCL:PCL = 1.25–1.35.

Comparison. Sazonov & Iwamoto (1992) distinguished *H. semipellucidus* from *H. neglectissimus* by a long black blotch on the dorsum (vs short and clear cut), shorter barbel, the higher number of pectoral rays (15–19 vs 13–16), the larger infraorbital width (9–11% HL vs 5–8% HL) and the slightly smaller orbit. It differs from *H. aeger*, *H. megalops* and *H. torvus* in the higher pectoral fin ray count (15–19 vs. 13–15, 14–16 and 12–14, respectively) and from *H. aeger*, *H. striatissimus* and *H. torvus* in the larger orbit (40–46% HL vs. 35–42% HL). An additional character to faultlessly distinguish *H. semipellucidus* from all species of the *striatissimus* Group is the outline of the otolith, with its less pronounced, triangular-shaped, pointed predorsal lobe.

Description. Head morphology (n = 1) (Fig. 35D): Snout short, slightly projecting, 15–20% HL, orbit diameter very large, 40–46% HL, 43–50% HL along the longest diameter, slightly obliquely oriented, interorbital width about 50–60% HW. Barbel, 10–17% HL (up to 22% HL according to Sazonov & Iwamoto). Head canals well developed, infraorbital width 9–11% HL, supraorbital canal with 4 segments, width 8% HL, supratemporal canal not identified, preopercular canal width 12% HL, postorbital-preopercular interspace 5% HL. Infranasal supporter short; infraorbital moderately long, narrow, 65% OD; preopercular supporter short, 5% HL, with straight rear margin.

Otolith morphology (n = 2) (Fig. 35E–H): Otolith large; OL:OH = 0.8–0.9; OH:OT = 3.2. Dorsal rim with rather short, broad, triangular shaped, pointed, smooth predorsal lobe, distally without marked indentation; posterior tip broadly rounded; ventral rim deep, regularly curved, smooth, deepest anterior of the middle; anterior rim high, subvertical vertical, slightly bent. Inner face slightly convex, with slightly suprmedian sulcus. Colliculi completely fused, terminating far from anterior and posterior tips of otolith, dorsally reduced and rather narrow, leaving depressed sulcus space without collicular filling above; pseudocolliculum very long. TCL:PCL = 1.25–1.35. No dorsal depression; ventral furrow narrow, close to ventral rim of otolith.

Distribution (Fig. 37). *Hymenocephalus neglectissimus* is only known from the Sala y Gomez Ridge.

Unidentifiable species

During the examination of the material, otoliths were extracted from two poorly preserved specimens, which seem

to represent two possibly undescribed species of the genus *Hymenocephalus*. The fish bodies are too poorly preserved to warrant any further description, let alone identification, but the otoliths are briefly described and figured below.

***Hymenocephalus* sp. 1**

Figs. 36A–C, 37

Material examined. 1 specimen MNHN 2006-0556, included in a jar of 20 specimens identified as *H. longiceps*, 08°16'S, 160°04'E, 430 m.

Description. Otolith large; OL:OH = 1.05; OH:OT = 2.7. Dorsal rim with short, broad, rounded, smooth predorsal lobe, distally with small indentation; posterior tip broadly rounded; ventral rim moderately deep, regularly curved, smooth, deepest at about its middle; anterior rim high, broadly rounded. Inner face slightly convex, with slightly suprmedian sulcus. Ostial and caudal colliculi small, short, very narrowly placed at collum, terminating at considerable distance from anterior and posterior tips of otolith; pseudocolliculum short. CCL:OCL = 1.0; TCL:PCL = 2.1. Dorsal indistinct; ventral furrow thin, close to ventral rim.

Discussion. This otolith morphology is clearly similar to the pattern found in the two species of the *longibarbis* Group, but differs in the regularly curved outline with the small predorsal lobe and thus could well represent an undescribed species.

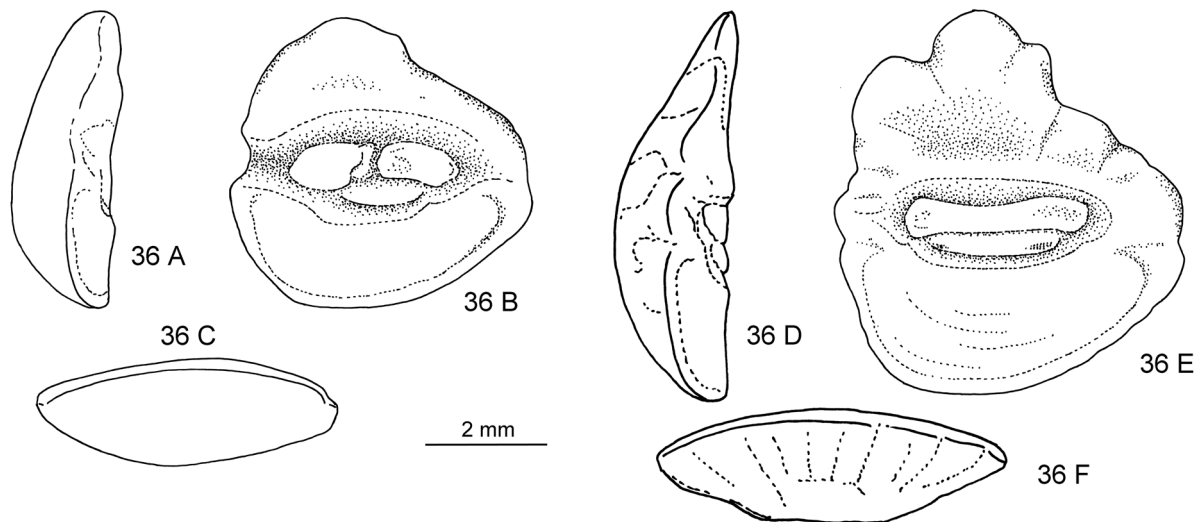


FIGURE 36. A–C: *Hymenocephalus* sp. 1, MNHN 2006-0556, otolith, A—Anterior view, B—Inner face, C—Ventral view. D–F: *Hymenocephalus* sp. 2, USNM 149049, D—Anterior view, E—Inner face, F—Ventral view.

***Hymenocephalus* sp. 2**

Figs. 36D–F, 37

Material examined. 1 specimen USNM 149049, 05°57'S, 81°50'E, 0–732 m.

Description. Otolith large; OL:OH = 0.9; OH:OT = 3.5. Dorsal rim with large, moderately high, broad, strongly undulating predorsal lobe, distally marked by small indentation; posterior tip rounded, positioned at about level of sulcus termination; ventral rim deep, regularly curved, smooth, deepest anterior of the middle; anterior rim high, nearly vertical. Inner face slightly convex, with median sulcus. Colliculi completely fused, narrow, terminating far from anterior and posterior tips of otolith; pseudocolliculum very long. TCL:PCL = 1.35. Dorsal depression moderately large, indistinct; ventral furrow moderately distinct, close to ventral rim.

Discussion. This otolith is from the only specimen of the genus collected off the western coast of the Americas (as noted in Cohen et al., 1990). The relatively large fish is almost completely disintegrated, but contained a well-preserved otolith, which closely resembles those of the *striatissimus* Group, for instance *H.*

striatissimus or *H. torvus*. The fish either represents a stray specimen of one of the two species, which cannot be identified from the otolith alone, or an unrecorded species.

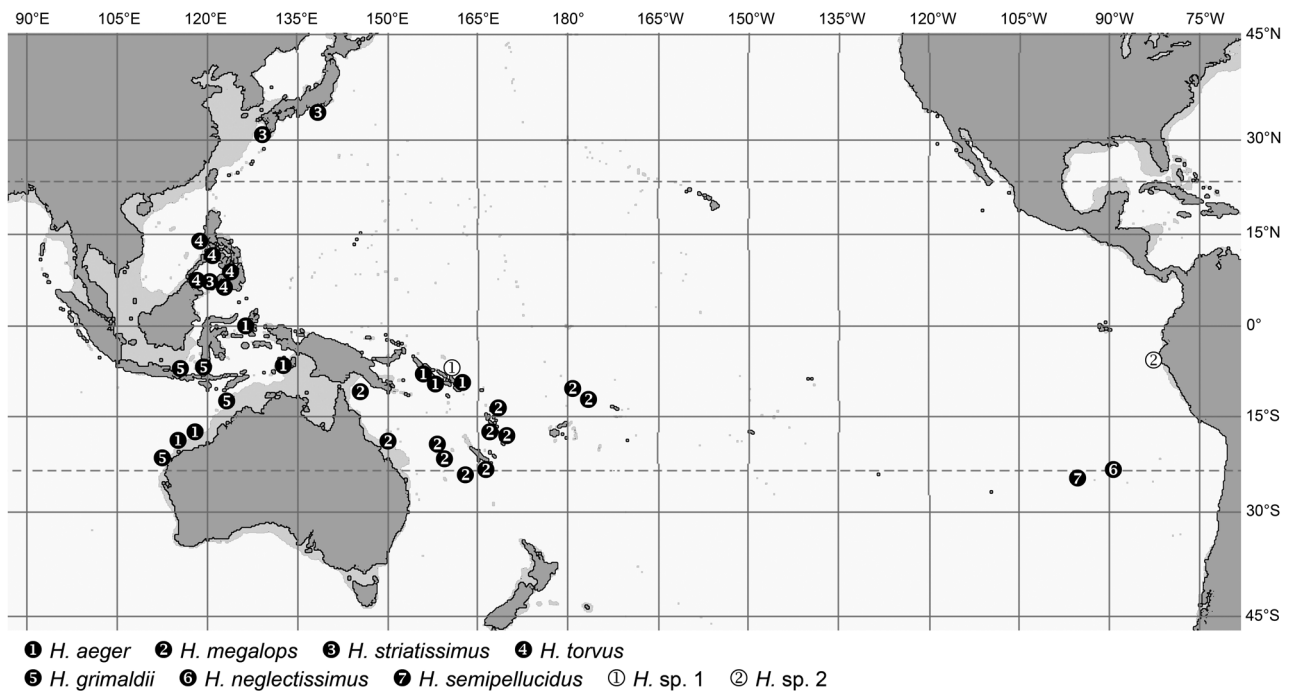


FIGURE 37. Geographical distribution of *Hymenocephalus aeger*, *H. megalops*, *H. striatissimus*, *H. torvus*, *H. grimaldii*, *H. neglectissimus*, *H. semipellucidus*, *H. sp. 1* and *H. sp. 2*.

Fossil record

Despite their Recent abundance, the fossil record of the genus *Hymenocephalus* is almost non-existent. The only valid record to date is the otolith-based species *H. rosenkrantzi* Schwarzahns, 2003 from the Middle Paleocene (62–59 Ma) of Denmark. This record confirms a geologically rather early occurrence of the genus together with a few other macrourid species of the same age. *Hymenocephalus rosenkrantzi* is characterized by a rather elongate shape (OL:OH = 1.5–1.65), a moderately developed predorsal lobe, the caudal colliculum being slightly longer than the ostial colliculum and a short pseudocolliculum positioned only inside the collum and with the ventral margin of the collum being slightly indented. This clearly is plesiomorphic otolith morphology, probably positioned phylogenetically near the dichotomy of the genera *Hymenogadus* and *Hymenocephalus*.

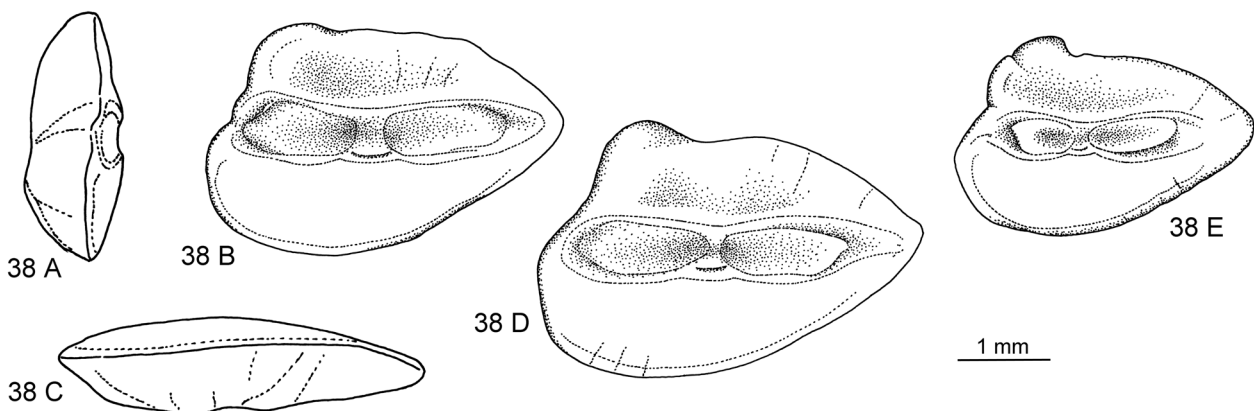


FIGURE 38. *Hymenocephalus rosenkrantzi*, fossil otoliths from the Middle Paleocene, Selandian of Kongedyb, Denmark: A—Anterior view, B, D, E—Inner faces, C—Ventral view, A–C—Holotype, MGUH 26150, D—Paratype, MGUH 26153, E—Paratype, 26151.

Phylogenetic interpretation

Geographical distribution and speciation (Figs. 5, 7, 12, 16, 21, 27, 29, 37)

Fishes of the genera *Hymenocephalus*, *Hymenogadus* and *Spicomacrurus* occur worldwide in tropical to temperate seas except along the continental margin of the eastern Pacific (one specimen found off Peru; see *Hymenocephalus* sp. 2 above). They live benthopelagically at depths chiefly between 300 and 1000 m over the continental slopes, oceanic island slopes, and above seamounts and guyots. They appear to be largely missing from open oceanic midwater environments.

Such a mode of living might support certain trends of geographic regionalization observed in the various species of the genera, although other species show a very wide, nearly cosmopolitan tropical distribution without any recognizable taxonomic diversification. The most outstanding ones in respect to wide geographical distribution are *Hymenogadus gracilis* and *Hymenocephalus aterrimus*. The distribution pattern of both species is discontinuous, patchy, but interestingly covers a certain proportion of common terrain in the Caribbean, the southwestern Pacific and the central Pacific Islands of Hawaii and Sala y Gomez seamounts, despite the fact that *H. gracilis* generally occurs in shallower water than *H. aterrimus*. In fact, *H. gracilis* is present over the Sala y Gomez Ridge, but replaced in Hawaii by the only other congener, *Hymenogadus tenuis*, while *H. aterrimus* is present off Hawaii, but replaced by the closely related *H. sazonomi* over the Sala y Gomez Ridge.

Some other species with relatively wide geographic distribution are *H. italicus* in the Atlantic and western Indian Ocean, the three closely related species *H. aeger*, *H. striatissimus* and *H. torvus* (considered as of subspecies ranking by Gilbert & Hubbs, 1920), the closely related pair *H. lethonemus* and *H. nascens*, and finally *H. longibarbis*, all in the same general area of the western Pacific, from southern Japan to Australia. Obviously, these species do show some regionalization. In the case of *H. italicus* there are some very subtle differences in fishes from the western Atlantic, eastern Atlantic and western Indian Ocean, but they are so small and inconsistent that they do not warrant differentiation into species or subspecies at this stage. The same is true for *H. longibarbis*, but the other two complexes mentioned above do show reasonable morphologically stable differentiation that in both instances led to the recognition of separate taxa in the area of southern Japan to Taiwan, as compared to the region from the Philippines to Australia. In the *H. striatissimus* complex even a separate species is recognized along the Philippines, viz. *H. torvus*. The differentiation of the respective species in these two species complexes depends on mostly subtle characters and still carries some tentative elements requiring more specific detailed analyses. Regardless of the outcome of such in-depth statistic analysis and whether differentiation is viewed as of species ranking or subspecies ranking, which appear to be the main alternatives, I think it is fair to assume that the systematic observations already made call for a rather young speciation event. A possible root cause for a geologically young speciation event might be expected in the rapid sea level changes during the Pleistocene and the temporary isolation effects that possibly came with it.

The genera *Spicomacrurus*, and much more so *Hymenocephalus*, also include a number of species with seemingly very restricted distributions, i.e. potentially endemic species. These occur in a variety of regions: *H. heterolepis* in the northeastern Indian Ocean and *H. punt* chiefly in the Gulf of Aden, but the majority of endemic species are found in the western and central Pacific. The areas richest with endemics are Japan (*Spicomacrurus kuronumai*, *Hymenocephalus lethonemus*, *H. papyraceus*, *H. striatissimus*) and the SW-Pacific from eastern Australia to New Caledonia, Vanuatu and Fiji (*Spicomacrurus dictyogadus*, *S. mccoskeri*, *Hymenocephalus megalops*, *H. nesaeae*). Of these, *S. dictyogadus*, *H. nesaeae* and *H. papyraceus* may be regarded as plesiomorphic species in their respective species groups. The Philippines, Hawaii and Sala y Gomez Ridge all have three species restricted to the specific areas, and Hawaii and Sala y Gomez a fourth species, *H. striatulus*, which they share. The high degree of endemism in Hawaii and Sala y Gomez reflects 'outposts' of the distribution range of the genus *Hymenocephalus* and most species are considered derived in respect to their species groups (i.e. *Hymenogadus tenuis*, *Hymenocephalus antraeus*, *H. neglectissimus*, *H. semipellucidus*), but two others are considered plesiomorphic counterparts, *H. sazonomi* for *H. aterrimus* and *H. striatulus* within their species group. Somewhat unexpectedly the NW Australian continental slope and the adjacent Timor and Java Seas have only yielded two endemic species so far—*Hymenogadus grimaldii* and *H. iwamotoi*—both with rather advanced morphologies when compared to their respective sister taxa, and at the same time rather isolated in their systematic position, which suggest a longer isolation time.

Phylogenetic trends and polarities of characters (Fig. 39)

The spectacular development of organs for visual, auditory and motion reception senses within the genus *Hymenocephalus* likely represents a functional morphological adaptation, which is yet to be fully understood (see also Marshall, 1979, pp. 276–277, 380–383, 413–420, 422–425). Irrespective of what the exact triggers for this evolution might eventually prove to be, it is already now clear that development of the specialization of these three traits follow specific patterns in the genera studied and in large part developed in parallel. In this respect, *Spicomacrurus* represents an evolutionary trend quite different from *Hymenocephalus*, with *Hymenogadus* plesiomorphic to both but probably closer to *Hymenocephalus*.

The species of *Spicomacrurus* show a remarkable development of large, robust and spatulate nasal bones not seen in any species of the two other genera and projecting forward above a ventrally flattened head profile. The eyes are oriented at about 60–45° angle to the fish axis resulting in a more dorsally oriented field of vision than the evolution of the visual field in *Hymenocephalus*. Both are aspects that probably speak for a rather benthic way of live, as already concluded in Okamura (1970). The otoliths do not show any specific specialization. Within *Spicomacrurus*, *S. dictyogadus* represents the most plesiomorphic species with the least strongly developed nasal bones and the least flattened ventral head profile. *Spicomacrurus mcoskeri* is the one with the longest nasal projection and the most dorsally oriented field of vision (indicated by the narrow interorbital ratio of 25% HW).

Eye size, head shape and otolith morphology exhibit a remarkable parallel evolution and polarity

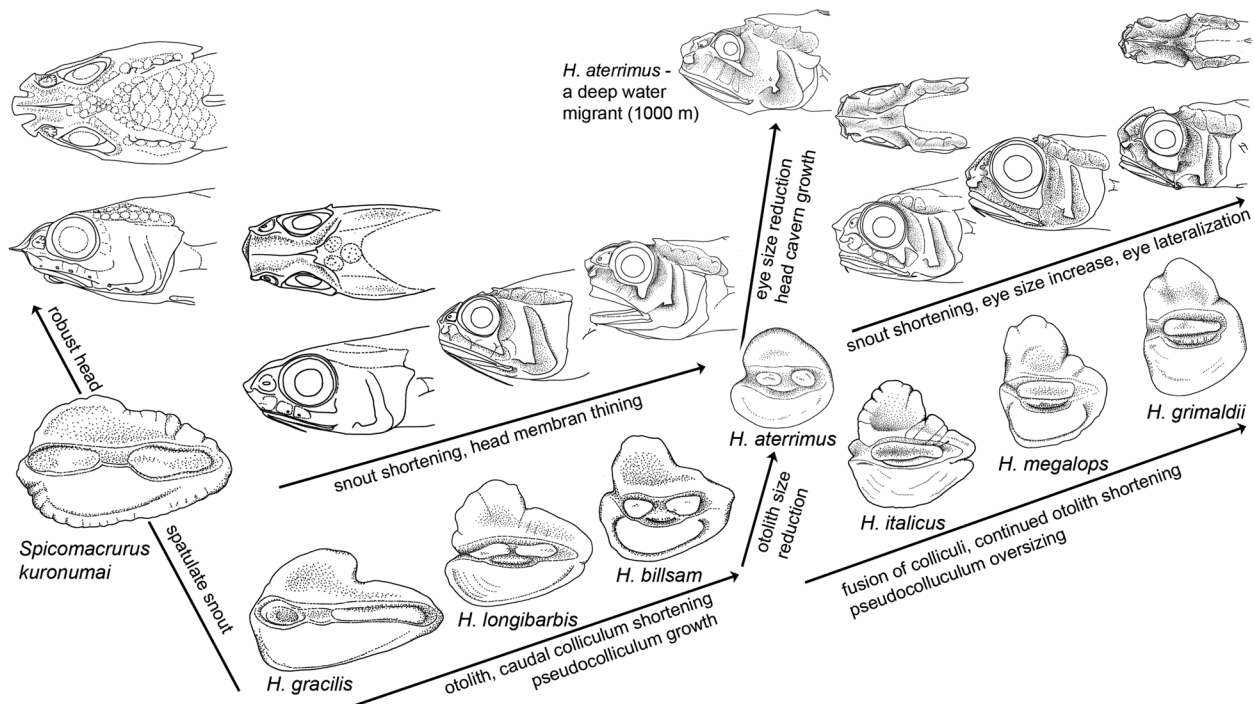


FIGURE 39. Evolutionary diagram depicting polarity in the development of otolith and head morphology of the genera *Hymenocephalus*, *Hymenogadus* and *Spicomacrurus*.

Three main trends of specialization are observed in the development of the sensory organs in *Hymenocephalus*.

1. Eye / orbit size and orientation. Orbit sizes range from 20–50% of HL in *Hymenocephalus*. Orbit sizes in the range of 28–35% of HL are found in species which I consider more basal within the genus, i.e. in the *longibarbis*, *striatulus* and *antraeus* Groups. Nevertheless, these are already fairly large diameters when compared to those of many other macrourids. Orbit sizes in the range of 40–50% of HL are reached in *H. antraeus* and the *striatissimus* and *grimaldii* Groups, whereby the latter two are considered amongst the most advanced in the genus. These observations document a clear polarity of characters related to the visual sense, but there is also a prominent polarity reversal evident in the *aterrimus* Group with small, supposedly reduced orbit sizes in the range of 20–25% of HL (only exception is *H. papyraceus* with up to 30% HL). The lateralization of the eyes / orbits is advanced in

most species of *Hymenocephalus* with interorbital values of 50% of HW or more except for the *longibarbis* Group and *H. megalops*. The highest values in the range of 70–80% of HW are found in *H. grimaldii* and *H. papyraceus*. The large eye size, the ‘parabolic’ shape of the orbit and its advanced lateralization combined with a relatively deep, laterally compressed body shape of the fishes all speak for a way of life detached from the sea bottom in free water, but not pelagic, since *Hymenocephalus* specimens are usually caught over continental and ocean island slopes and not or very rarely in the open ocean. The polarity reversal in the development of the eye and orbit sizes in the *aterrimus* Group probably represents an adaptive regression as a result of a somewhat deeper mode of life of these species (generally 700–1000 m) in an area with further reduced light than that for most other species of the genus (generally 300–600 m).

2. Head canals / lateral line system on head. One of the most striking specializations found in the genus *Hymenocephalus* is the development of very spacious and deep head canals housing the lateral line system on the head and its rarely preserved thin skin cover (‘integument’ or ‘hymen’) spanned over the canals with the help of supporters. This specialization is not seen in *Spicomacrurus* and only incipiently in the outgroup constituted by *Hymenogadus*. Not much is to be recognized within *Hymenocephalus* in terms of polarity of character development related to head canals. The two species of the *longibarbis* Group are remarkable for their relatively narrow supraorbital cavern width (6–10% vs 9–20% HL in other species of the genus, except 5–8% HL in *H. neglectissimus* and *H. semipellucidus*), and a relatively wide postorbital-preopercular interspace (10–14% vs 4–10% HL in most other species of the genus, except 10–14% in *H. aterrimus* and *H. sazoni*). Both character states are considered plesiomorphic within the genus and hence support the basal phylogenetic position of the *longibarbis* Group. The one species group sticking out from the remainder of the genus is the *aterrimus* Group, which shows the widest head canals of all *Hymenocephalus* species: infraorbital width 16–23% HL (vs 6–17% HL), supraorbital width mostly 13–20% HL (vs 9–16, except up to 18% HL in *H. grimaldii*) and preopercular cavern width mostly 15–22% HL (vs 8–16%, except up to 19% HL in *H. grimaldii*). Again, the size increase of the head canal system observed in the *aterrimus* Group might be an adaptation to their way of life in deeper waters when compared to other species of the genus, with probable orientation towards motion-capturing senses at the expense of visual and hearing capacities (see above and below).

3. Sagittal otolith size and morphology. Four individual trends of specialization are observed in sagittal otoliths: the increase of relative size to more than 20% HL in some species (Fig. 2A), the foreshortening of the shape with an enormously large and high predorsal lobe, the development of an extremely long pseudocolliculum in the ventral part of the collum extending well beyond the ostial and caudal colliculi, and the fusion of the ostial and caudal colliculi. In all these aspects otoliths of the genus *Hymenogadus*, representing the outgroup for *Hymenocephalus*, show a plesiomorphic character state. The otolith morphology found in the *longibarbis* Group shows a transitional status, advanced in comparison to *Hymenogadus*, but basal in respect to all other species groups of *Hymenocephalus* except for the *aterrimus* Group. In fishes of the *aterrimus* Group, otolith sizes are regressed between 10–15% HL, being smallest in *H. aterrimus* at about 10–11% HL. The pseudocolliculum is still short (TCL:PCL = 1.8–2.8), the outline is compressed (OL:OH = 0.8–1.2), and the predorsal lobe well developed except for *H. aterrimus* where it is shallow and rounded, probably as an indication of reversed polarity, like the overall reduction of otolith size. The reduction of otolith size appears to be related to life in deeper waters, as demonstrated by Wilson (1985) for several macrourid fishes, and sometimes observed within the same species caught at different water depths. The compression of the otolith shape shows a character polarity from an OL:OH ratio of 1.1–1.3 in the *longibarbis* Group to 0.75–0.8 found in the *striatissimus* and *grimaldii* Groups. The relative length of the pseudocolliculum shows a character polarity from a ratio TCL:PCL of 1.7–2.8 in the *longibarbis*, *iwamotoi*, *aterrimus* and *billsam* Groups to a ratio of less than 1.35 found in the *grimaldii* Group and certain species of the *striatissimus* Group. Otoliths with a similar outline are found in other macrourid genera as well, for instance in *Squalogadus*, *Macrouroides* and *Trachyrincus* (Nolf & Steurbaut, 1989), but, as stated before, the very large size of the pseudocolliculum is a unique character so far observed in teleost otoliths. The fusion of the ostial and caudal colliculi finally is observed in the *italicus*, *striatissimus* and *grimaldii* Groups and incipiently though only occasionally in *H. antraeus*. The fusion of the colliculi into a single undivided feature is commonly observed in benthic and benthopelagic fishes and certainly reflects a case of functional morphological adaptation, which is not yet understood. A number of studies exist that evaluate the pattern of the hair cell orientation of nerve ciliae attached to the sulcus of the sagittal otolith; these show great variation, but the effect on the otolith or sulcus morphology is not yet understood. The only gadiforms seemingly studied in this respect are bregmacerotids

(Popper, 1980), merlucciids (Lombarte & Popper, 2004) and morids (Deng *et al.*, 2011), but no macrourid. Schwarzahns (1981) has shown the occurrence of multiple, unrelated developments of fused colliculi in the Ophidiiformes, sometimes within a genus, similar to that in *Hymenocephalus*. Similar observations no doubt could be made with otoliths of the Macrouridae, but in *Hymenocephalus* there is no indication that fusion of the colliculi has occurred more than once.

In summary, it appears that the specializations of characters associated with the visual, auditory and motion-capturing senses (eye / orbit size, sagittal otolith morphology and head canal system) have developed in parallel and along similar polarities within the genus *Hymenocephalus*, with the *longibarbis* Group the most basal and the *striatissimus* and *grimaldii* Groups the most advanced (Fig. 39). Polarity reversal is observed in two of the three main trends (visual and auditory) in the *aterrimus* Group, which is probably a result of adaptation to a life in deeper waters.

Conclusions

This detailed study of the head and otolith morphology of the species of *Hymenocephalus* has clarified the taxonomic status of several of the species, which have been under discussion in recent literature. In certain instances, however, the taxonomic status still remains poorly or tentatively resolved (*H. lethonemus* vs *H. nascens* and the three nominal species *H. aeger*, *H. striatissimus* and *H. torvus*). Specific large-scale statistical evaluations could contribute further to the clarification of these remaining problematic species, or DNA-analyses, when available, will yield better perspectives.

The genera *Hymenocephalus* and *Spicomacrurus* contain a number of geographically restricted species, particularly in the western Pacific, and it may well be that the recognition of individual species is still incomplete. The otoliths of two poorly preserved fishes are described under Unidentifiable Species, and probably represent two undescribed species. Also, certain regions are under-explored, particularly continental and island margins of the Indian Ocean and the tropical eastern Atlantic. Once more extensively covered we might expect not only unrecorded and possibly new species, but also recognition of wider geographical ranges of known species. A recent study on otoliths dredged from Holocene sea bottom sediments in the Gulf of Guinea and off the Azores (Schwarzahns, 2013) has already indicated the potential for the latter: the presence of at least one other previously unrecorded species of the genus *Hymenocephalus* in the eastern Atlantic, probably *H. billsam* in this case.

The value of otolith morphology in the taxonomy of the Gadiformes, and particularly the Macrouridae seems high, as has been demonstrated in this study. Therefore, I expect that studies of the otolith morphology of other macrourid genera will contribute valuable taxonomic data as demonstrated here for the genus *Hymenocephalus*.

Acknowledgements

I wish to thank the following persons for providing data and / or information: P. Bearez (MNHN), D. Catania (CAS), G. Duhamel (MNHN), H. Endo (BSKU), E. Evsenko (IORAS), R. Feeney (LACM), K. Hartel (MCZ), M. McGrouther (AMS), J. Maclaine (BMNH), P. Møller (ZMUC), S. Morrison (WAM), N. Nakayama (BSKU), J. Nielsen (ZMUC), D. Nolf (IRSNB), S. Raredon (USNM), G. Shinohara (NSMT), R. Thiel (ZMH), E. Vasileva (ZMMGU), J. Williams (USNM). I particularly thank T. Iwamoto (CAS) for very valuable advice and encouragement during the early phases of the project and N. Nakayama (BSKU) for the fruitful discussion about the cephalic canal system. M. Krag (ZMUC) is thanked for the photographs and S. Raredon (USNM) for the radiographs of type specimens at USNM. Finally I wish to thank T. Iwamoto (CAS) and H. Endo (BSKU) for their constructive review of the manuscript.

References

- Alcock, A. (1889) Natural history notes from H.M. Indian Marine Survey Steamer 'Investigator', Commander Alfred Carpenter, R.N., D.S.O., commanding No. 13. On the bathybial fishes of the Bay of Bengal and neighboring waters, obtained during the seasons 1885-1889. *Annals and Magazine of Natural History*, Series 6, 4, 376-399.
<http://dx.doi.org/10.1080/00222938909460547>

- Alcock, A. (1891) On the deep-sea fishes collected by the 'Investigator' in 1890-1891. *Annals and Magazine of Natural History*, Series 6, 8, 119–138.
<http://dx.doi.org/10.1080/00222939109460407>
- Alcock, A. (1899) *A Descriptive Catalogue of the Indian Deep-Sea Fishes in the Indian Museum*. Indian Museum, Calcutta, 211 pp.
<http://dx.doi.org/10.5962/bhl.title.4684>
- Cohen, D.M., Inada, T., Iwamoto, T. & Scialabba, N. (1990) FAO species catalogue Vol. 10. Gadiform fishes of the world (Order Gadiformes). *FAO Fisheries Synopsis*, 125(10), 442 pp. [Rome]
- Deng, X., Wagner, H.-J. & Popper, A.N. (2011) The inner ear and its coupling to the swim bladder in the deep-sea fish *Antimora rostrata* (Teleostei: Moridae). *Deep-Sea Research I*, 58, 27–37.
<http://dx.doi.org/10.1016/j.dsr.2010.11.001>
- Fricke, R. & Eschmeyer, W.N. (2011) A guide to fish collections in the Catalog of Fishes. Available from: <http://researcharchive.calacademy.org/research/Ichthyology/catalog/collections.asp> (accessed 5 May 2014)
- FishBase (2014) World Wide Web Electronic Publication. Version (04/2014), Ed. by R. Froese & Pauly, D. Available from: <http://www.fishbase.org> (accessed 12 November 2014)
- Garman, S. (1899) The Fishes. In: Reports on an exploration off the west coasts of Mexico, Central and South America, and off the Galapagos Islands, in charge of Alexander Agassiz, by the U.S. Fish Commission steamer 'Albatross,' during 1891, Lieut. Commander Z.L. Tanner, U.S.N., commanding. No. XXVI. *Memoirs of the Museum of Comparative Zoology*, 24, pp. 1–431, Atlas: pls. 1–85 + A–M.
- Giglioli, E.H. (1884) *Issel Pelagos. Saggi sulla vita e sui prodotti del mare*. Tipografia del R. Istituto de' Sordo-Muti, Genoa, 436 pp.
<http://dx.doi.org/10.5962/bhl.title.42527>
- Gilbert, C.H. (1905) The deep-sea fishes of the Hawaiian Islands. In: Jordan & Evermann (Eds.), The aquatic resources of the Hawaiian Islands. *Bulletin of the United States Fishery Commission*, 22 (2), 575–713.
<http://dx.doi.org/10.5962/bhl.title.12624>
- Gilbert, C.H. & Cramer, F. (1897) Report on the fishes dredged in deep water near the Hawaiian Islands, with descriptions and figures of twenty-three new species. *Proceedings of the United States National Museum*, 19 (1114), 403–448.
<http://dx.doi.org/10.5479/si.00963801.19-1114.403>
- Gilbert, C.H. & Hubbs, C.L. (1916) Report on the Japanese macrouroid fishes collected by the United States fisheries steamer 'Albatross' in 1906, with a synopsis of the genera. *Proceedings of the United States National Museum*, 51 (2149), 135–214.
<http://dx.doi.org/10.5479/si.00963801.51-2149.135>
- Gilbert, C.H. & Hubbs, C.L. (1917) Description of *Hymenocephalus tenuis*, a new macrouroid fish from the Hawaiian Islands. *Proceedings of the United States National Museum*, 54 (2231), 173–175.
<http://dx.doi.org/10.5479/si.00963801.54-2231.173>
- Gilbert, C.H. & Hubbs, C.L. (1920) The macrouroid fishes of the Philippine Islands and the East Indies. *United States National Museum Bulletin*, 100 (1), 369–588.
<http://dx.doi.org/10.5962/bhl.title.13637>
- Goode, G.B. & Bean, T.H. (1885) Descriptions of new fishes obtained by the United States Commission mainly from deep water off the Atlantic and Gulf coasts. *Proceedings of the United States National Museum*, 8, 589–605.
<http://dx.doi.org/10.5479/si.00963801.8-543.589>
- Goode, G.B. & Bean, T.H. (1896) *Oceanic ichthyology, a treatise on the deep-sea and pelagic fishes of the world. Special Bulletin 2*, Smithsonian Institution, United States National Museum, Washington, 553 pp., plus atlas.
<http://dx.doi.org/10.5962/bhl.title.48521>
- Günther, A. (1887) Report on the deep-sea fishes collected by HMS 'Challenger' during the years 1873-1876. *Report of the scientific results of the voyage of H.M.S. Challenger during the years 1873-76, Zoology*, 22, 1–335.
<http://dx.doi.org/10.5962/bhl.title.15693>
- Iwamoto, T. & McCosker, J.E. (2014) Deep-water fishes of the 2011 Hearst Philippine biodiversity expedition of the California Academy of Sciences. In: Williams, G.C. & Gosliner, T.M. (Eds.), *The Coral Triangle. The 2011 Hearst Philippine Biodiversity Expedition*. California Academy of Sciences, San Francisco, pp. 263–332.
- Iwamoto, T. & Merrett, N.R. (1997) Pisces Gadiformes: Taxonomy of grenadiers of the New Caledonian region, southwest Pacific. *Mémoires du Muséum national d'Histoire naturelle*, 176, 473–570.
- Iwamoto, T., Shao, K.-T. & Ho, H.-C. (2011) Elevation of *Spicomacrus* (Gadiformes: Macrouridae) to generic status, with descriptions of two new species from the southwestern Pacific. *Bulletin of Marine Science*, 87 (3), 513–530.
<http://dx.doi.org/10.5343/bms.2011.1004>
- Iwamoto, T. & Williams, A. (1999) Grenadiers (Pisces, Gadiformes) from the continental slope of Western and northwestern Australia. *Proceedings of the California Academy of Sciences*, 51 (3), 105–243.
- Jordan, D.S. & Gilbert, C.H. (1904) *Macrouridae*. In: Jordan, D.S. & Starks, E.C. *List of fishes dredged by the steamer Albatross off the coasts of Japan in the summer of 1900, with descriptions of new species and a review of the Japanese Macrouridae*. *Bulletin of the United States Fishery Commission*, 22, 577–630.
- Kamohara, T. (1938) *On the offshore bottom fishes of Prov. Tosa, Shikoku, Japan*. Tokyo, 86 pp.

- Koken, E. (1884) Über Fisch-Otolithen, insbesondere über diejenigen der norddeutschen Oligocän-Ablagerungen. *Zeitschrift der deutschen Geologischen Gesellschaft*, 36, 500–565.
- Lombarte, A. & Popper, A.N. (2004) Quantitative changes in the otolithic organs of the inner ear during the settlement period in European hake *Merluccius merluccius*. *Marine Ecology progress series*, 267, 233–240.
<http://dx.doi.org/10.3354/meps267233>
- Marshall, N.B. (1979) *Developments in deep-sea biology*. Blandford Press Ltd, Dorset, 566 pp.
- Marshall, N.B. & Iwamoto, T. (1973) Genus *Hymenocephalus*. In: Cohen, D.M. (Ed.), *Fishes of the Western North Atlantic. Memoires of the Sears Foundation Marine Research*, 1 (6), 601–612.
- Merrett, N.R. & Iwamoto, T. (2000) Pisces Gadiformes: Grenadier fishes of the New Caledonian region, southwest Pacific Ocean. Taxonomy and distribution with ecological notes. *Mémoires du Muséum national d'Histoire naturelle*, 184, 723–781.
- Nolf, D. & Steurbaut, E. (1989) Evidence from otoliths for establishing relationships within gadiforms. *Natural History Museum of Los Angeles County, science series*, 32, 89–112.
- Okamura, O. (1970) *Fauna Japonica. Macrourina (Pisces)*. Academic Press of Japan, Tokyo, pp. 1–216.
- Okamura, O. (1984) *The Fishes of the Japanese Archipelago. Vol. 1. & 2*. Tokai University Press, 437 pp. & 370 pls. [Masuda, H., Amaoka, K., Araga, C., Uyeno, T. & Yoshino, T.]
- Popper, A.N. (1980) Scanning electron microscopic study of the sacculus and lagena in several deep-sea fishes. *The American Journal of Anatomy*, 157, 115–136.
<http://dx.doi.org/10.1002/aja.1001570202>
- Prokofiev, A.M. & Kukuev, E.I. (2009) New findings of rare fish species from families Mitsukurinidae (Chondrichthyes), Muraenidae, Lophiidae, Macrouridae, and Psychrolutidae (Teleostei) on raises of the Atlantic Ocean with description of *Gymnothorax walvisensis* sp. nova. *Journal of Ichthyology*, 49 (3), 215–227.
<http://dx.doi.org/10.1134/s0032945209030023>
- Sazonov, Y.I. & Iwamoto, T. (1992) Grenadiers (Pisces, Gadiformes) of the Nazca and Sala y Gomez Ridges, southeastern Pacific. *Proceedings of the California Academy of Sciences*, 48 (2), 27–95.
- Schwarzahns, W. (1978) Otolith-morphology and its usage for higher systematical units, with special reference to the Myctophiformes s.l. *Mededelingen van de Werkgroep voor Tertiaire en Kwartaire Geologie*, 15, 167–185.
- Schwarzahns, W. (1981) Vergleichende morphologische Untersuchungen an rezenten und fossilen Otolithen der Ordnung Ophidiiformes. *Berliner geowissenschaftliche Abhandlungen, Reihe A*, 26, 1–211.
- Schwarzahns, W. (2003) Fish otoliths from the Paleocene of Denmark. *Geological Survey of Denmark and Greenland Bulletin*, 2, 1–94.
<http://dx.doi.org/10.13140/2.1.2532.4164>
- Schwarzahns, W. (2010) *The otoliths from the Miocene of the North Sea Basin*. Backhuys Publishers, Leiden; Margraf Publishers, Weikersheim, 350 pp.
- Schwarzahns, W. (2013) Otoliths from dredges in the Gulf of Guinea and off the Azores - an actuo-paleontological case study. *Palaeo Ichthyologica*, 13, 7–40.
<http://dx.doi.org/10.13140/2.1.1299.5209>
- Smith, H.M. & Radcliffe, L. (1912) in Radcliffe. Descriptions of a new family, two new genera, and twenty-nine new species of anacanthine fishes from the Philippine Islands and contiguous waters. *Proceedings of the United States National Museum*, 43(1924), 105–140.
<http://dx.doi.org/10.5479/si.00963801.43-1924.105>
- Vaillant, L.L. (1888) *Expéditions scientifiques du TRAVAILLEUR et du TALISMAN pendant les années 1880, 1881, 1882, 1883*. Poissons, Paris, 406 pp.
<http://dx.doi.org/10.5962/bhl.title.13677>
- Weber, M. (1913) Die Fische der SIBOGA-Expedition. *Siboga Expedition*, 57, 1–179.
<http://dx.doi.org/10.5962/bhl.title.35825>
- Weiler, W. (1942) Die Otolithen des rheinischen und nordwestdeutschen Tertiärs. *Abhandlungen des Reichsamts für Bodenforschung*, 206, 1–140. [NF]
- Wilson, R.R. Jr. (1985) Depth-related changes in sagitta morphology in six macrourid fishes of the Pacific and Atlantic Oceans. *Copeia*, 4, 1011–1017.
<http://dx.doi.org/10.2307/1445256>